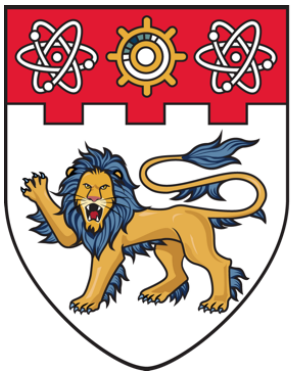

NANYANG TECHNOLOGICAL UNIVERSITY

SINGAPORE

THE CHEMISTRY OF MUCIN GLYCOPROTEIN

IN SWIFTLET (*AERODRAMUS FUCIPHAGUS*)

EDIBLE BIRD'S NEST

ERIC SHIM KIAN SHIUN

SCHOOL OF PHYSICAL AND MATHEMATICAL SCIENCES

2019

THE CHEMISTRY OF MUCIN GLYCOPROTEIN

IN SWIFTLET (*AERODRAMUS FUCIPHAGUS*)

EDIBLE BIRD'S NEST

ERIC SHIM KIAN SHIUN

SCHOOL OF PHYSICAL AND MATHEMATICAL SCIENCES

A thesis submitted to the Nanyang Technological University in partial fulfilment of the requirement for the degree of Doctor of Philosophy

2019

Statement of Originality

I hereby certify that the work embodied in this thesis is the result of original research done by me except where otherwise stated in this thesis. The thesis work has not been submitted for a degree or professional qualification to any other university or institution. I declare that this thesis is written by myself and is free of plagiarism and of sufficient grammatical clarity to be examined. I confirm that the investigations were conducted in accord with the ethics policies and integrity standards of Nanyang Technological University and that the research data are presented honestly and without prejudice.

14 Feb 2019

. . . . . .

Date

. . . . . .

Eric Shim Kian Shiun

Supervisor Declaration Statement

I have reviewed the content and presentation style of this thesis and declare it of sufficient grammatical clarity to be examined. To the best of my knowledge, the thesis is free of plagiarism and the research and writing are those of the candidate's except as acknowledged in the Author Attribution Statement. I confirm that the investigations were conducted in accord with the ethics policies and integrity standards of Nanyang Technological University and that the research data are presented honestly and without prejudice.

14 Feb 2019

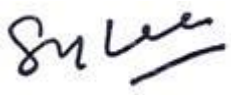

. . . . . .

Date

. . . . . .

Professor Lee Soo Ying

Authorship Attribution Statement

This thesis contains material from 4 papers published in the following peer-reviewed journals where I was the first author.

Chapter 2 is published as Shim, Eric Kian-Shiun; Chandra, Gleen Fernando; Pedireddy, Srikanth; Lee, Soo-Ying, Characterization of swiftlet edible bird nest, a mucin glycoprotein, and its adulterants by Raman microspectroscopy. *Journal of Food Science and Technology* **2016**, *53*, 3602-3608. (Permission for reproducing the content in this thesis has been obtained from Springer Nature, License Number 4302330646383)

and

Shim, Eric Kian-Shiun; Lee, Soo-Ying, Raman microspectroscopy is a rapid technique to authenticate edible bird's nest—a glycoprotein. *Spectroscopy Europe* **2017**, *29*, 10-13. (Permission for reproducing the content in this thesis has been obtained from John Wiley & Sons Ltd and IM Publications LLP)

The contributions of the co-authors are as follows:

- Prof Lee Soo Ying provided the initial project direction and hypothesis.
- I prepared the manuscript drafts and the manuscript was revised and edited by Prof Lee Soo Ying.
- I co-designed the study with Prof Lee Soo Ying and performed all the laboratory work at Division of Chemistry and Biological Chemistry, School of Physical and Mathematical Sciences. I also conducted the data processing and analysis.
- Gleen F. Chandra assisted in the sample preparation and collection of the Raman microspectroscopy data.

- Dr Srikanth Pedireddy provided guidance in the operation of the Raman microspectrometer.

Chapter 3 is published as Shim, Eric Kian-Shiun; Chandra, Gleen Fernando; Lee, Soo-Ying, Thermal analysis methods for the rapid identification and authentication of swiftlet (Aerodramus fuciphagus) edible bird's nest – A mucin glycoprotein. *Food Research International* **2017**, *95*, 9-18. (Permission for reproducing the content in a thesis has been obtained from Elsevier)

The contributions of the co-authors are as follows:

- Prof Lee Soo Ying provided the initial project direction and hypothesis.
- I prepared the manuscript drafts and the manuscript was revised and edited by Prof Lee Soo Ying.
- I co-designed the study with Prof Lee Soo Ying and performed all the laboratory work at Division of Chemistry and Biological Chemistry, School of Physical and Mathematical Sciences. I also conducted the data processing and analysis.
- Gleen F. Chandra assisted in the sample preparation and collection of the data of thermogravimetry and differential scanning calorimetry.

Chapter 4 is published as Shim, Eric Kian-Shiun; Lee, Soo-Ying, Nitration of tyrosine in the mucin glycoprotein of edible bird's nest changes its color from white to red. *Journal of Agricultural and Food Chemistry* **2018**, 66, 5654-5662. (The content is reprinted (adapted) with permission from American Chemical Society © 2018 American Chemical Society.

The contributions of the co-authors are as follows:

- Prof Lee Soo Ying provided the initial project direction and hypothesis.
- I prepared the manuscript drafts and the manuscript was revised and edited by Prof Lee Soo Ying.
- I co-designed the study with Prof Lee Soo Ying and performed all the laboratory work, data processing, and analysis at Division of Chemistry and Biological Chemistry, School of Physical and Mathematical Sciences.

14 Feb 2019

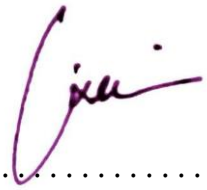

. . . . . .

Date

. . . . . .

Eric Shim Kian Shiun

Abstract

The chemistry of mucin glycoprotein in edible bird's nest (EBN), an esteemed delicacy and broad-spectrum supplement, produced by swiftlet *Aerodramus fuciphagus* has been explored in this thesis.

In the first part of the project, the use of Raman microspectroscopy and thermal analysis tools (thermogravimetry, differential thermogravimetry, and differential scanning calorimetry) has provided new insights into the understanding of the properties of EBN mucin glycoprotein. The unique Raman spectrum shows characteristic bands of both protein and carbohydrate, justifying that EBN is a mucin glycoprotein, while the unique thermal analysis curves show the moisture content, thermal decomposition pattern, and ceramic ash content of EBN. Adulteration of EBN will give rise to a different Raman spectrum or thermal analysis curve, and thus the unique fingerprinting can be used to authenticate EBN samples. Overall, these analytical tools show high potential as rapid, simple, and label-free techniques to contend with the rampant adulteration of EBN.

In the second part of the project, the molecular basis and chemistry behind the color of the more desirable red EBN or 'blood' nest that has been a puzzle for a long time have been investigated. Through the qualitative and quantitative analysis by Raman microspectroscopy, enzyme-linked immunosorbent assay, and UV-visible absorption spectroscopy, the nitration of protein tyrosine, which is recognized as ubiquitous in several diseases, to produce 3-nitrotyrosyl residue in mucin glycoprotein is found to be the real cause of the red coloration. The discovery of the underlying mechanism is useful when it comes to achieving a holistic evaluation of the benefits and values of EBN, and the findings could have refined the putative benefits of red EBN, which might have been touted for centuries.

Acknowledgment

First and foremost, I would like to express my extreme gratitude towards my supervisor, Professor Lee Soo Ying for his constant guidance and advice. I really could not have made it without his support and guidance. Thank you for being patient with me and instilling in me an appreciation for true scientific research, and it was a great honor to be part of your research group.

Secondly, I would like to thank my co-supervisors- Assoc Prof Liu Xuewei and Dr Alessandra Bonanni, Thesis Advisory Committee members- Prof Leung Pak Hing and Assoc Prof Koh Cheng Gee, and Qualifying Examination examiners- Assoc Prof Leong Weng Kee and Asst Prof Hajime Hirao for all the advice and support for my project. In addition, I would like to thank for the guidance received from Dr Sumod, Prof Li Tianhu, Prof Bates, Dr Boontawee, and Dr Julia while I was doing teaching duties. The financial support from the NTU research scholarship over the last three years is also gratefully acknowledged.

Thirdly, I would like to express my gratitude to the following people who have been there in my Ph.D. journey, whether it was through physical or emotional support, all the help were greatly appreciated:

- To my fellow lab neighbors, thank you for all the assistance in CBC as well as the times we had: Asyifah, my senior in CBC-04-39; Alan, Desiree, Kiran, Krishna, JiaZi, and Zhiyu from Prof Chen group; Yingzhou, YuQian, ZhiYong, BoYang, WeiXiang, PoKai, and Carmen from Prof Leong group; He Lei, Jingyuan, Wenping, and Liying from Prof Shao group; Alan from Prof Xing group; Charlynn, CheeLeng, Yang Zhe, Yijie, and Srikanth from Prof Ling group; Hiro from Prof Chiba group; ShuHui from Prof Liu group; Maja from Prof Webster group; Andrew from Prof Soo group, Fiona from Prof Zhao group;

Jonathan and Ronald from Prof Leung group, CherChiek from Prof So group and Benny from Prof England group, and *etc*.

- AiHua, Charlene, EeLing, YeanChin and all the CBC/SPMS staffs, thanks for your expertise, technical support, and training for the instruments in teaching lab and central facilities lab.
- SiewKheng, VoonChin and YaWen, thanks for your efforts and assistance in the lab.

I would also like to extend my appreciation to my friends who have kept me going through the times and inject liveliness in my life, all these years:

- HongTak, Noel, Jossent, YeeWei, YiJye, HuiHwa, Okie, Levin, Chiewsian, JiaJia, JiunnLong, YeuDe, ZhiTing, ChongAih and WeiLeong, thanks for all the endless enthusiasm.
- ChingHui, Deacon, XianQi, JingXuan, Benjamin, WangWei, JaeYu, SiokWei, TeckWan, ShengYuan, MayChear, SeanJon, ZhengXian, LiangJie, Evillion, and HongHeem, thanks for all the interesting and meaningful days.
- Noel, ZhiPei, Michelle, HaoHao, ChunHung, LeeTian, SiJia, Marshall, and FongChin, I will miss the music and performance we did together.
- My volunteer-mates from Welfare Service Club Youth- Daphne, Brandon, LingYong, RuiLiang, WeiShuen, Jessica, PeiYu, Reuben, GuanMing, and *etc*.
- And all the people that I could not have listed down here, you know who you are. Thank you for being in my life.

Last but not least, my deepest gratitude to my family for their love, unwavering support, trust and encouragement in all my pursuits, especially my parents, for their upbringing, unspoken love for the past 26 years. You will always be the pillars of my strength.

Table of Contents

List of Figures

320-600 nm have been scaled up by an appropriate factor, as indicated, for visualization.

List of Tables and Reaction Schemes

Abbreviations

3-NT	3-nitrotyrosine
3-NTyr	3-nitrotyrosine residue in the glycoprotein
4-NP	4-nitrophenylalanine
AAS	atomic absorption spectrophotometer
AC	acidic chitinase
AD	*Anno Domini*
AMCase	acidic mammalian chitinase
BSM	bovine submaxillary mucin
CCD	charge-coupled device
CM	Chinese medicine
DMPD	N,N-dimethyl-ρ-phenylenediamine
DNA	deoxyribonucleic acid
DSC	differential scanning calorimetry
DTG	differential thermogravimetry
EBN	edible bird's nest
EGF	epidermal growth factor
ELISA	enzyme-linked immunosorbent assay
ESEM	environmental scanning electron microscope
ESI	electrospray ionization
F-C	Folin-Ciocalteu
FT-IR	Fourier-transform infrared

GAGs	chondroitin glycosaminoglycans
GalNAc	N-acetylgalactosamine
GC	gas chromatography
GlcNAc	N-acetylglucosamine
HPLC	high-performance liquid chromatography
HRP	horseradish peroxidase
HWIF	hot water insoluble fraction
ICP-MS	inductively coupled plasma-mass spectroscopy
kDa	kilodalton
LC-MS	liquid chromatography-mass spectroscopy
MSG	monosodium glutamate
NA	numerical aperture
NADH	nicotinamide adenine dinucleotide with hydrogen
NANA	N-acetylneuraminic acid
NCBI	National Center for Biotechnology Information
Neu5Ac	N-acetylneuraminic acid
NMR	nuclear magnetic resonance
PC	principle component
PCA	principal component analysis
PG	proteoglycan
Phe	phenylalanine
RNS	reactive nitrogen species

RP-HPLC	reversed-phase high-performance liquid chromatography
SDS-PAGE	sodium dodecyl sulfate-polyacrylamide gel electrophoresis
TG	thermogravimetry
Tyr	tyrosine
UV-Vis	UV-Visible
w/w	weight to weight ratio

List of Publications

1. Shim, Eric Kian-Shiun; Chandra, Gleen Fernando; Pedireddy, Srikanth.; Lee, Soo-Ying, Characterization of swiftlet edible bird nest, a mucin glycoprotein, and its adulterants by Raman microspectroscopy. *Journal of Food Science and Technology* **2016**, *53*, 3602-3608.

2. Shim, Eric Kian-Shiun; Lee, Soo-Ying, Raman microspectroscopy is a rapid technique to authenticate edible bird's nest—a glycoprotein. *Spectroscopy Europe* **2017**, *29*, 10-13.

3. Shim, Eric Kian-Shiun; Chandra, Gleen Fernando; Lee, Soo-Ying, Thermal analysis methods for the rapid identification and authentication of swiftlet (*Aerodramus fuciphagus*) edible bird's nest – A mucin glycoprotein. *Food Research International* **2017**, *95*, 9-18.

4. Shim, Eric Kian-Shiun; Lee, Soo-Ying, Nitration of tyrosine in the mucin glycoprotein of edible bird's nest changes its color from white to red. *Journal of Agricultural and Food Chemistry* **2018**, 66, 5654-5662.

Chapter 1 Introduction

1.1 The origin of edible bird's nest

The edible bird's nests (EBN), or cubilose, produced by the swiftlet is a fascinating natural product. The nest cement formed from the glutinous salivary secretion of swiftlets can be made into a delicacy - bird's nest soup. It has been served as an esteemed food and broad-spectrum health supplement, particularly by Asians, for centuries due to its exclaimed health benefits and medicinal functions.

The nest cement itself is a composite material made almost entirely out of the mucin glycoprotein from a peculiar kind of secretion from the swiftlet's paired sublingual glands.[1] A unique morphological feature of the glands contributes significantly to the activity of nest building. The swiftlet's hypertrophic salivary glands distributed within the lingual apparatus enlarge and reach their maximum secretory activity during the breeding season.[2] The viscid mucin secreted is bound together with feathers and impregnated with tiny sand grains regurgitated from the bird's gizzard to form a composite material. It is attached to the vertical walls of caves or human-made bird houses, which is a purpose-built structure that simulates the natural cave environment with dark and humid conditions and plays recordings of bird calls on the roof to attract swiftlets, and hardened as it layered into the form of a solid half bowl-shaped nest to bear the nestlings.[3] A completed nest typically weighs one to two times the swiftlet's body weight.[4]

After the breeding season, the raw nests are collected and sent for cleaning. The cleaning process is highly labor-intensive and time-consuming. Primarily, there are three major steps for the cleaning process. At first, the raw nest is soaked in water until the nest cement is softened and expanded. The interwoven feathers, fine plumage, eggshells, sand particles and any other impurities are then removed carefully with forceps with sharp tips. This step requires

a tremendous amount of human effort and can take estimate 0.8 hours for a trained operator to clean a nest.[5] Lastly, the cleaned moistened strands of nest cement are rearranged and molded into a cup, biscuit or other shape and air-dried to obtain cleaned EBN product that is marketable.

Figure 1.1 Raw white EBN (left) and cleaned white EBN (right) collected from Malaysia.

Generally, the grade of EBN is dependent on three key criteria- the purity, shape and also the color of the EBN cement. In the market, the cleaned EBN is sold in various shapes, such as cup (Figure 1.2A - C), biscuit (Figure 1.2D - F), strips, and the lowest grade is sold in the form of coarse powder. Also, the EBN differs in color from ivory white, yellow to red (Figures 1.2A - C).

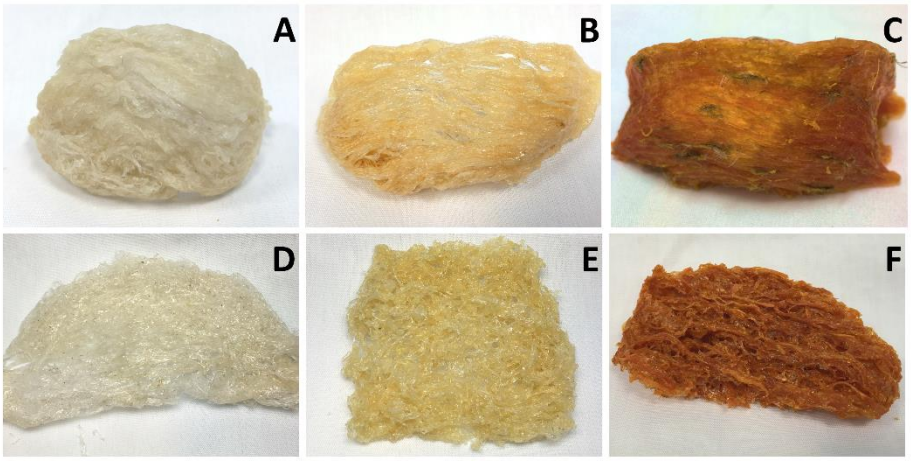

Figure 1.2 Types and colors of EBN found in the market. A. white EBN cup; B. yellow EBN cup; C. red EBN cup; D. white EBN biscuit; E. yellow EBN biscuit and F. red EBN biscuit. The EBNs were purchased from local Traditional Chinese Medicine (TCM) stores in Singapore or Malaysia.

It is presumed that red EBN has higher medicinal and nutritional properties than yellow and white ones although no scientific evidence on the chemical basis has been provided. The premium grade EBN fetches a premium price from US$3000 per kilogram, and therefore EBN is honored as the "Caviar of the East".[3]

Among the three genera (*Aerodramus*, *Collocalia*, and *Hydrochous)* under the Swift family of *Apodidae*,[6] the genus of *Aerodramus* is of higher commercial values as it produces a higher grade of the edible nest with trace impurities.[7] For this reason, the majority of EBN traded worldwide come from two heavily exploited "edible-nest swiftlet" species under the genus of *Aerdramus*, which are the white-nest swiftlet (*Aerodramus fuciphagus*) and the black-nest swiftlet (*Aerodramus maximus*). These species are native to the Nicobar Islands in the Indian Ocean and the sea caves in the coastal regions of Thailand, Vietnam, Indonesia, Borneo as well as the Palawan Islands in the Philippines, as indicated in Figure 1.3.[8] In this thesis, the premium grade EBN produced by the species *Aerodramus fuciphagus* is featured in the experiments.

Figure 1.3 Map of South-East Asia[9] showing the distribution of *Aerodramus* genus (area in the rectangular box).

1.2 Historical background of edible bird's nest

Human consumption of bird's nest soup has been a symbol of wealth, prestige, and power as well as being used medicinally in Chinese medicine (CM). It is reputed to possess medicinal properties that nourish and tone up the organ systems of the body, help to dissolve phlegm, relieve gastric problems, aid kidney function, enhance complexion, alleviate asthma, suppress coughing, cure tuberculosis, improve the immune system, energy, and metabolism.[7, 10] Practitioners of CM have consistently recommended that the consumption of EBN is beneficial for the treatment of a variety of health problems.[8] In the last few decades, the nutraceutical effect of EBN has been investigated, which reveals the anti-influenza properties against human, avian, and porcine influenza viruses,[11-13] cognitive-enhancing properties in memory and learning ability,[14-15] cell-proliferation simulative properties,[16-18] anti-oxidative properties,[19-23] ability of lowering risk of cardiovascular disease,[24-25] skin-whitening properties,[26-27] and *etc.* Therefore, it is suggested that EBN has the potential to be a functional food that provides substantial benefits to our body.

The consumption of EBN as a quintessential delicacy in ancient China can be traced back to Tang Dynasty (618-907 AD).[8] There are also historical sources stated that Admiral Zheng He bring back EBN to the imperial court of Ming Dynasty (1368-1644 AD) in his voyage to the South China Sea. Since then, the existence of EBN has been reported in the Chinese literature , such as "Eastern Western" or "Dōng Xi Yáng Kǎo" (东西洋考) written in Ming Dynasty (Figure 1.4 A) which describes the exotic herbal, spices, foods and other items found in South-East Asia and East Asia, and "Supplements to the Compendium of Materia Medica" or "Běn Cǎo Gāng Mù Shí Yí" (本草纲目拾遗) written in Qing Dynasty (1636-1912) (Figure 1.4 B), a herbology volume listing the plants, animals, minerals and other items that were believed to have medicinal properties.

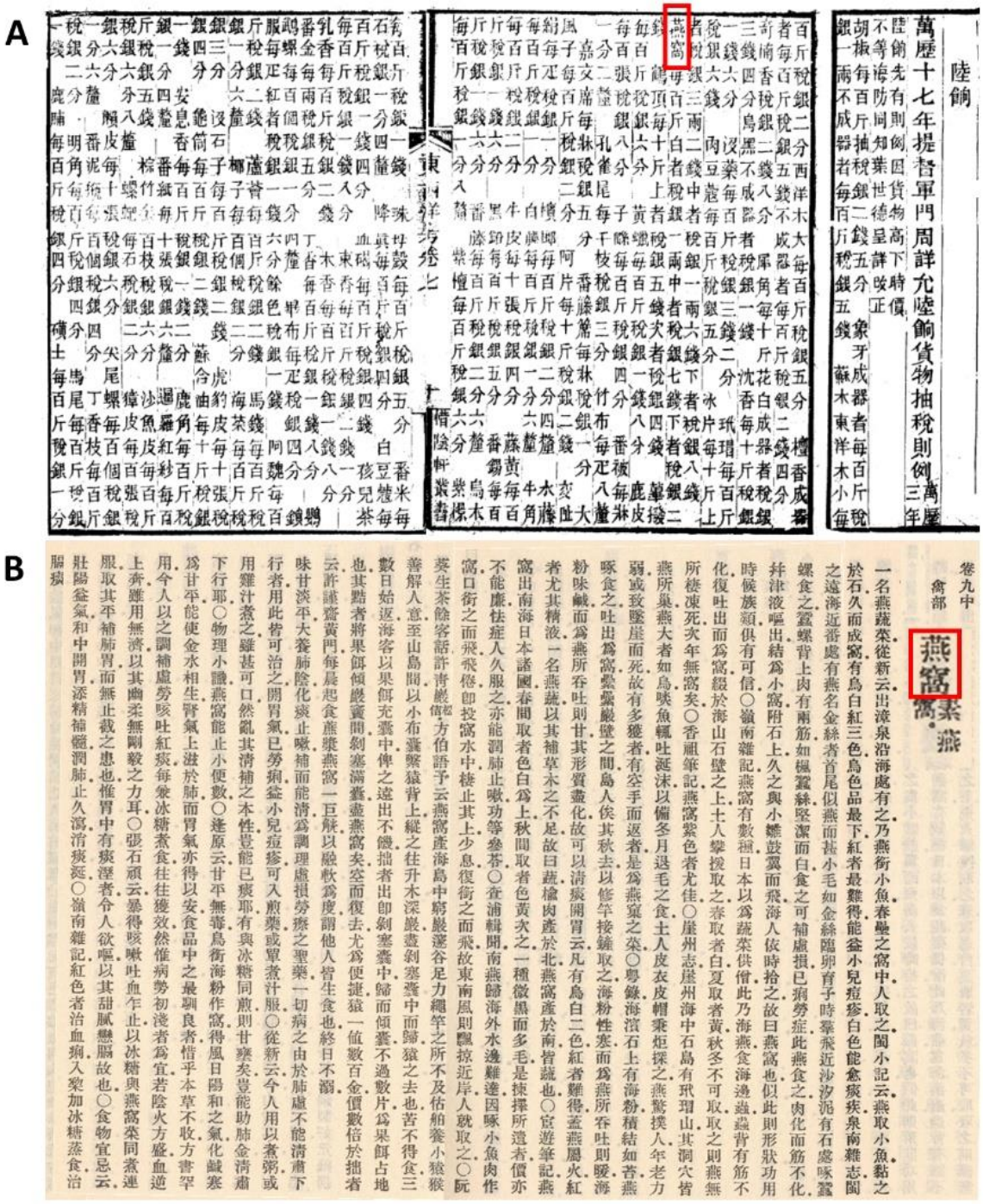

Figure 1.4 Excerpt of records on EBN (in Chinese characters, 燕窝 yàn wō) in ancient Chinese literature: A. "Eastern Western" written in Ming Dynasty; B. "Supplements to the Compendium of Materia Medica" written in Qing Dynasty. (Adapted from physical books in Nanyang Technological University's Chinese Library and Wang Gungwu Library)

This delicacy long held in high esteem in China was brought into prominence to the western countries in the 19th century when an England's scientist reported descriptive statements concerning the occurrence and appearance of the nest in a scientific symposium.[28] After that, the study of EBN has increased exponentially, and the reputation of EBN has spread all over the world. Nowadays, the consumption of EBN is no longer a privilege for wealthy. Despite being one of the most expensive food commodities, various processed EBN and ready-to-drink health tonics are appearing in the supermarkets and shops across the world, and the benefits of EBN are increasingly being promoted to domestic consumers.[29]

1.3 The composition of edible bird's nest

Despite the long history of EBN consumption, the earliest composition analysis of EBN was only conducted by a female scientist Wang Chi Che from the University of Chicago in the early 20th century. In her research, she found that the EBN belongs to the class of glycoprotein that has the properties of both protein and carbohydrate,[30] and successfully isolated several amino sugars from EBN.[31] She further commented that the EBN glycoprotein has a structure that is more complicated than a boiled egg as the digestion rate of EBN with pepsin and trypsin is slower than that of boiled egg.[30]

Her observation is found to be in accord with other research, which shows that in addition to the glycoprotein, EBN also contains moisture, mineral and trace amount of lipid. The composition of EBN is briefly discussed in the following section.

1.3.1 Mucin glycoprotein

The mucin glycoprotein of EBN has a structure containing both O- and N-glycosylproteins with sialic acid occupying the non-reducing terminal position of oligosaccharides chains (Figure 1.5).[32] The dendritic carbohydrates are O-glycosidically attached to the protein backbone by linkages involving N-acetylgalactosamine (GalNAc) and

an amino acid consists of a hydroxyl group (serine or threonine), and N-glycosidically attached by linkages involving N-acetylglucosamine (GlcNAc) and asparagine. In particular, O-glycosidically linked oligosaccharides are the major components of the EBN glycoproteins while N-glycosidically linked glycans are the minor components.[33] A wide range of amino acids and monosaccharides can be found in the EBN glycoprotein, and this unique structure makes it differ from other glycoproteins, in terms of functionality and properties. Herein, the literature review of the protein and carbohydrate components of EBN mucin glycoprotein is included.

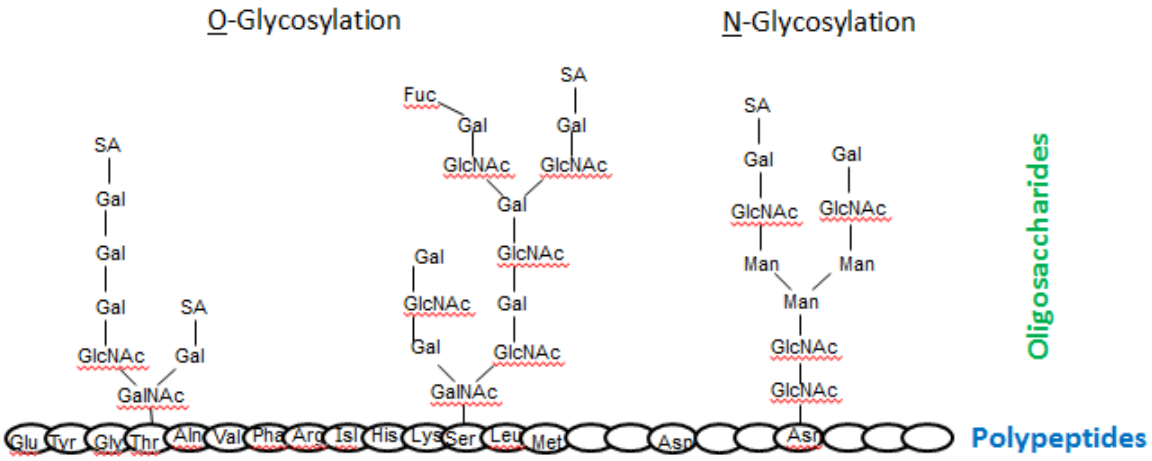

Figure 1.5 Schematic diagram of the EBN mucin glycoprotein drawn using information from literature.[3, 32]

1.3.1.1 Protein

The protein component in mucin glycoprotein is found to be the major component of EBN. It is contributing up to its 61% by weight reported by Zhu *et al.*,[34] 62% reported by Marcone,[3] and 64% reported by Sengkrajang *et al.*[35] and Wang[30]. As it is difficult to isolate a single pure protein from EBN, a complex natural product, the protein content was estimated using the Kjeldahl method, which quantitatively measures the nitrogen content of the sample and multiplies with a specific conversion factor (6.25) to correlate with the protein content.

However, the following proteomics research of EBN has reached a bottleneck because of the difficulties in the extraction, purification, and identification. Primarily due to the different extraction approaches, the proteins extracted in the supernatant has often been not identical. Hence, a non-repeatable protein fingerprint and not well-resolved streaking bands on sodium dodecyl sulfate-polyacrylamide gel electrophoresis (SDS-PAGE) are commonly observed in the proteomics research of EBN.

Briefly, in the literature, decoction method which is akin to the traditional way of preparing the bird's nest soup was frequently used by the researcher to prepare the solubilized EBN protein extract. However, different results are often observed for the aqueous extract decocted at the different temperature as EBN protein exhibits a broad distribution of molecular weight. Tukiran *et al.*[36] observed two intense protein bands at 128 kDa and 106 kDa in the 50°C aqueous-extract of EBN, which was also observed in the extracts prepared with ultrasonication or urea solution.[37-38] Kong *et al.*[16] isolated and obtained two proteins with the molecular weight ranging from 6 kDa to 8 kDa with epidermal growth factor (EGF) activity in the 60°C aqueous-extract of EBN.

Several studies were conducted with the 100°C aqueous-extract of EBN; Wong *et al.*[39] identified a 150 kDa acidic mammalian chitinase (AMCase)-like protein, which is known to be found in animals that need to digest chitin-containing prey and chitinase-like proteins. Goh *et al.*[40] performed an allgerosorbent test on the protein smaller than 100 kDa and successfully identified a 66 kDa protein band that is postulated to be the major putative allergen for EBN-induced anaphylaxis. Additionally, Kong *et al.*[41] performed simulated gastrointestinal digestion on the hot water insoluble fraction (HWIF) of EBN after the decoction at 100°C to investigate the peptides released from HWIF in our body, where an abundant 50 kDa protein band was visualized and suggested to be a mucin-5 like peptide. Moreover, the other peptides were compared and matched with the sequences in the National Center for Biotechnology

Information (NCBI) protein database with the aid of the algorithm, and the presence of mucin AC-like protein, nicotinamide adenine dinucleotide with hydrogen (NADH) dehydrogenase, AMCase, *etc*. was identified.[41]

To further explore the chemical properties and understand the specific composition of the protein in EBN, the protein was broken down with acid at a carefully controlled condition (6 N HCl at 105°C for 24 h),[42] to yield the free amino acid profile. The amino acids profile obtained is essential for understanding its functional properties and nutritional value. According to Marcone,[3] the protein is made up of 17 types of amino acids: serine (15.4%), valine (10.7%), isoleucine (10.1%), tyrosine (10.1%), aspartic acid, asparagine (9.5%), glutamic acid, glutamine (7.0%), phenylalanine (6.8%), arginine (5.4%), glycine (5.9%), threonine (4.4%), alanine (4.0%), lysine (3.5%), histidine (3.3%), leucine (3.0%) and methionine (0.8%). There is a distinct absence of two essential amino acids, tryptophan, and cysteine. Therefore, it cannot be used to serve as a sole source of protein as it is not a complete source of food protein, which has also been demonstrated in a rat feeding experiment.[30]

However, from the amino acid profile, we can observe that the nutritional value of EBN is high as it consists of many essential amino acids that are required to be supplied to the human body in the diet. Moreover, Chua *et al.*[42] remarked that the amino acids (both essential and non-essential) in EBN were at a higher concentration than typical protein-rich food like milk and egg and hence suggested EBN as a premium grade protein-source supplement.

1.3.1.2 Carbohydrate

Carbohydrate is the second major component in EBN, and it ranged from 10.6 to 27.3% by weight, across different studies.[3, 30, 43-44] The carbohydrate in EBN presents as the dendritic oligosaccharides on the glycoprotein, and its linkage and structures have been established in several publications.[32, 45-46] Akin to protein structure analysis, complex patterns are observed

in the separation and the purification. Therefore, it is suggested that the oligosaccharides present in EBN are more complicated than that of other glycoproteins, for example, bovine submaxillary mucin (BSM).[45]

Neutral monosialyl and disialyl oligosaccharides were released from the glycoprotein after alkaline reductive treatment.[32] Abundant oligosaccharides, such as chondroitin glycosaminoglycans (GAGs),[47] non-sulfated chondroitin proteoglycan (PG),[48] and numerous O-glycans and N-glycans[33] can be found in EBN. The oligosaccharides were further breakdown to liberate the monosaccharides for the quantitative analysis. It was revealed that EBN contains galactose (16.9%), sialic acid (9.0%), N-acetylgalactosamine (7.2%), N-acetylglucosamine (5.3%), fucose (0.7%), and mannose (0.6%) as the main saccharides,[49] with glucose, xylose, rhamnose, and ribose as the minor saccharides.[42] The diversified monosaccharides profile of EBN made it different from other types of food such as egg white and infant formula.[42] Among the saccharides, a high concentration of N-acetylgalactosamine and N-acetylglucosamine was observed as they are the linkers between dendritic oligosaccharides chains with the protein backbone, which suggested the presence of numerous glycosylated site on the mucin glycoprotein of EBN.

On the other hand, sialic acid, especially N-acetylneuraminic acid (Neu5Ac or NANA),[46, 48] is present in an unusually high concentration in the EBN mucin glycoprotein.[3, 43] The high concentration of sialic acid can be explained by the presence of the MGAT gene, which is essential for the biosynthesis of sialic acid, that is highly expressed in the *Aerodramus* swiftlets.[50] Structurally, sialic acid is a non-reducing α-glycoside in the mucin glycoprotein, usually found attached to the outermost ends of the dendritic hetero-oligosaccharides chains.[51] The negative charge on the carboxyl group of sialic acid (Figure 1.6) contributes to the biophysical features and the physiological effect of the biological system.[52]

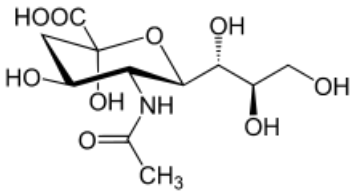

Figure 1.6 Structure of N-acetylneuraminic acid, a sialic acid. Sialic acid imparts negative charges to the glycoproteins due to its carboxyl group.

These functions made sialic acid a valuable monosaccharide, and its isolation from EBN has recently attracted significant attention. Kathan *et al.*[49] reported that sialic acid could be quantitatively released from EBN by mild acid hydrolysis without the simultaneous release of any other saccharides. Alternatively, Martin *et al.*[53] reported a relatively moderate process of separating sialic acid from EBN glycoproteins by hot-water extraction, followed by ultrafiltration and ion-exchange chromatographic separation. These methods provide substantial quantities of sialic acid which is useful for the further application.

1.3.2 Moisture

Beside the mucin glycoprotein, EBN cement contains a significant amount of moisture from the environment due to its hygroscopic nature. The moisture content of EBN is proximately estimated from the weight loss during dehydration in an oven and found to be at around 7.5 to 12.9% by weight.[3, 21, 35] However, since it is a prevalent phenomenon to find loosely bound moisture and tightly bound moisture in a hygroscopic material, more advanced thermal analysis techniques (thermogravimetry and differential scanning calorimetry) are required to provide more information on the dehydration and decomposition of EBN cement. The more detailed experiments and quantification of the total moisture content in EBN will be shown in chapter 3.

1.3.3 Mineral

The residual mass left behind from the combustion is often used to estimate the ashes and mineral content of a sample. It is found that the ashes content of EBN from different geographical origin was similar (2-5%).[3, 35, 54] The elemental analysis of the ashes was achieved with atomic absorption spectrophotometer (AAS) or inductively coupled plasma-mass spectroscopy (ICP-MS). AAS revealed that the cleaned EBN contains Na (650-700 ppm), Ca (798-1298 ppm), Mg (330-500 ppm), K (110-165 ppm), Fe (30-60 ppm) and P (40-45 ppm).[3] Huda *et al.*[55] indicated that cave nests have higher levels of Na and Ca than house nests due to the leaching from the limestone walls of the cave. On the other hand, ICP-MS detected Na (15241 ppm), Ca (3811 ppm), Mg (2488 ppm), K (1433 ppm), Fe (156 ppm) and Sr (368 ppm) as the major element in EBN.[56] The higher concentration of the minerals might arise from the higher sensitivity of the technique or due to sample's batch difference.

Nevertheless, those minerals detected in EBN are essential micro-nutrients which serve as cofactors to activate many enzymatic reactions in the body, and therefore, the findings suggest that EBN is an excellent source for the essential mineral that is required by the human body and could be included in daily intake.

1.3.4 Lipid

Saengkrajang *et al.*[35] found that the content of crude lipid for EBN collected from Thailand ranged from 0.4 to 1.3% by weight while Huda *et al.*[55] reported about 0.4 to 2.0% of lipid is in the white EBN from Indonesia and Malaysia. Similarly, Marcone[3] showed that 0.1 and 1.3% lipid could be found in white and red EBN, respectively.

The characterization of lipid in EBN with gas chromatography showed three saturated fatty acids - palmitric acid (C16:0), stearic acid (C18:0), and behenic acid (C22:0), and eight unsaturated fatty acids- myristoleic acid (C14:1), pentadecanoic acid (C15:1), palmitoleic acid

(C16:1), heptadecenoic acid (C17:1), oleic acid (18:1), linoleic acid (C18:2), eicosenoic acid (C20:1), and arachidonic acid (C20:4).[55] The fatty acids are suggested to be originated from the diets as swiftlets are feed exclusively on insects which are rich in fatty acids.[55]

In summary, numerous studies have been conducted to elucidate the nature of EBN, especially on their composition and structural characteristic. However, the relationships of carbohydrate with proteins backbone in the mucin glycoprotein are still not comprehensively elucidated, and there are many questions left unresolved. Thus, there is still a need to develop our understanding of the chemical and physical properties of EBN. Nevertheless, evidence has shown that the protein and carbohydrate content in EBN from the different geographical locations did not differ significantly,[57-59] suggesting that the EBN is a consistent biopolymer built of protein and carbohydrate. Hence, if the structure, sequence, and linkage of the amino acids and carbohydrate moiety in the glycoprotein can be understood, we will get a better comprehension of the properties and functions of EBN, and more importantly, the synthesis of the glycoprotein might be possible.

1.4 Key research questions on edible bird's nest

1.4.1 Adulteration

As mentioned above, EBN is one of the most favorable nutraceutical delicacies in Asian culture, and it is reputed to be "undoubtedly one of the most expensive foods in the world".[8] However, the nature of EBN mucin glycoprotein is still unclear, and it is impossible to synthesize EBN from other precursors. In addition, the supply of EBN is very limited due to the low production level and the labor-intensive cleaning process. Due to these reasons, EBN is firmly regarded as an exquisite material and is sold at a premium price in the market. Commercially, a kilogram of the cleaned white EBN costs about US$3,000 today, and red EBN

retails at a price that is several times higher. Given a global output of about a million kilogram per year, this translates to an annual trade worth more than US$1.5 billion

Due to the substantial lucrative return of EBNs, the adulteration is a widespread and rampant issue, although their excessive profit is at the cost of consumer trust and confidence. Some unscrupulous and unethical EBN processors use various methods to adulterate it to increase profits, including using lower grade EBN to imitate high-grade EBN, incorporating some cheaper materials which are similar in appearance into the cleaned EBN to increase the net weight and its market value, or dyeing the white EBN with food coloring or industrial dyes to produce red 'blood' nest that is higher-priced.

The commonly used edible adulterants in EBN can be classified into two types: (a) Type I adulterants which are solids with a similar appearance to EBN cement and can be adhered externally to the surface of EBN cement, for example, tremella fungus (*Tremella fuciformis*) and coralline seaweed which are often introduced in the form of thin slivers. Type I adulterants may be introduced by up to 10% in weight to evade detection by the naked eyes. However, they can be detected with a microscope due to differences in their morphological structure; (b) Type II adulterants which are water-soluble substances that can be incorporated internally into the EBN cement matrix, for example, saccharides (e.g. glucose, sucrose), polypeptides (e.g. hydrolyzed marine collagen), and salts (e.g. monosodium glutamate) that can be absorbed by the moist EBN hydrogel and embedded in the EBN cement to form a composite material upon drying. The Type II adulterants which are embedded in the EBN cement are more covert and difficult to detect visually. More sophisticated techniques and tools are required to identify and distinguish Type II adulterants.

Unfortunately, though many consumers are aware of the benefits of EBN and the premium price they are paying for it, most are unaware of how to choose and differentiate

superior quality or genuine ones from fakes or adulterated products. They rely on the empirical identification method, including sensory testing on the characteristic traits, or examiner's experience on choosing the commodities but it is highly inefficient to provide conclusive results on the authenticity of EBN. Therefore, many analytical techniques have been developed to check for the presence of adulterants in EBN, mainly including microscopic identification, chromatographic identification, biological identification, spectral identification, as well as combinations from the above. However, it is clear that all the proposed techniques have their own strengths and weakness.

Under an optical stereoscope, the fiber array of EBN is semitransparent and fine cracks are present on the cement.[60] In addition, Yang *et al.*[61] showed that the EBN displays a crater-like structure of irregularly shaped three-dimensional network under environmental scanning electron microscope (ESEM). However, only the adulterants that have very detailed striations (Type I) can be distinguished from the highly amorphous strands of EBN.

The metabolite fingerprinting of EBN obtained from chromatographic separation is often used as a standard for the authentication of EBN, for example, the unique gas chromatography (GC) fingerprinting of saccharides,[61-63] and the high-performance liquid chromatography (HPLC) fingerprinting of amino acids.[64-65] Any adulteration with other constituents can be determined by comparing with the standard. However, this method is destructive and time-consuming, and the adulterant needs to be present in a substantial amount for the detection.

Enzyme-linked immunosorbent assay (ELISA) is developed to differentiate EBN sample. It is used to detect the sialoglycoproteins in EBN,[38, 66] or the presence of a particular type of adulterant.[36, 67] Similarly, molecular genetic identification or deoxyribonucleic acid (DNA)-based methods have also been applied on EBN after the successful extraction of DNA

in EBN.[68] The DNA profile is used to establish the phylogenetic tree of EBN which demonstrates the genetic origin of EBN sample,[69-70] and it is used to authenticate EBN from its counterfeits and the adulterants.[70-72] However, non-biological adulterants that do not contain DNA can evade the detection easily.

Spectroscopic method, such as Fourier-transform infrared (FTIR) spectroscopy is used to ascertain the presence of adulterants by comparing the absorption bands around the fingerprint regions.[73-75] However, the interpretation of the FTIR spectrum is often hindered by the presence of moisture in the hygroscopic EBN cement, and the FTIR spectrometer might not be sensitive enough to detect adulterants added in a tiny amount.

Despite the vast variability of the analytical method used to detect adulterants, the absolute quality of EBN cannot be thoroughly evaluated as all the methods have their limitation. Moreover, no official regulatory protocol has been established for the authentication or quality surveillance of EBN products till now. Therefore, consumers or dealers have experienced an urgent need to identify the purity of EBN as there is an increasing trend in illegal adulterated EBN products.

1.4.2 The scientific explanation for the red color of 'blood' nest

Apart from the common white EBN, EBN also exists in the much sought after yellow or red color. The molecular basis and chemistry behind the red color in the red EBN have intrigued the community for a long time, and numerous conjectures for the red color have been proposed. It was claimed to be from the blood spat by exhausted swiftlets during the nest building, and hence red EBN is commonly referred as "blood" nest. However, it was proved that red EBN does not contain any hemoglobin.[76] Following that, it was fabricated by Marcone[3] that the red EBN contains ovotransferrin, as the color of the "blood" nest is very similar to the

color of purified ovotransferrin in its iron complexed state whereas the white nest is similar in the color to non-iron complexed ovotransferrin.

Recently, But *et al.*[77] demonstrated that white EBN could be turned red by fumigating with vapors generated either from a solution of sodium nitrite in dilute hydrochloric acid or unwashed bird's droppings. It was then suggested that the color of the EBN profoundly relates to the prevalence of nitrite and nitrate.[76, 78] The determination of nitrite and nitrate content in red EBN was carried out by several groups after a high concentration of nitrite and nitrate content exceeding the legal limits was detected in the red EBN imported in China mainland and Hong Kong.[29, 79] This incident pressed the authorities to tighten the control on EBN products and leading to a significant trade reduction in the last decade. Through the studies,[76, 78-80] it was concluded that the reddening agent accounts for the contents of nitrites and nitrate in red EBN as EBN with darker and redder color generally have higher nitrite and nitrate contents than the brighter and whiter EBN.

However, no conclusive evidence has been reported on the underlying chemistry on how the nitrite and nitrate bind to EBN and no molecular based explanation on the origin of yellow or red EBN can be found in the literature. The color-changing principle has remained elusive for this ethnomedicinal commodity. Hence, more efforts are needed to shed light on this mystery that has mystified the Chinese community for centuries.

1.5 Motivations and aims of the study

Since the composition, chemical and physical properties of EBN are still unclear, the characteristics of EBN should be extensively investigated with different techniques to improve our understanding of this natural product so that chemical synthesis might be possible in the future. In addition, the comprehension of the nature of EBN can also address the problem of EBN adulteration. It is perceptible that the industry is in urgent need of a tool to detect the

adulteration of EBN. However, most of the current analytical tools for the authentication of EBN are either time-consuming, destructive, require large sample size or specialized personnel. Therefore, new methods with the advantages such as rapid experimental time, small sample size required, no pretreatment needed have to be proposed so that the procedure can be standardized, and more predictable and reproducible results can be achieved in various conditions.

On the other hand, the myth of the red color in the red EBNs has perpetuated for over centuries among Chinese communities. The majority of consumers believe in the legend which regards the red EBN as of higher nutritional and medicinal value, and hence it fetches a steep price than the white EBN. The chemical nature and mechanisms of the color change are to be studied so that we can offer some sound findings to refine the understanding of this gastronomic delicacy. Once the chemical explanation for the color change has been established, then the evaluation of the difference between the white, yellow, and red EBN is plausible. The study could bring public awareness regarding the difference of the nutritional and medicinal value between the more common white EBN and the rarer red EBN, so that the consumers will have better knowledge when selecting EBN products.

Therefore, in this thesis, we aim

1. to characterize the physical properties of EBN mucin glycoprotein with advanced analytical tools- Raman microspectroscopy, thermogravimetry (TG) and differential scanning calorimetry (DSC).
2. to explore the potential of Raman microspectroscopy as a rapid, non-invasive, moisture-insensitive, and label-free technique for studying the properties of EBN and detecting any adulterants which might be introduced into EBN.

3. to introduce TG and DSC as fast and straightforward techniques that require only a small sample size to authenticate and check for adulterants which might be present in EBN.
4. to elucidate the underlying chemistry of the reddening process of the EBN, account for the color of yellow and red EBN and refine consumer's understanding of this exquisite food material.

1.6 Organization of this thesis

In this thesis, the introductory first chapter gives a brief literature review of the origin, history, and the composition of EBN, and includes a conceptual overview of the key research questions of EBN, the motivations and the aims of the study.

We will characterize EBN and tackle the challenges of the authentication of EBN by the utilization of advanced analytical tools- Raman microspectroscopy and thermal analysis instruments in the second and third chapters. The second chapter will describe the characterization of the mucin glycoprotein of EBN and its adulterants with Raman microspectroscopy. We introduce the concept of classifying the common edible adulterants into two types: Type I adulterants and Type II adulterants. The Raman spectra of unadulterated EBN, various Type I adulterants and EBN sample adulterated with Type II adulterants are collected with Raman microspectrometer. The characteristics Raman lines of EBN and adulterants are assigned and tabulated for easy reference in the future. Using Raman microspectroscopy, the unique Raman spectrum of amorphous mucin glycoprotein in swiftlet edible birdnest is reported, and the ability to detect adulterants is assessed.

The third chapter will describe the thermal analysis methods for the rapid identification and authentication of EBN. The thermal properties of EBN are investigated, and the unique thermogravimetry (TG), differential thermogravimetry (DTG) and differential scanning calorimetry (DSC) are used for the identification and authentication of EBN. The thermal

decomposition characteristics of EBN are shown for the first time, which also include the detection of loosely-bound and tightly-bound moisture with DSC. The ability of these curves serving as an analytical reference standard to detect adulteration in EBN was also assessed.

The fourth chapter will describe the underlying chemistry of the origin of yellow or red EBNs that have mystified the Chinese community for centuries. The nitration of tyrosine in the mucin glycoprotein of EBN is the real cause of the red color. Conclusive evidence on the chemical nature and reddening mechanism is obtained from the detection and quantification of 3-nitrotyrosine residue in EBN by ELISA, the UV-Vis absorption spectra of red EBN as a function of pH being similar to 3-nitrotyrosine and the Raman spectrum of red EBN showing strong Raman nitro bands with 532 nm laser as the excitation source.

Lastly, the final chapter will give a broad overview of the conclusions of this thesis work, and the future scope is discussed.

1.7 References

1. Shah, S. W.; Aziz, N. A., Morphology of the lingual apparatus of the Swiftlet, Aerodramus fuciphagus (Aves, Apodiformes, Apodidae). *Journal of Microscopy and Ultrastructure* **2014,** *2* (2), 100-103.

2. Medway, L., The relation between the reproductive cycle, moult and changes in the sublingual salivary glands of the swiftlet Collocalia Maxima Kijme. *Proceedings of the Zoological Society of London* **1962,** *138* (2), 305-315.

3. Marcone, M. F., Characterization of the edible bird's nest the "Caviar of the East". *Food Research International* **2005,** *38* (10), 1125-1134.

4. Marcone, M. F., Origins and compositional analysis of novel foods: Kopi luwak coffee and bird's nest soup. In *Comprehensive Biotechnology (Second Edition)*, Academic Press: Burlington, 2011; pp 683-702.

5. Meng, G. K.; Kin, L. W.; Han, T. P.; Koe, D.; Keen Raymond, W. J., Size characterisation of edible bird nest impurities: a preliminary study. *Procedia Computer Science* **2017,** *112*, 1072-1081.

6. Lee, P., L. M. ; Clayton, D. H.; Griffiths, R.; Roderic, D. M. P., Does behavior reflect phylogeny in swiftlets (Aves: Apodidae)? a test using cytochrome b mitochondrial DNA sequences. *Proceedings of the National Academy of Sciences of the United States of America* **1996,** *93* (14), 7091-7096.

7. Wong, R. S. Y., Edible bird's nest: Food or medicine? *Chinese Journal of Integrative Medicine* **2013,** *19* (9), 643-649.

8. Koon, L. C.; Cranbrook, E., *Swiftlets of Borneo: Builders of edible nests*. Natural History Publication (Borneo) Sdn Bhd: 2002; p 1-171.

9. Mouse, O., Maps of Southeast Asia. 2015.

10. Chua, L. S.; Zukefli, S. N., A comprehensive review of edible bird nests and swiftlet farming. *Journal of Integrative Medicine* **2016,** *14* (6), 415-428.

11. Guo, C.-T.; Takahashi, T.; Bukawa, W.; Takahashi, N.; Yagi, H.; Kato, K.; Hidari, K. I. P. J.; Miyamoto, D.; Suzuki, T.; Suzuki, Y., Edible bird's nest extract inhibits influenza virus infection. *Antiviral Research* **2006,** *70* (3), 140-146.

12. Howe, C.; Lee, L. T.; Rose, H. M., Collocalia mucoid: a substrate for myxovirus neuraminidase. *Archives of Biochemistry and Biophysics* **1961,** *95* (3), 512-520.

13. Haghani, A.; Mehrbod, P.; Safi, N.; Kadir, F. A. i. A.; Omar, A. R.; Ideris, A., Edible bird's nest modulate intracellular molecular pathways of influenza A virus infected cells. *BMC Complementary and Alternative Medicine* **2017,** *17* (1), 22.

14. Hou, Z.; He, P.; Imam, M. U.; Qi, J.; Tang, S.; Song, C.; Ismail, M., Edible bird's nest prevents menopause-related memory and cognitive decline in rats via increased hippocampal sirtuin-1 expression. *Oxidative Medicine and Cellular Longevity* **2017,** *2017*, 8.

15. Xie, Y.; Zeng, H.; Huang, Z.; Xu, H.; Fan, Q.; Zhang, Y.; Zheng, B., Effect of maternal administration of edible bird's nest on the learning and memory abilities of suckling offspring in mice. *Neural Plasticity* **2018,** *2018*, 13.

16. Kong, Y. C.; Keung, W. M.; Yip, T. T.; Ko, K. M.; Tsao, S. W.; Ng, M. H., Evidence that epidermal growth factor is present in swiftlet's (Collocalia) nest. *Comparative Biochemistry and Physiology Part B: Comparative Biochemistry* **1987,** *87*.

17. Zainal Abidin, F.; Hui, C. K.; Luan, N. S.; Mohd Ramli, E. S.; Hun, L. T.; Abd, G. N., Effects of edible bird's nest (EBN) on cultured rabbit corneal keratocytes. *BMC Complement Altern Med* **2011,** *11*.

18. Roh, K.-B.; Lee, J.; Kim, Y.-S.; Park, J.; Kim, J.-H.; Lee, J.; Park, D., Mechanisms of edible bird's nest extract-induced proliferation of human adipose-derived stem cells. *Evidence-Based Complementary and Alternative Medicine* **2012,** *2012*, 11.

19. Hou, Z.; Imam, M. U.; Ismail, M.; Azmi, N. H.; Ismail, N.; Ideris, A.; Mahmud, R., Lactoferrin and ovotransferrin contribute toward antioxidative effects of edible bird's nest against hydrogen peroxide-induced oxidative stress in human SH-SY5Y cells. *Bioscience, Biotechnology, and Biochemistry* **2015,** *79* (10), 1570-1578.

20. Muhammad, N. N.; Babji, A. S.; Ayub, M. K., Antioxidative activities of hydrolysates from edible birds nest using enzymatic hydrolysis. *AIP Conference Proceedings* **2015,** *1678* (1), 050038.

21. Gan, S. H.; Ong, S. P.; Chin, N. L.; Law, C. L., Kinetic retention of sialic acid and antioxidants in Malaysian edible bird's nest during low-temperature drying. *Drying Technology* **2016**, 1-11.

22. Ghassem, M.; Arihara, K.; Mohammadi, S.; Sani, N. A.; Babji, A. S., Identification of two novel antioxidant peptides from edible bird's nest (Aerodramus fuciphagus) protein hydrolysates. *Food & Function* **2017,** *8* (5), 2046-2052.

23. Zhang, Y.; Imam, M. U.; Ismail, M., In vitro bioaccessibility and antioxidant properties of edible bird's nest following simulated human gastro-intestinal digestion. *BMC Complementary and Alternative Medicine* **2014,** *14*, 468.

24. Nurfatin, M. H.; Etty Syarmila, I. K.; Nur Aliah, D.; Zalifah, M. K.; Babji, A. S.; Ayob, M. K., Effect of enzymatic hydrolysis on Angiotensin converting enzyme (ACE) inhibitory activity in swiftlet saliva. *International Food Research Journal* **2016,** *23* (1), 141-146.

25. Zhang, Y.; Imam, M. U.; Ismail, M.; Ismail, N.; Hou, Z., Edible bird's nest attenuates procoagulation effects of high-fat diet in rats. *Drug Design, Development and Therapy* **2015,** *9*, 3951-3959.

26. Mohd Taib, S. H.; Abd Gani, S. S.; Ab Rahman, M. Z.; Basri, M.; Ismail, A.; Shamsudin, R., Formulation and process optimizations of nano-cosmeceuticals containing purified swiftlet nest. *RSC Advances* **2015,** *5* (53), 42322-42328.

27. Chan, G.; Wong, Z.; Lam, K.; Cheng, L.; Zhang, L.; Lin, H.; Dong, T.; Tsim, K., Edible bird's nest, an asian health food supplement, possesses skin lightening activities: Identification of N-acetylneuraminic acid as active ingredient. *Journal of Cosmetics, Dermatological Sciences and Applications* **2015,** *5* (4), 262-274.

28. Green, J. R., The edible bird's-nest, or nest of the Java swift (Collocalia Nidifica). *The Journal of Physiology* **1885,** *6* (1-2), 40-45.

29. Thorburn, C. C., The edible nest swiftlet industry in Southeast Asia: Capitalism meets commensalism. *Human Ecology* **2015,** *43* (1), 179-184.

30. Wang, C. C., The composition of Chinese edible bird's nest and the nature of their proteins. *Journal of Biological Chemistry* **1921,** *49* (2), 429-439.

31. Wang, C. C., The isolation and the nature of the amino sugar of chinese edible birds' nests. *Journal of Biological Chemistry* **1921,** *49* (2), 441-452.

32. Wieruszeski, J. M.; Michalski, J. C.; Montreuil, J.; Strecker, G.; Peter-Katalinic, J.; Egge, H.; van Halbeek, H.; Mutsaers, J. H.; Vliegenthart, J. F., Structure of the monosialyl oligosaccharides derived from salivary gland mucin glycoproteins of the Chinese swiftlet (genus Collocalia). Characterization of novel types of extended core structure, Gal beta(1----3)[GlcNAc beta(1----6)] GalNAc alpha(1----3)GalNAc(-ol), and of chain termination, [Gal alpha(1----4)]0-1[Gal beta(1----4)]2GlcNAc beta(1----.). *Journal of Biological Chemistry* **1987,** *262* (14), 6650-6657.

33. Franz-Georg, H.; Gerhard, U., Structural Studies on O- and N-Glycosidically Linked Carbohydrate Chains on Collocalia Mucin. In *Hoppe-Seyler´s Zeitschrift für physiologische Chemie*, 1984; Vol. 365, p 119.

34. Zhu, C.; Yong, W.; Xu, L., Methods to identify true edible bird's nest. *Chinese Journal of Food Hygiene* **2007,** *19* (31), 206-209.

35. Saengkrajang, W.; Matan, N.; Matan, N., Nutritional composition of the farmed edible bird's nest (Collocalia fuciphaga) in Thailand. *Journal of Food Composition and Analysis* **2013,** *31* (1), 41-45.

36. Tukiran, N. A.; Ismail, A.; Mustafa, S.; Hamid, M., Determination of porcine gelatin in edible bird's nest by competitive indirect ELISA based on anti-peptide polyclonal antibody. *Food Control* **2016,** *59*, 561-566.

37. Liu, X.; Lai, X.; Zhang, S.; Huang, X.; Lan, Q.; Li, Y.; Li, B.; Chen, W.; Zhang, Q.; Hong, D.; Yang, G., Proteomic Profile of Edible Bird's Nest Proteins. *Journal of Agricultural and Food Chemistry* **2012,** *60* (51), 12477-12481.

38. Zhang, S.; Lai, X.; Liu, X.; Li, Y.; Li, B.; Huang, X.; Zhang, Q.; Chen, W.; Lin, L.; Yang, G., Competitive enzyme-linked immunoassay for sialoglycoprotein of edible bird's nest in food and cosmetics. *Journal of Agricultural and Food Chemistry* **2012,** *60* (14), 3580-3585.

39. Wong, Z. C. F.; Chan, G. K. L.; Wu, L.; Lam, H. H. N.; Yao, P.; Dong, T. T. X.; Tsim, K. W. K., A comprehensive proteomics study on edible bird's nest using new monoclonal antibody approach and application in quality control. *Journal of Food Composition and Analysis* **2018,** *66*, 145-151.

40. Goh, D. L. M.; Chua, K. Y.; Chew, F. T.; Liang, R. C. M. Y.; Seow, T. K.; Ou, K. L.; Yi, F. C.; Lee, B. W., Immunochemical characterization of edible bird's nest allergens. *Journal of Allergy and Clinical Immunology* **2001,** *107* (6), 1082-1088.

41. Kong, H.-k.; Wong, K.-H.; Lo, S. C.-l., Identification of peptides released from hot water insoluble fraction of edible bird's nest under simulated gastro-intestinal conditions. *Food Research International* **2016,** *85*, 19-25.

42. Chua, Y. G.; Chan, S. H.; Bloodworth, B. C.; Li, S. F. Y.; Leong, L. P., Identification of edible bird's nest with amino acid and monosaccharide analysis. *Journal of Agricultural and Food Chemistry* **2015,** *63* (1), 279-289.

43. Ma, F.; Liu, D., Sketch of the edible bird's nest and its important bioactivities. *Food Research International* **2012,** *48* (2), 559-567.

44. Quek, M. C.; Chin, N. L.; Yusof, Y. A.; Law, C. L.; Tan, S. W., Characterization of edible bird's nest of different production, species and geographical origins using nutritional composition, physicochemical properties and antioxidant activities. *Food Research International* **2018,** *109*, 35-43.

45. Kakehi, K.; Susami, A.; Taga, A.; Suzuki, S.; Honda, S., High-performance capillary electrophoresis of O-glycosidically linked sialic acid-containing oligosaccharides in glycoproteins as their alditol derivatives with low-wavelength UV monitoring. *Journal of Chromatography A* **1994,** *680* (1), 209-215.

46. Yagi, H.; Yasukawa, N.; Yu, S.-Y.; Guo, C.-T.; Takahashi, N.; Takahashi, T.; Bukawa, W.; Suzuki, T.; Khoo, K.-H.; Suzuki, Y.; Kato, K., The expression of sialylated high-antennary N-glycans in edible bird's nest. *Carbohydrate Research* **2008,** *343* (8), 1373-1377.

47. Matsukawa, N.; Matsumoto, M.; Bukawa, W.; Chiji, H.; Nakayama, K.; Hara, H.; Tsukahara, T., Improvement of bone strength and dermal thickness due to dietary edible bird's nest extract in ovariectomized rats. *Bioscience, Biotechnology, and Biochemistry* **2011,** *75* (3), 590-592.

48. Nakagawa, H.; Hama, Y.; Sumi, T.; Li, S.-C.; Maskos, K.; Kalayanamitra, K.; Mizumoto, S.; Sugahara, K.; Li, Y.-T., Occurrence of a nonsulfated chondroitin proteoglycan in the dried saliva of Collocalia swiftlets (edible bird's-nest). *Glycobiology* **2007,** *17* (2), 157-164.

49. Kathan, R. H.; Weeks, D. I., Structure studies of Collocalia mucoid.1. Carbohydrate and amino acid composition. *Arch. Biochem. Biophys.* **1969,** *134*, 576.

50. Looi, Q. H.; Amin, H.; Aini, I.; Zuki, M.; Omar, A. R., De novo transcriptome analysis shows differential expression of genes in salivary glands of edible bird's nest producing swiftlets. *BMC Genomics* **2017,** *18* (1), 504.

51. Maru, I.; Ohnishi, J.; Ohta, Y.; Tsukada, Y., Why is sialic acid attracting interest now? complete enzymatic synthesis of sialic acid with N-acylglucosamine 2-epimerase. *Journal of Bioscience and Bioengineering* **2002,** *93* (3), 258-265.

52. Varki, A., Sialic acids in human health and disease. *Trends in molecular medicine* **2008,** *14* (8), 351-360.

53. Martin, J. E., A facile procedure for the isolation of N-acetylneuraminic acid from edible bird's-nest. *Carbohydr. Res.* **1977,** *56*, 423-425.

54. Shim, E. K. S.; Chandra, G. F.; Lee, S.-Y., Thermal analysis methods for the rapid identification and authentication of swiftlet (Aerodramus fuciphagus) edible bird's nest – a mucin glycoprotein. *Food Research International* **2017,** *95*, 9-18.

55. Huda, M. Z. N.; Zuki, A. B. Z.; Azhar, K.; Goh, Y. M.; Suhaimi, H.; Hazmi, A. J. A.; Zairi, M. S., Proximate, elemental and fatty acid analysis of pre-processed edible birds nest (Aerodramus fuciphagus): a comparison between regions and type of nest. *Journal of Food Technology* **2008,** *6* (1), 39-44.

56. Zhao, B.; Deng, X.-M.; Wang, L.-L.; Liu, J.; Lai, X.-P., Principal component analysis and cluster analysis of inorganic elements in edible bird's nest imported from Southeast Asia by ICP-MS. *Journal of Chinese Medicinal Materials* **2015,** *38* (4), 697-700.

57. Zainab, H.; Nur Hulwani, I.; J, S.; Kamarudin, H.; Othman, H.; Lee, B.-B., Nutritional properties of edible bird nest. *Journal of Asian Scientific Research* **2013,** *3* (6), 600-607.

58. Wong, C.-F.; Chan, G. K.-L.; Zhang, M.-L.; Yao, P.; Lin, H.-Q.; Dong, T. T.-X.; Li, G.; Lai, X.-P.; Tsim, K. W.-K., Characterization of edible bird's nest by peptide fingerprinting with principal component analysis. *Food Quality and Safety* **2017,** *1* (1), 83-92.

59. Shim, E. K. S.; Chandra, G. F.; Pedireddy, S.; Lee, S.-Y., Characterization of swiftlet edible bird nest, a mucin glycoprotein, and its adulterants by Raman microspectroscopy. *Journal of Food Science and Technology* **2016,** *53* (9), 3602-3608.

60. Lin, J.; Zhou, H.; Lai, X.-P., Application of stereoscopy on edible birds nest identification. *Journal of Chinese Medicinal Materials* **2006,** *29* (3), 219-221.

61. Yang, M.; Cheung, S.-H.; Li, S. C.; Cheung, H.-Y., Establishment of a holistic and scientific protocol for the authentication and quality assurance of edible bird's nest. *Food Chemistry* **2014,** *151*, 271-278.

62. Tung, C.-H.; Pan, J.-Q.; Chang, H.-M.; Chou, S.-S., Authentic determination of bird's nests by saccharides profile. *Journal of Food Drug Analysis* **2008,** *16* (4), 86-91.

63. Yu, Y.-Q.; Xue, L.; Wang, H.; Zhou, H.-X.; Zhu, X.-F.; Li, B.-S., Determination of edible bird's nest and its products by gas chromatography. *Journal of Chromatographic Science* **2000,** *38* (1), 27-32.

64. Ismail, A. M.; Amin, A.; Hashim, D. M.; Ismail, A., Using amino acids composition combined with principle component analysis to differentiate house and cave bird's nests. *Current Trends in Technology and Science* **2013,** *2* (6), 353-366.

65. Seow, E.-K.; Ibrahim, B.; Muhammad, S. A.; Lee, L. H.; Cheng, L.-H., Differentiation between house and cave edible bird's nests by chemometric analysis of amino acid composition data. *LWT - Food Science and Technology* **2015,** *65*, 428-435.

66. Zhang, S.; Lai, X.; Liu, X.; Li, Y.; Li, B.; Huang, X.; Zhang, Q.; Chen, W.; Lin, L.; Yang, G., Development of monoclonal antibodies and quantitative sandwich enzyme linked

immunosorbent assay for the characteristic sialoglycoprotein of edible bird's nest. *Journal of Immunoassay and Immunochemistry* **2013,** *34* (1), 49-60.

67. Tukiran, N. A.; Ismail, A.; Mustafa, S.; Hamid, M., Enzyme immunoassay for the detection of porcine gelatine in edible bird's nests. *Food Additives & Contaminants: Part A* **2015,** *32* (7), 1023-1028.

68. Wu, R.; Chen, Y.; Wu, Y.; Ge, Y., Comparison of DNA extraction methods from birds' nest. *Food and Fermentation Industries* **2008,** *34* (3), 33-36.

69. Lin, J.; Zhou, H.; Lai, X.; Hou, Y.; Xian, X.; Chen, J.; Wang, P.; Zhou, L.; Dong, Y., The DNA extraction method of edible bird's nest. In *Modernization of Traditional Chinese Medicine and Materia Medica-World Science and Technology*, University, H. K. B., Ed. Hong Kong,China, 2010.

70. Lin, J.-R.; Zhou, H.; Lai, X.-P.; Hou, Y.; Xian, X.-M.; Chen, J.-N.; Wang, P.-X.; Zhou, L.; Dong, Y., Genetic identification of edible birds' nest based on mitochondrial DNA sequences. *Food Research International* **2009,** *42* (8), 1053-1061.

71. Wu, Y.; Chen, Y.; Wang, B.; Bai, L.; han, W. r.; Ge, Y.; Yuan, F., Application of SYBRgreen PCR and 2DGE methods to authenticate edible bird's nest food. *Food Research International* **2010,** *43* (8), 2020-2026.

72. Guo, L.; Wu, Y.; Liu, M.; Wang, B.; Ge, Y.; Chen, Y., Authentication of Edible Bird's nests by TaqMan-based real-time PCR. *Food Control* **2014,** *44*, 220-226.

73. Set, J. *Fast, effective evaluation of edible bird nests using the handheld Agilent 4100 ExoScan FTIR.*; Agilent Technologies.: Petaling Jaya, 2012.

74. Zainab, H., Prof. Madya Dr., *A rapid technique to determine purity of edible bird nest*. AENSI Publisher: 2014.

75. Deng, Y.; Sun, S.; Zhou, Q.; Li, A., Analysis of edible bird's nest quality with FTIR spectrocopy *Spectroscopy and Spectral Analysis* **2006,** *7*, 1242-1245.

76. Paydar, M.; Wong, Y. L.; Wong, W. F.; Hamdi, O. A. A.; Kadir, N. A.; Looi, C. Y., Prevalence of nitrite and nitrate contents and its effect on edible bird nest's color. *Journal of Food Science* **2013,** *78* (12), T1940-T1947.

77. But, P. P.-H.; Jiang, R.-W.; Shaw, P.-C., Edible bird's nests—How do the red ones get red? *Journal of Ethnopharmacology* **2013,** *145* (1), 378-380.

78. Quek, M. C.; Chin, N. L.; Yusof, Y. A.; Tan, S. W.; Law, C. L., Preliminary nitrite, nitrate and colour analysis of Malaysian edible bird's nest. *Information Processing in Agriculture* **2015,** *2* (1), 1-5.

79. Chan, G. K. L.; Zhu, K. Y.; Chou, D. J. Y.; Guo, A. J. Y.; Dong, T. T. X.; Tsim, K. W. K., Surveillance of nitrite level in cubilose: Evaluation of removal method and proposed origin of contamination. *Food Control* **2013,** *34* (2), 637-644.

80. Gan, S. H.; Ong, S. P.; Chin, N. L.; Law, C. L., Color changes, nitrite content, and rehydration capacity of edible bird's nest by advanced drying method. *Drying Technology* **2016,** *34* (11), 1330-1342.

Chapter 2 Characterization of Swiftlet Edible Bird Nest, a Mucin Glycoprotein, and its Adulterants by Raman Microspectroscopy

Abstract

Edible bird's nest (EBN) is made from the glutinous salivary secretion of highly concentrated mucin glycoprotein by swiftlets (genus *Aerodramus* or *Collocalia*) native to the Indo-Pacific region. The unique Raman spectrum of EBN has vibrational lines that can be assigned to peptides and saccharides in the glycoprotein, and it can be used to screen for adulteration. The common edible adulterants are here classified into two types. Type I adulterants, such as fish bladder, pork skin, karaya gum, coralline seaweed, agar strips, and tremella fungus, are solids which adhere *externally* on the surface of the EBN cement. They can usually be detected with a microscope based on differences in the surface structure. Type II adulterants are water-soluble substances such as saccharides (e.g. glucose, sucrose), polypeptides (e.g. hydrolyzed collagen) and salts (e.g. monosodium glutamate) which can be readily soaked up by the EBN hydrogel when moist and adsorbed *internally* in the EBN cement matrix forming a composite upon drying, making them difficult to detect visually. We show that Raman microspectroscopy offers a rapid, non-invasive, and label-free technique to detect both Type I and II adulterants in EBN.

2.1 Introduction

Raw white edible bird's nest (EBN), also known as cubilose or nest cement, is a relatively strong, hardened, amorphous composite material made mainly of dried strands of mucin glycoprotein, secreted by male swiftlets of genus *Aerodramus* or *Collocalia* during the nesting and breeding season from a pair of sublingual glands under the tongue. The strands are bound together with feathers and occasionally impregnated with tiny sand grains regurgitated from the birds gizzard, making a strong composite material to bear the weight of the nestlings. These swiftlets are native to the Indo-Pacific region and commonly found in South-East Asian countries, predominantly in Indonesia, Malaysia, Thailand, and Vietnam. The raw EBN, carefully cleaned of feathers, sand grains, etc., by soaking and picking of impurities with tweezers, besides being a Chinese food delicacy, has been a part of traditional Chinese medicine for more than 1000 years, and is reputed to have nutritional and medicinal properties.[1-3]

Analysis of EBN using modern chemical methods can be traced back to 1921 where it was shown that EBN is a mucin glycoprotein with properties of both carbohydrate and protein.[4] Structurally, a glycoprotein is a dendritic polymer, like a bottle brush, with a polypeptide backbone and hundreds of polysaccharide chains attached to it by O- or N-glyosidic linkages, and has molecular weight of 40-130 kDa.[5] By proximate analysis on EBN,[6] it was found that the protein portion constitutes ~ 62% by weight and is made up of 17 types of amino acids, with serine, valine, isoleucine, tyrosine, aspartic acid and asparagine as the major components, but with an absence of proline and two essential amino acids - tryptophan and cysteine. The carbohydrate portion makes up ~28% by weight, and the major saccharides are sialic acid (N-acetylneuraminic acid), galactose, N-acetylgalactosamine, N-acetylglucosamine, fucose, and mannose. The rest are moisture (~ 8%), ash/minerals (~ 2%), and fat (< 1%).

A kilogram of the cleaned white EBN retails for more than US$3,000 per kg today as the supply is limited due to the labor-intensive manual cleaning process, increasing labor cost, and high demand for EBN especially in China with growing affluence among the population. Given a global output of about a million kg per year, this translates to a trade worth US$1.5 billion per year. The high price of EBN is an inducement for EBN processors to adulterate it to increase profits. Consumers and retailers often rely on sight and smell to try to pick out the genuine EBN. It is often difficult to detect adulterated EBN by such simple (macroscopic) physical means, especially when the adulteration level is no more than 10% by weight. An official or standard method has yet to be found for the authentication and quality surveillance of EBN.

Various physical, analytical and chemical techniques have been designed to check for the presence of adulterants in EBN. The authentication techniques so far can generally be classified under: microscopy,[6-7] chromatography,[8-9] spectroscopy,[6, 10] enzymatic and genomic methods,[7, 11] and qualitative analysis.[6] However, most of the techniques are invasive, require tedious sample preparation, slow and generally not easy to use.

We can divide the edible adulterants in EBN into two types: (a) **Type I adulterants** are solid substances with similar appearance and can be adhered *externally* to the EBN cement. (b) **Type II adulterants** are incorporated *internally* into the EBN cement matrix, and not yet discussed in the literature. They are water-soluble substances that can be absorbed by the moist EBN hydrogel and are embedded in the EBN cement to form a composite upon drying. The hydrogel character of EBN arises from the presence of hydrophilic polysaccharides in the glycoprotein polymer, and the EBN cement can soak up about five times its weight of moisture at room temperature. Based on the EBN mucin glycoprotein structure, adulterants can be carbohydrates, proteins, other glycoproteins, or salts. Typical Type I adulterants are solid polysaccharides (karaya gum, *tremella fungus*, coralline seaweed, agar strips) and polypeptides

(fish bladder, pork skin), while the common Type II adulterants are water-soluble saccharides (e.g. glucose, sucrose), polypeptides (e.g. hydrolyzed marine collagen), and salts (e.g. monosodium glutamate).

Edible adulterants are incorporated into the cleaned EBN to increase its weight, and Type I adulterants may be introduced by up to 10% in weight to evade detection with the naked eye. Type I adulterants which are external to the EBN cement, however, can be detected with a microscope due to differences in their surface structure. Type II adulterants which are embedded in the EBN cement are more covert and difficult to detect visually. More sophisticated techniques and tools are required to identify and detect Type II adulterants.

Spectroscopic methods can provide a simple, non-invasive and fast way to detect both Type I and II adulterants. Fourier transform-infrared (FT-IR) spectroscopy, an absorption technique, has been used for detecting Type I adulterants which can be picked out from the EBN by examining the bands of the adulterants in the fingerprint region. If the adulterants are embedded in the EBN cement in small amounts, as in the case of Type II adulterants, FT-IR might not be sensitive enough to detect the adulterants.

Raman spectroscopy is a scattering technique, complementary to absorption FT-IR, often able to give a richer vibrational spectrum with sharper lines due to differences in spectral selection rules. It is non-invasive, applicable to opaque samples, is not affected by moisture in the sample, but has yet to be employed as an authentication method of EBN. The frequencies of the Raman lines correspond to vibrational modes in a molecule, and each molecule has a distinct set of vibrational modes. The intensity of a Raman line is proportional to the concentration of the molecule present. Hence the vibrational fingerprint of both frequency and intensity in Raman spectroscopy is routinely used in the analysis to determine the kind of molecule and its concentration. Raman microspectroscopy, with spatial resolution of about

1μm, also has an advantage over FT-IR in being able to focus on tiny spots over various regions of the sample, and therefore it is a good tool to identify both Type I and II adulterants that may either be lumpy or uniformly distributed across the EBN cement. Raman spectroscopy has been used successfully in food analysis and in the study of various agricultural products.[12-14] The aim of this work is to investigate the potential of Raman microspectroscopy as a *rapid*, non-invasive, and label-free technique for studying EBN and detecting adulterants in EBN.

2.2 Materials and methods

2.2.1 Edible bird's nest (EBN) samples

Raw, white EBN samples produced by *Aerodramus fuciphagus* were obtained from bird houses in widely separated geographical locations in South-East Asia - Kuantan (West Malaysia), Kuching (East Malaysia), and Jakarta (Indonesia).

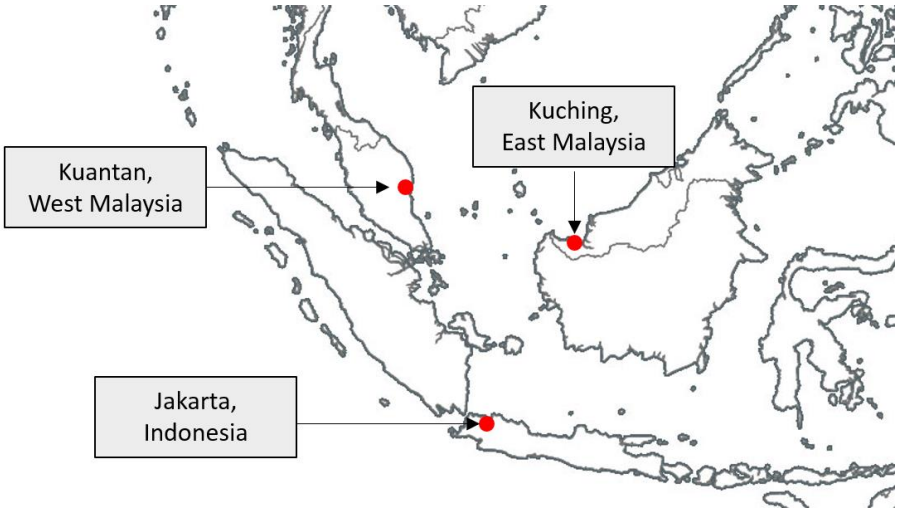

Figure 2.1 Map of South-East Asia showing the geographical locations of Kuantan (West Malaysia), Kuching (East Malaysia), and Jakarta (Indonesia).

2.2.2 Raman Microspectroscopy

Raman spectra were collected with the Nanophoton Inc. Ramantouch microspectrometer (Osaka, Japan) with a charge-coupled device (CCD) detector, using a

linearly polarized laser of 785 nm wavelength as an excitation laser, with a spectral grating of 600 gr/mm and an excitation power of 140 mW on the sample. A clear piece of EBN sample was placed on a silicon substrate glass slide, and the Raman spectrum was collected in the range 724-1800 cm^{-1}. 10 spots were examined for each EBN sample via simple random sampling technique and the spot was chosen from the smooth surface without any microscopic impurities.

The spectra were calibrated with the 520 cm^{-1} silicon peak. The excitation laser light was focused into a single spot on the sample through a cylindrical lens and an air objective lens (LU Plan Fluor 20x, numerical aperture (NA) 0.45). The back-scattered Raman signal from the spot-illuminated site was collected with the same objective lens. The exposure time for each spot was 60 s. The Origin Pro 8.0 software (Northampton, MA) was used to make the background correction, the intensities of the spectra were normalized with respect to the amide I band at 1671 cm^{-1}.

2.2.3 Adulterant samples

Tremella fungus, coralline seaweed, Japanese agar strips, fish bladder, pork skin, glucose, sucrose, and monosodium glutamate were purchased from grocery stores. Karaya gum and hydrolyzed marine collagen were purchased from suppliers of food chemicals and ingredients. Ultrapure water used in experiments was generated with the Merck Millipore ultrapure water system (Germany).

2.2.4 Uptake of Type II adulterants by EBN

About 1 g of EBN was carefully weighed and soaked overnight in 50 mL of 10% w/w aqueous solutions of glucose, sucrose, hydrolyzed marine collagen, and monosodium glutamate. The EBN samples were sieved, rinsed with ultrapure water and air-dried with fan to constant weight (about 3 days) at a room temperature of 24°C and under relative humidity

of about 50%, simulating conditions used by EBN processors. The samples were weighed to estimate the amount of adulterant that was absorbed by and embedded in the EBN cement. Five samples were prepared for each adulterant. Raman spectra were taken on the dried samples.

2.3 Results and Discussion

2.3.1 Raman spectra of EBN

The Raman spectra of the EBN samples from geographically different places – Kuantan (West Malaysia), Kuching (East Malaysia), and Jakarta (Indonesia) – are shown in Figure 2.2. They show identical vibrational bands in the fingerprint region, suggesting that they are generally made of the same material by the same species of swiftlets.

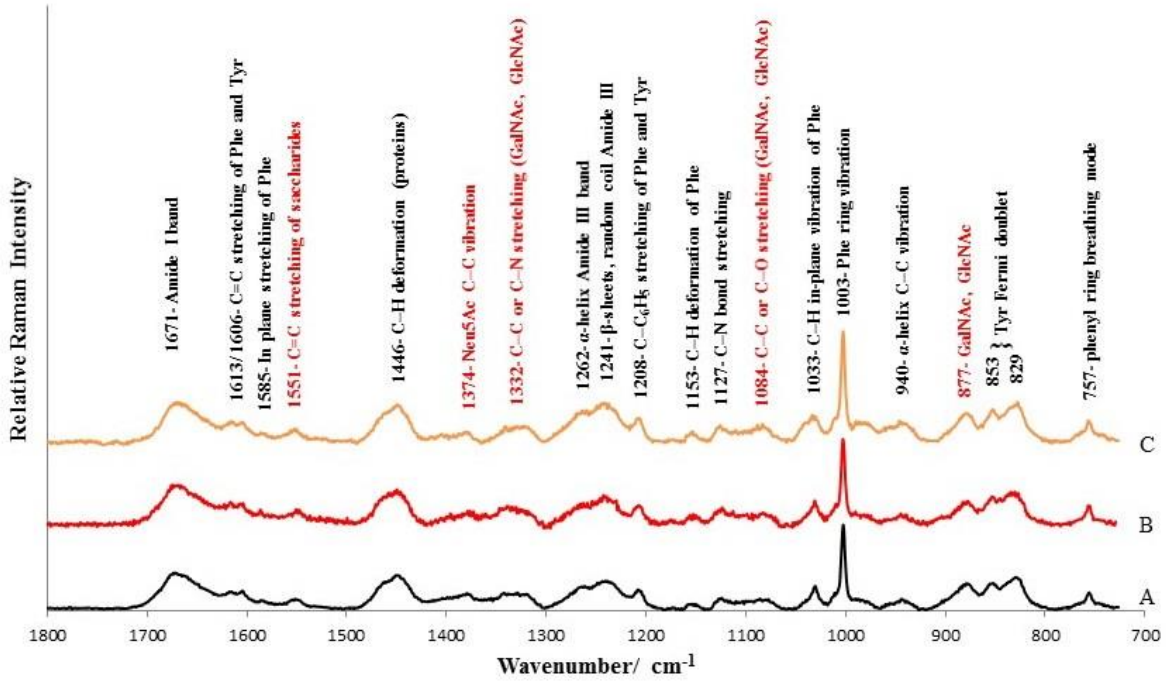

Figure 2.2 Unique Raman spectra of EBN samples collected from different geographical locations: A. Kuantan, West Malaysia (black line); B. Kuching, East Malaysia (red line); C. Jakarta, Indonesia (orange line). The band assignments attributed to peptides are shown in black, and those that are attributed to saccharides are shown in red.

Table 2.1 Assignment of vibrational lines in the EBN Raman spectrum.

Raman shift (cm^{-1})	**Contributor**	**Assignments**
1671(s)	Peptide	Amide I band
1613(m)	Peptide	C=C stretching of Phe and Tyr
1606(m)	Peptide	C=C stretching of Phe and Tyr
1585(w)	Peptide	In-plane stretching of Phe
1551(w)	Saccharide/Peptide	C=C stretching of saccharides, Amide II band
1446(s)	Peptide	C–H deformation (proteins)
1374(w)	Saccharide	Neu5Ac C–C vibration
1332(w)	Saccharide	C–C or C–N bond stretching (GalNAc, GlcNA)
1262(m)	Peptide	α-helix Amide III band
1241(s)	Peptide	β-sheets, random coil Amide III
1208(m)	Peptide	C- C_6H_5 stretching of Phe and Tyr
1153(w)	Peptide	C–H deformation of Phe
1127(w)	Peptide	C–N bond stretching (proteins)
1084(m)	Saccharide	C–C or C–O bond stretching (GalNAc, GlcNAc)
1033(s)	Peptide	C–H in-plane vibration of Phe
1003(vs)	Saccharide/Peptide	Neu5Ac C–C or C-N vibration , Phe ring vibration
940(w)	Peptide	α-helix C–C vibration
877(s)	Saccharide	GalNAc, GlcNAc
853(s)	Peptide	} Tyr Fermi doublet
829(s)	Peptide	
757(m)	Peptide	Phenyl ring breathing mode

The Raman lines, shown in Figure 2.2, were assigned using data for other glycoproteins,[15] soy protein isolate,[16] tyrosine,[17] collagens,[18] and N-acetylneuraminic acid, a

sialic acid.[19] The Raman spectrum of EBN clearly shows that it is a glycoprotein with vibrational lines of both peptides and saccharides. Table 2.1 gives a summary of the vibrational lines and assignments.

2.3.2 Type I adulterants

Although Type I adulterants, being solids with different surface structure from EBN, can be picked out using a microscope, Raman microspectroscopy offers a definitive way to identify Type I adulterants as each has a unique Raman spectrum different from that of genuine EBN. The Raman spectra of the common Type I adulterants – fish bladder and pork skin which are largely collagens (protein); karaya gum, coralline seaweed and Japanese agar which are polysaccharides; and tremella fungus which is largely a polysaccharide – in comparison to an unadulterated EBN sample are shown in Figure 2.3.

The fish bladder and pork skin would have the polypeptide amide lines, but generally lack the polysaccharide lines, and so they differ significantly from EBN in the 1300-1400 cm^{-1}, 1050-1150 cm^{-1}, and 800-980 cm^{-1} regions. There is also a relatively higher concentration of phenylalanine in EBN (intense 1003 cm^{-1} line) compared to the collagens. The karaya gum, coralline seaweed, and Japanese agar, being polysaccharides, lack the strong Amide I band at 1671 cm^{-1}, the strong C-H deformation of polypeptide band at 1446 cm^{-1}, and the strong phenylalanine ring vibration at 1003 cm^{-1} of EBN. The composition of tremella fungus is largely carbohydrate (78.3%) with a small amount of protein (6.6%) and crude fiber, and so the Raman spectrum would be more like that of the polysaccharides. The characteristic Raman bands of Type I adulterants are summarized in Table 2.2.

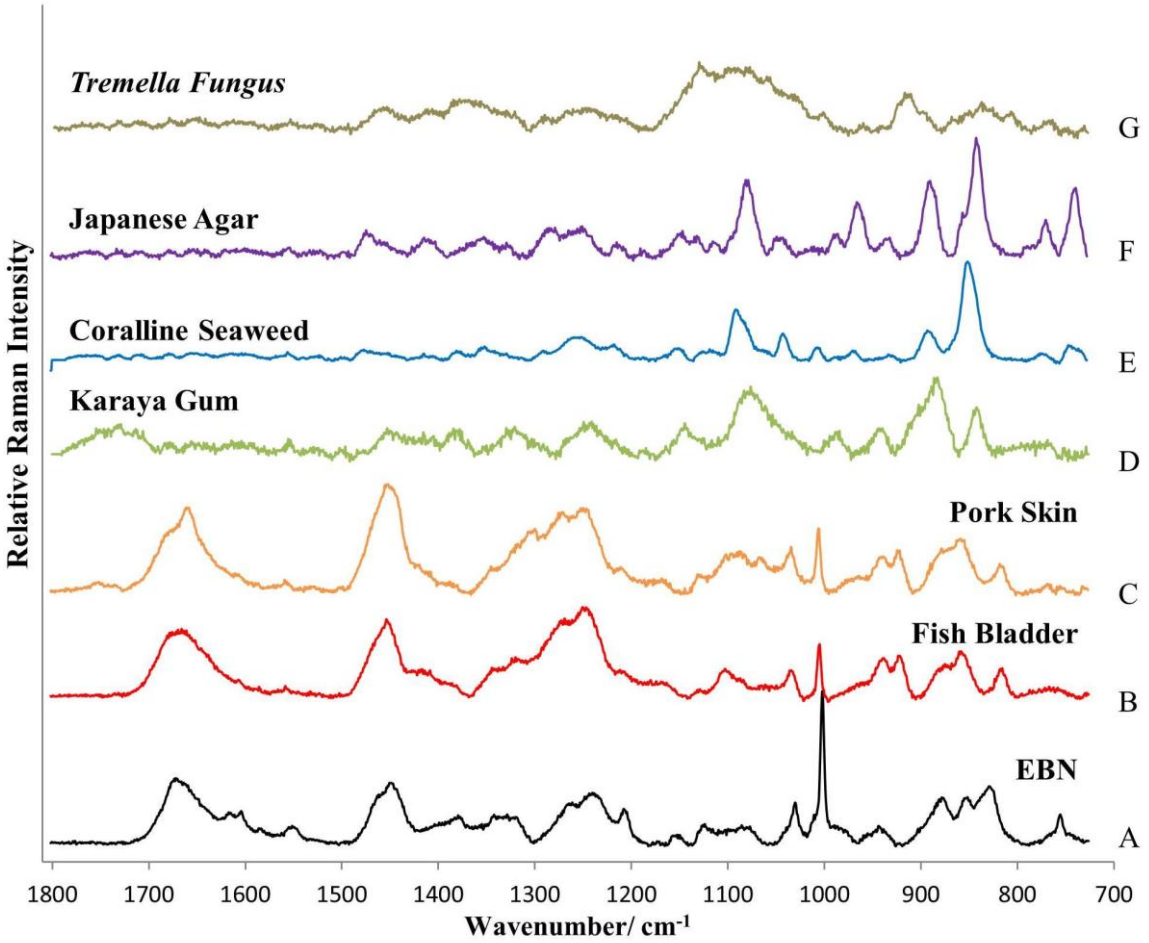

Figure 2.3 Raman spectra of common Type I adulterants compared to EBN: A. EBN from Kuantan (black line); B. Fish bladder (red line); C. Pork skin (orange line); D. Karaya gum (green line). E. Coralline seaweed (blue line); F. Japanese agar (purple line); G. Tremella fungus (brown line). Sample A is a glycoprotein; Samples B and C are collagens, i.e., proteins; while Samples D-G are largely polysaccharides.

Table 2.2 Characteristic Raman bands of common Type I adulterants

Type I adulterants	**Characteristic Raman band (cm^{-1})**
Fish bladder	1668(s), 1654(s), 1448(s), 1411(m), 1306(sh), 1263(sh), 1243(s), 1099(m), 1028(m), 1003(s), 933(m), 917(s), 874(m), 853(m)
Pork skin	1669(s), 1654(s), 1448(s), 1411(m), 1263(sh), 1240(s), 1094(m), 1028(m), 1001(s), 930(m), 917(m), 877(m), 851(m), 810(m)
Karaya gum	1729(m), 1446(m), 1377(m), 1318(m), 1240(m), 1147(m), 1070(s), 983(m), 989(m), 882(s), 840(s)
Coralline seaweed	1249(m), 1090(s), 1040(m), 889(m), 849(vs)
Japanese agar-agar	1471(m), 1079(s), 963(m), 890(s), 837(s), 770(m), 738(m)
Tremella fungus	1452(m), 1374(m), 1126 (s), 1087(s), 1074(s), 1056(m), 910(m)

2.3.3 Type II adulterants

Four common kinds of Type II adulterants are glucose, sucrose, (hydrolyzed marine) collagen, and monosodium glutamate (MSG). Fructose can also be a Type II adulterant, but it is not used because it can more readily undergo a Maillard reaction with the amino acids present in EBN, which may lead to undesirable coloration in the presence of heat. Type II adulterants in solution can be absorbed by the EBN hydrogel. EBN samples were soaked in the 10% w/w aqueous solutions of the adulterants overnight. It is useful to note that bottled EBN, a popular Asian tonic drink, would contain added sweeteners like sucrose and glucose, supplements like collagen, and taste enhancers like MSG. The EBN, acting as a hydrogel, absorbs about 5 times its weight of the solution and expands. The moist EBN was fan dried to constant weight as

described above, and the adulterant was left behind, adsorbed together with some water in the glycoprotein chains of the EBN cement to form an amorphous composite material. The average weight increases for five runs of each adulterant were as follows: glucose (34 ± 10%), sucrose (66 ± 15%), collagen (42 ± 10%), and MSG (26 ± 8%). Experiments were also carried out where the EBN was soaked in 5% w/w aqueous solutions of the adulterants overnight, and the average weight increases were about half that for the 10% w/w aqueous solutions. The weight increase is largely due to adsorbed adulterant, as can be shown by thermo-gravimetric analysis which will be reported in a future study. The adsorption of the adulterants in EBN by weight percentage shows the following order: sucrose > glucose ~ collagen > MSG. Or, generally, saccharides > peptides > salts, which can be explained by the structure of the EBN glycoprotein which has a polypeptide backbone with numerous polysaccharide chains attached to it and saccharides are more easily adsorbed on the exposed polysaccharide chains.

There was generally no observable change in physical appearance of the EBN strands after the absorption of the Type II adulterants, except for salts which may leave some shiny crystals on the surface of the EBN strands, as seen through the microscope of the Raman instrument. The Raman spectra of the adulterated EBN (blue line), the unadulterated EBN (black line), the difference spectrum between the adulterated and unadulterated EBN (red line), and the pure adulterant (green line), are shown in Figure 2.4. Clearly, the difference spectra (red line) show the main bands of the pure adulterants. The boxes in each figure show the regions where the Raman spectrum of the adulterated EBN differ from the unadulterated EBN, with new lineshapes, intensities, or new lines which are attributed to the additional Raman scattering by the adsorbed adulterant, and they are summarized in Table 2.3.

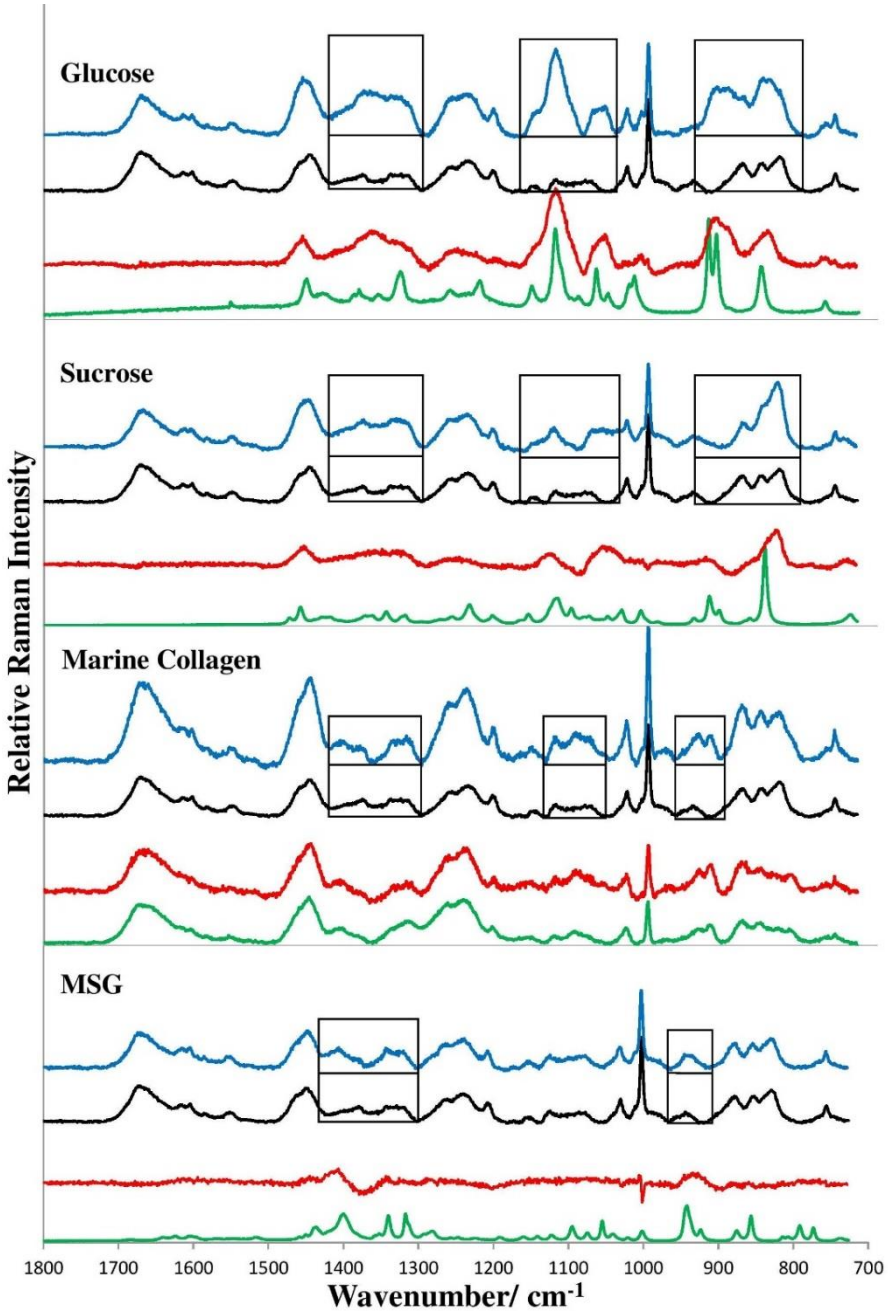

Figure 2.4 Comparison of Raman spectra of EBN adulterated with Type II adulterants (blue line) unadulterated EBN (black line), the difference spectra (red line) and the pure adulterant (green line). The adulterants, from top to bottom, are glucose, sucrose, hydrolyzed marine collagen and monosodium glutamate (MSG). The rectangular boxes show the spectral regions where the adulterated EBN differ from the unadulterated EBN in lineshape and intensity, and they are due to the additional Raman scattering of the adsorbed adulterant.

Table 2.3 Frequency ranges where the Raman spectra of adulterated EBN differ from the unadulterated EBN, and new Raman lines for the adulterated EBN.

Type (II) adulterants	**Frequency Ranges (cm^{-1}) where Raman spectra are significantly different from unadulterated EBN**	**New lines (cm^{-1})**
Glucose	1425-1300, 1160-1050, 925-780	1115(vs), 1060(m), 900(s), 825(s)
Sucrose	1425-1300, 1165-1050, 925-780	1135(m), 830(s)
Hydrolyzed Marine Collagen	1425-1300, 1130-1050, 960-890	1406(w), 1323(m), 1100(m), 920(m)
Monosodium glutamate (MSG)	1430-1300, 970-910	1410(m), 1341(m), 940(m)

Generally, new lines appear for the adulterated EBN in regions where the Raman bands for the pure adulterant are relatively strong. They may not occur exactly at the same frequencies as those in the pure adulterant, and the bands may also be broadened, indicating that physical adsorption and caging of the adulterant molecules has occurred forming a composite material with the amorphous EBN. The strong Raman intensity of the band at 1130 cm^{-1} for glucose and at 850 cm^{-1} for sucrose,[20-22] as seen in Figure 2.4, can be used for quantification of glucose and sucrose adsorbed in EBN, with the construction of a calibration curve as in a Beer-Lambert plot for absorbance vs concentration. Interestingly, the Raman spectrum of marine collagen, a common supplement taken for skin health, has many spectral similarities to EBN due to similar amino acid constituents, which would make it a choice adulterant. The Raman spectrum of

EBN+MSG also has many similarities to unadulterated EBN because there are no strong protein or saccharide bands in MSG. However, there are still frequency regions where the spectra of the EBN+adulterant differ sufficiently in lineshape and intensity from that of unadulterated EBN for collagen and MSG, as shown by the boxes in Figure 2.4.

A principal component analysis (PCA) of all the Raman spectra comprising the EBN+adulterant Raman spectra, for samples soaked in 5% and 10% w/w aqueous solutions of the adulterants, Raman spectrum of hydrolyzed marine collagen, and the unadulterated EBN Raman spectra from four different geographical regions, using the intensities of the Raman lines with frequencies listed in Tables 3.1 and 3.3, was carried out. From the PCA score plot (Figure 2.5), we can distinguish three clusters. One cluster for EBN adulterated with glucose and sucrose is due to the characteristic strong Raman bands at 1130 cm^{-1} (glucose) and 830 cm^{-1} (sucrose) arising from the CH out-of-plane deformation with the peptide bands of EBN relatively unchanged in frequency and intensity. A second cluster is for the EBN adulterated with marine collagen as the Raman spectrum for marine collagen lacks saccharides bands, while a third cluster is for the rest of the samples where the Raman bands for MSG are relatively weak and therefore the dominant Raman bands in EBN+MSG arise from EBN

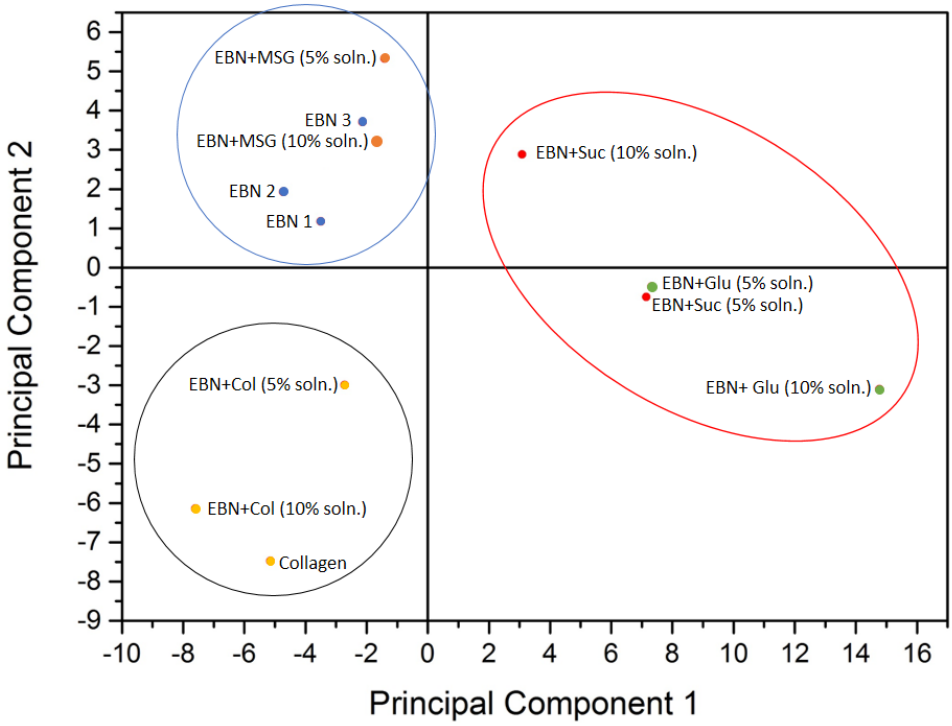

Figure 2.5 2-dimensional PCA score plot of all the Raman spectra comprising the EBN+Adulterant Raman spectra, for samples soaked in 5% and 10% w/w aqueous solutions of the adulterants, Raman spectrum of hydrolyzed marine collagen, and the unadulterated EBN Raman spectra from four different geographical regions.

2.4 Conclusion

We have categorized the common adulterants of EBN into Type I and II. Within each type, the adulterants may be largely saccharides or peptides. Type I adulterants which are external to the EBN cement can be detected with a microscope whereas water-soluble Type II adulterants are physically adsorbed into the EBN cement matrix to form a composite and so are not visible microscopically. We showed that Raman microspectroscopy provides a simple, fast, effective, and non-destructive way to analyze for both Type I and Type II adulterants with unique Raman spectra for the adulterated samples and the unadulterated EBN. It was also shown that saccharides (glucose, sucrose), peptides (hydrolyzed marine collagen), and salt (MSG) are physically adsorbed and embedded in the glycoprotein chains of the EBN. This

functionality of EBN as a hydrogel which can also adsorb drugs can be further explored in future as it could provide an edible and nutritious substrate for drug delivery. The present work demonstrates that Raman microspectroscopy is a powerful tool to provide direct information about the authenticity of EBN samples.

2.5 References

1. Vimala, B.; Hussain, H.; Nazaimoon, W. M. W., Effects of edible bird's nest on tumour necrosis factor-alpha secretion, nitric oxide production and cell viability of lipopolysaccharide-stimulated RAW 264.7 macrophages. *Food and Agricultural Immunology* **2012,** *23* (4), 303-314.

2. Guo, C.-T.; Takahashi, T.; Bukawa, W.; Takahashi, N.; Yagi, H.; Kato, K.; Hidari, K. I. P. J.; Miyamoto, D.; Suzuki, T.; Suzuki, Y., Edible bird's nest extract inhibits influenza virus infection. *Antiviral Research* **2006,** *70* (3), 140-146.

3. Haghani, A.; Mehrbod, P.; Safi, N.; Aminuddin, N. A.; Bahadoran, A.; Omar, A. R.; Ideris, A., In vitro and in vivo mechanism of immunomodulatory and antiviral activity of Edible Bird's Nest (EBN) against influenza A virus (IAV) infection. *Journal of Ethnopharmacology* **2016,** *185*, 327-340.

4. Wang, C. C., The composition of Chinese edible bird's nest and the nature of their proteins. *Journal of Biological Chemistry* **1921,** *49* (2), 429-439.

5. Wieruszeski, J. M.; Michalski, J. C.; Montreuil, J.; Strecker, G.; Peter-Katalinic, J.; Egge, H.; van Halbeek, H.; Mutsaers, J. H.; Vliegenthart, J. F., Structure of the monosialyl oligosaccharides derived from salivary gland mucin glycoproteins of the Chinese swiftlet (genus Collocalia). Characterization of novel types of extended core structure, Gal beta(1----3)[GlcNAc beta(1----6)] GalNAc alpha(1----3)GalNAc(-ol), and of chain termination, [Gal alpha(1----4)]0-1[Gal beta(1----4)]2GlcNAc beta(1----.). *Journal of Biological Chemistry* **1987,** *262* (14), 6650-6657.

6. Marcone, M. F., Characterization of the edible bird's nest the "Caviar of the East". *Food Research International* **2005,** *38* (10), 1125-1134.

7. Yang, M.; Cheung, S.-H.; Li, S. C.; Cheung, H.-Y., Establishment of a holistic and scientific protocol for the authentication and quality assurance of edible bird's nest. *Food Chemistry* **2014,** *151*, 271-278.

8. Chua, Y. G.; Chan, S. H.; Bloodworth, B. C.; Li, S. F. Y.; Leong, L. P., Identification of edible bird's nest with amino acid and monosaccharide analysis. *Journal of Agricultural and Food Chemistry* **2015,** *63* (1), 279-289.

9. Hun, L. T.; Wani, W. A.; Poh, H. Y.; Baig, U.; Ti Tjih, E. T.; Nashiruddin, N. I.; Ling, Y. E.; Aziz, R. A., Gel electrophoretic and liquid chromatographic methods for the identification and authentication of cave and house edible bird's nests from common adulterants. *Analytical Methods* **2016,** *8* (3), 526-536.

10. Ma, F.; Liu, D., Sketch of the edible bird's nest and its important bioactivities. *Food Research International* **2012,** *48* (2), 559-567.

11. Zhang, S.; Lai, X.; Liu, X.; Li, Y.; Li, B.; Huang, X.; Zhang, Q.; Chen, W.; Lin, L.; Yang, G., Development of Monoclonal Antibodies and Quantitative Sandwich Enxyme Linked Immunosorbent Assay for the Characteristic Sialoglycoprotein of Edible Bird's Nest. *Journal of Immunoassay and Immunochemistry* **2013,** *34* (1), 49-60.

12. Yang, D.; Ying, Y., Applications of Raman spectroscopy in agricultural products and food analysis: a review. *Applied Spectroscopy Reviews* **2011,** *46* (7), 539-560.

13. Martin, C.; Bruneel, J.-L.; Guyon, F.; Médina, B.; Jourdes, M.; Teissedre, P.-L.; Guillaume, F., Raman spectroscopy of white wines. *Food Chemistry* **2015,** *181*, 235-240.

14. Pereira, L.; Sousa, A.; Coelho, H.; Amado, A. M.; Ribeiro-Claro, P. J. A., Use of FTIR, FT-Raman and 13C-NMR spectroscopy for identification of some seaweed phycocolloids. *Biomolecular Engineering* **2003,** *20* (4–6), 223-228.

15. Ashton, L.; Pudney, P. D. A.; Blanch, E. W.; Yakubov, G. E., Understanding glycoprotein behaviours using Raman and Raman optical activity spectroscopies:

Characterising the entanglement induced conformational changes in oligosaccharide chains of mucin. *Advances in Colloid and Interface Science* **2013,** *199–200,* 66-77.

16. Herrero, A. M.; Jiménez-Colmenero, F.; Carmona, P., Elucidation of structural changes in soy protein isolate upon heating by Raman spectroscopy. *International Journal of Food Science & Technology* **2009,** *44* (4), 711-717.

17. Hernández, B.; Coïc, Y.-M.; Pflüger, F.; Kruglik, S. G.; Ghomi, M., All characteristic Raman markers of tyrosine and tyrosinate originate from phenol ring fundamental vibrations. *Journal of Raman Spectroscopy* **2016,** *47* (2), 210-220.

18. Nguyen, T. T.; Gobinet, C.; Feru, J.; -Pasco, S. B.; Manfait, M.; Piot, O., Characterization of type I and IV collagens by Raman microspectroscopy: Identification of spectral markers of the dermo-epidermal junction. *Spectroscopy: An International Journal* **2012,** *27* (5-6), 7.

19. Vinogradova, E.; Tlahuice-Flores, A.; Velazquez-Salazar, J. J.; Larios-Rodriguez, E.; Jose-Yacaman, M., Surface-enhanced Raman scattering of N-acetylneuraminic acid on silver nanoparticle surface. *Journal of Raman Spectroscopy* **2014,** *45* (9), 730-735.

20. Ilaslan, K.; Boyaci, I. H.; Topcu, A., Rapid analysis of glucose, fructose and sucrose contents of commercial soft drinks using Raman spectroscopy. *Food Control* **2015,** *48*, 56-61.

21. Mathlouthi, M.; Vinh Luu, D., Laser-Raman spectra of d-glucose and sucrose in aqueous solution. *Carbohydrate Research* **1980,** *81* (2), 203-212.

22. Söderholm, S.; Roos, Y. H.; Meinander, N.; Hotokka, M., Raman spectra of fructose and glucose in the amorphous and crystalline states. *Journal of Raman Spectroscopy* **1999,** *30* (11), 1009-1018.

Chapter 3 Thermal Analysis Methods for the Rapid Identification and Authentication of Swiftlet Edible Bird's Nest – a Mucin Glycoprotein

Abstract

Edible bird's nest of the swiftlet Aerodramus fuciphagus, is an unusual dried mucin glycoprotein, which has been used, particularly by Asians, as a premium food and wide spectrum health supplement for centuries. For the first time, thermogravimetry, differential thermogravimetry, and differential scanning calorimetry methods are used for the rapid identification and authentication of edible bird's nest. It is shown that edible bird's nest has a total moisture content of 12.6% which is removed below 200°C, followed by two major decomposition steps on heating under nitrogen gas. The first decomposition step (200-735°C) has a mass loss of 68.0% with maximum rate of mass loss at about 294°C, and the second decomposition step (735-1000°C) has a mass loss of 15.4% with maximum rate of mass loss at about 842°C, leaving a ceramic residue of about 4.0%. Differential scanning calorimetry shows that there are two kinds of bound water in edible bird's nest: (a) loosely bound water (about 7.5%) that dehydrates from edible bird's nest first, largely below 110°C, which can also be removed by lyophilization, and (b) tightly bound water (about 5.0%), still present in the edible bird's nest after lyophilization, that dehydrates from edible bird's nest between 100-200°C. The unique thermogravimetry and differential thermogravimetry curves of edible bird's nest serve as analytical standards and offer a simple, fast technique that requires only a small sample size (5- 10 mg) without the need for sample pretreatment to authenticate and check for edible adulterants which may be introduced into edible bird's nest with a profit motive.

3.1 Introduction

The raw, white edible bird's nest (EBN) of the swiftlet of genus *Aerodramus* or *Collocalia* fuciphaga is built from a viscous, sticky secretion of mucin glycoprotein from a pair of sublingual glands beneath the tongue of the swiftlet. The strands of mucin glycoprotein are interlaced with feathers to form a strong composite material when dried to carry the weight of the eggs or hatchlings and a pair of parent swiftlets. The swiftlet is native to South East Asia, and the EBNs are built on the vertical walls of caves and, in more recent times, in human-made bird houses.

The raw EBN is soaked in water to facilitate removal of feathers, wood chips, egg shells, and tiny sand grains with tweezers, before being sold as cleaned, dried nest cement. Cleaned EBN is coveted and one of the most expensive foods in Chinese cuisine, and for that reason, it has been termed "Caviar of the East" but it has no relation to fish eggs. It has been used as a health food in Chinese Medicine (CM) since the Tang dynasty (618-907 AD). EBN has about 10% by weight of sialic acid in the glycoprotein which could account for the many anecdotal health benefits associated with its consumption. One kg of the cleaned, dried EBN often retails for more than US$3,000 today due to market forces of supply and demand. The high demand of EBN globally, especially from China, Hong Kong, and Taiwan has given rise to a large market valued at billions of US dollars annually.

EBN has been shown to be a mucin glycoprotein, a biopolymer, having the properties of both carbohydrate and protein by chemical tests.[1] Structurally, the mucin glycoprotein is made up of a protein backbone with side chains of sugars, like a bottlebrush.[2] By proximate analysis, it has been reported that ~62% by weight of EBN is protein built from 17 types of amino acids, ~28% is carbohydrates/sugars, and the rest are moisture (~ 8%), ash/minerals (~ 2%), and fat (< 1%).[3]

The high cost of EBN is a temptation for unethical suppliers to introduce cheaper edible adulterants into the EBN to boost profits. We have recently shown that the adulterants can be classified into two types.[4] Type I adulterants are solids which are rendered to have a similar appearance to EBN cement by the naked eye, and can be adhered externally to the surface of the nest cement. They may be largely polysaccharides or polypeptides, e.g. coralline seaweed, tremella fungus, and agar which are polysaccharides; and fish bladder and pork rind which are largely polypeptides. Such adulterants tend to have a distinct difference in their microstructure from EBN and so that they can be detected with a microscope. On the other hand, Type II adulterants are water-soluble and can be absorbed by the EBN cement when it is soaked in the adulterant solution. They may be saccharides, polypeptides or salts, e.g. glucose and sucrose are saccharides, hydrolyzed marine collagen is a polypeptide, and monosodium glutamate is a salt. When the water is evaporated, the adulterants are incorporated into the EBN cement to form a new, uniform composite material. Such adulterated EBN has the same appearance as the unadulterated one under a microscope.

With the increasing occurrence of adulteration, there has been widespread interest in developing techniques to check for the quality and authenticity of EBN. Many physical, analytical and chemical techniques have been developed. For example, the microstructure of EBN fiber array was observed through microscopy and X-ray microanalysis,[3, 5] and the shape of EBN was inspected by imaging analysis and machine vision technology.[6] Separation techniques such as gas chromatography and liquid chromatography have been used to generate chromatographic metabolite mapping which reveals the composition of saccharides, amino acids and peptides to provide a chemical fingerprint for the EBN.[5, 7-9] Spectrophotometric methods (absorption and scattering spectroscopy) have been used to determine the sialic acid and protein content in EBN.[3, 10] Enzymatic and genomic methods can detect some of the specific compounds present in EBN and differentiate heterogeneous protein from adulterants.[5,

[11-13], and the use of qualitative analysis to provide information on its constituents.[3] Through the use of these techniques, authentication of EBN may be achievable. However, many of the techniques require expensive instrumentation, large sample sizes, and tedious sample preparation, and therefore may not be suitable for routine use.

EBN has not been studied before by thermal analysis. Thermogravimetry (TG) is a thermal analysis method in which changes in physical transition (to the gas phase) and chemical decomposition of a material is measured in terms of mass loss as a function of increasing temperature (with constant heating rate), as used here, or as a function of time in isothermal condition. TG and the corresponding differential thermogravimetry (DTG) have been useful for the study of complex materials like polymers and food substances.[14-18] Differential scanning calorimetry (DSC) technique is another appropriate thermal analysis method that measures the heat difference between sample and reference material to study thermo-physical transitions. It is has been used to study the thermal behavior of pharmaceutical and food systems to provide a predictive model for thermal stability with kinetic data,[19-23] and to detect adulteration in food products.[24-26] Both TG/DTG and DSC are useful tools for packaging materials and food characterization. They can provide rapid analysis with no sample pre-treatment and uses small quantities (5-10 mg). Here, we use thermal analysis by TG/DTG and DSC for the first time to study the thermal decomposition characteristics of EBN, the Type I adulterants, and new composite EBN incorporating Type II adulterants. The unique TG/DTG and DSC curves of EBN provide a reference to check for adulteration.

3.2 Materials and Methods

3.2.1 Edible bird's nest (EBN) and adulterant samples

Raw, white EBN samples produced by the species *Aerodramus fuciphagus* were obtained from bird houses from different geographical locations in South-East Asia: Port Dickson (West Malaysia), Lahad Datu (East Malaysia), and Pekan Baru (Indonesia).

Coralline seaweed, tremella fungus, agar, fish bladder, and pork rind were purchased from grocery stores. Glucose, sucrose, hydrolyzed marine collagen and monosodium glutamate were purchased from suppliers of food chemicals and ingredients. Ultrapure water (18.2 MΩ·cm) used in experiments was generated with the Merck Millipore ultrapure water system (Germany). The fish bladder and pork rind were cleaned of any remaining oil by soaking in warm water overnight, rinsed, and the moisture was squeezed out followed by air drying. Coralline seaweed and fish bladder were also bleached with 3% H_2O_2 solution for 30 min and air-dried to obtain a color to blend in better with EBN. All samples were kept at room temperature of 24°C and relative humidity of 50%.

3.2.2 Microscope

Carl Zeiss Stemi 305 Trino Greenough system with Stand K EDU and spot illuminator K LED a (Germany) was used to obtain the microscopic images of EBN and Type I adulterants. The images were captured and recorded with Carl Zeiss Microscopy Camera Axiocam 105 color and ZEN Lite software.

3.2.3 Thermogravimetric analysis (TGA)

TA Instruments Thermal Advantage Instruments TGAQ500 (New Castle, DE) and the Universal TA Instruments Analysis software were used in acquisition and processing of the curves. TA Instruments Platinum sample crucible (100 μL) was used as the sample container, and the nitrogen gas flux was set at 60.0 mL/ min to create a reproducible and dry atmosphere.

About 3.0 to 4.0 mg of crushed powder from each sample was accurately weighed and placed on the tared platinum crucible. The crucible was then heated from 30°C to 1000°C and 800°C for unadulterated and adulterated samples, respectively, at a heating rate of 15°C/ min.

The results were presented in curves of mass percentage versus temperature, TG curve, and the first derivative DTG curve which gave the rate of change of mass loss percentage (a positive number) versus temperature.

3.2.4 Differential Scanning Calorimetry (DSC)

Calorimetric measurements were performed with a TA Instruments DSCQ20 and the data processed with the same software used for TGA. The DSC profile was recorded as heat flow (W/g) versus temperature (°C). Calorimetric standards used for instrument calibration were indium and ultrapure water; 3.0-4.0 mg of powder form sample were sealed in a 40 μL aluminum Tzero pan and used for measurements. A purge flow (nitrogen gas) was maintained at 50 mL/min at all times. The standby temperature of the instrument was set at 40°C, and each sample was then cooled from 40°C to 0°C and equilibrated for 60 seconds prior to measurement. The ramping rate (heating or cooling) was set at 5°C/min. Triplicate analyses were carried out for each sample to ensure consistency in the results.

3.2.5 Uptake of Type II adulterants by EBN

Glucose, sucrose, hydrolyzed collagen, and MSG are water soluble and can be absorbed by the EBN cement. The adulterated EBN samples were prepared according to a recently reported procedure.[4] About 1 g (weighed accurately) of EBN was soaked overnight in 50 mL of 1%, 2%, 5% or 10% solution of various Type II adulterants. Triplicate samples were made for each concentration of adulterant solutions. The samples were fan-dried at room temperature and 50% relative humidity for four days and then used for thermal analysis.

3.2.6 Principal component analysis (PCA)

The principal component analysis was performed by using the OriginLab Origin 9.0 software (Northampton, MA). Principle component (PC) 1 is using as the horizontal coordinate and PC2 as the vertical coordinate to generate a score plot.

3.3 Results and discussion

3.3.1 TG and DTG

Similar TG and DTG curves of EBNs from different geographical origins were obtained as shown in Figure 3.1. Earlier, through the physical characterization of EBN by Raman microspectroscopy, it was shown that these EBNs also have a similar unique Raman spectrum indicative of a generally consistent biopolymer built of polysaccharides and polypeptides.[4] The observation of unique TG and DTG curves for EBN is consistent with that finding.

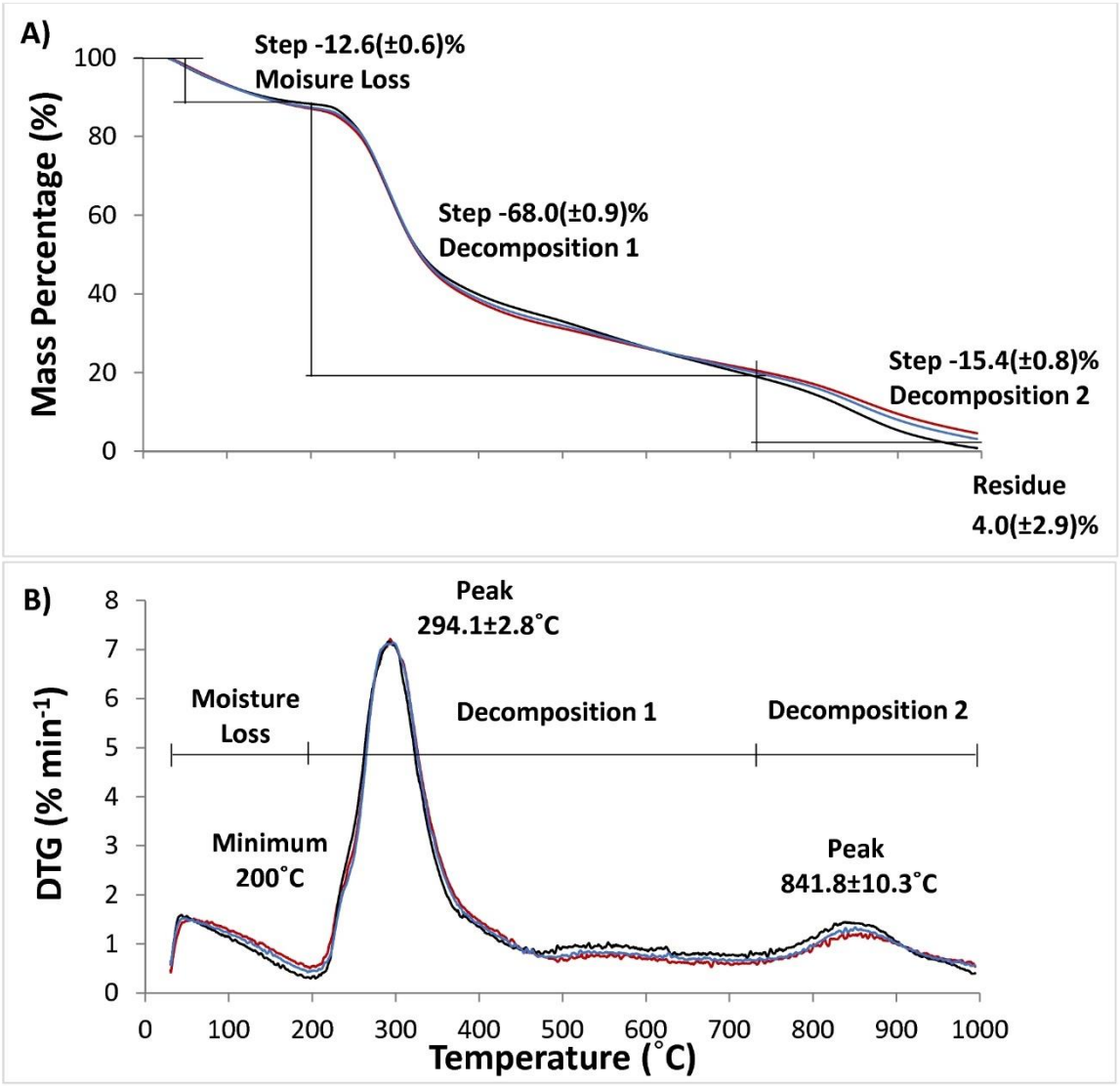

Figure 3.1 (A) Thermogravimetry (TG) curves, (B) Differential thermogravimetry (DTG) curves of EBN samples collected from different geographical locations: a. Port Dickson, West Malaysia (black line); b. Lahad Datu, East Malaysia (red line); c. Pekan Baru, Indonesia (blue line).

There are three main regions in the curve. The first region from 25-200°C corresponds to a physical dehydration of EBN. The DTG curve presents a minimum at 200°C and corresponds to a TG mass loss of 12.6(±0.6)% of moisture for raw EBN. By proximate analysis with drying to constant weight at 100°C, Marcone reported that (white) EBN contained 7.5% moisture.[3] Indeed, on the TG curve, the loss of moisture is about 7.5% at 100°C. As shown by

the DSC study below, this loss of moisture corresponds largely to the loosely bound water, but EBN also has tightly bound water and it would require heating to 200°C to remove both the loosely and tightly bound water.

After the complete loss of moisture at about 200°C and on further heating, the DTG curve shows that there are two major regions where the anhydrous EBN chemically degrades with significant mass loss. The first chemical decomposition region is from 200-735°C with a mass loss of 68.0(±0.9)%, and the DTG shows a maximum rate of mass loss at 294(±3)°C. The mass loss in this region is attributed to: (a) decarboxylation and bond breaking of the protein in the glycoprotein backbone which occurs at around 300°C, as is also seen in collagen,[27-28] and (b) breakdown of the dendritic polysaccharide chains in the glycoprotein into smaller fragments, releasing volatiles and resulting in mass loss. In addition, the reducing sugar molecules in the polysaccharide chains of the glycoprotein can undergo the Maillard reaction with the amino acids from the protein chain in the presence of heat, and the volatiles released through the Maillard reaction also contribute to the mass loss.

The second decomposition region is from 735-1000°C with a mass loss of 15.4(±0.8)%, and the maximum rate of mass loss is at 842(±10)°C. This high-temperature region would correspond to the complex decomposition of multicomponent inorganic oxides, nitrates, and carbonates [29-32]. Swiftlets are insectivores scooping up airborne flying insects and ingesting sand and mineral-rich water from a river for grinding their feed of insects in the gizzard, and these are primary sources of inorganic minerals in the EBN strands. Elemental analysis of EBN has shown the presence of calcium, sodium, magnesium, potassium, and iron ranging from tens to a thousand ppm.[3] Finally, at 1000°C, a ceramic ash of 4.0(±2.9)% was obtained.

The unique TG and DTG curves of unadulterated EBN can be used to check for adulterants which may be introduced into EBN with a profit motive. In particular, there will be major differences in the DTG curves between unadulterated and adulterated EBNs.

3.3.2 DSC

The DSC curves, Figures 3.2a-e, show that there are two kinds of bound water in EBN. Figure 3.2a is the DSC curve for raw EBN heated from 0-400°C. There is a broad endothermic band between 0-200°C associated with the physical loss of water, with a peak at about 83°C. This is followed by another endothermic band between 200-260°C, with a relatively sharp peak at 233°C which is due to the breakdown of the anhydrous EBN structure, akin to melting, with simultaneous chemical decomposition and volatilization. Subsequently, there's a broad endothermic band in the 260-400°C range within the first decomposition stage of EBN as seen in the TG curve in Figure 3.1.

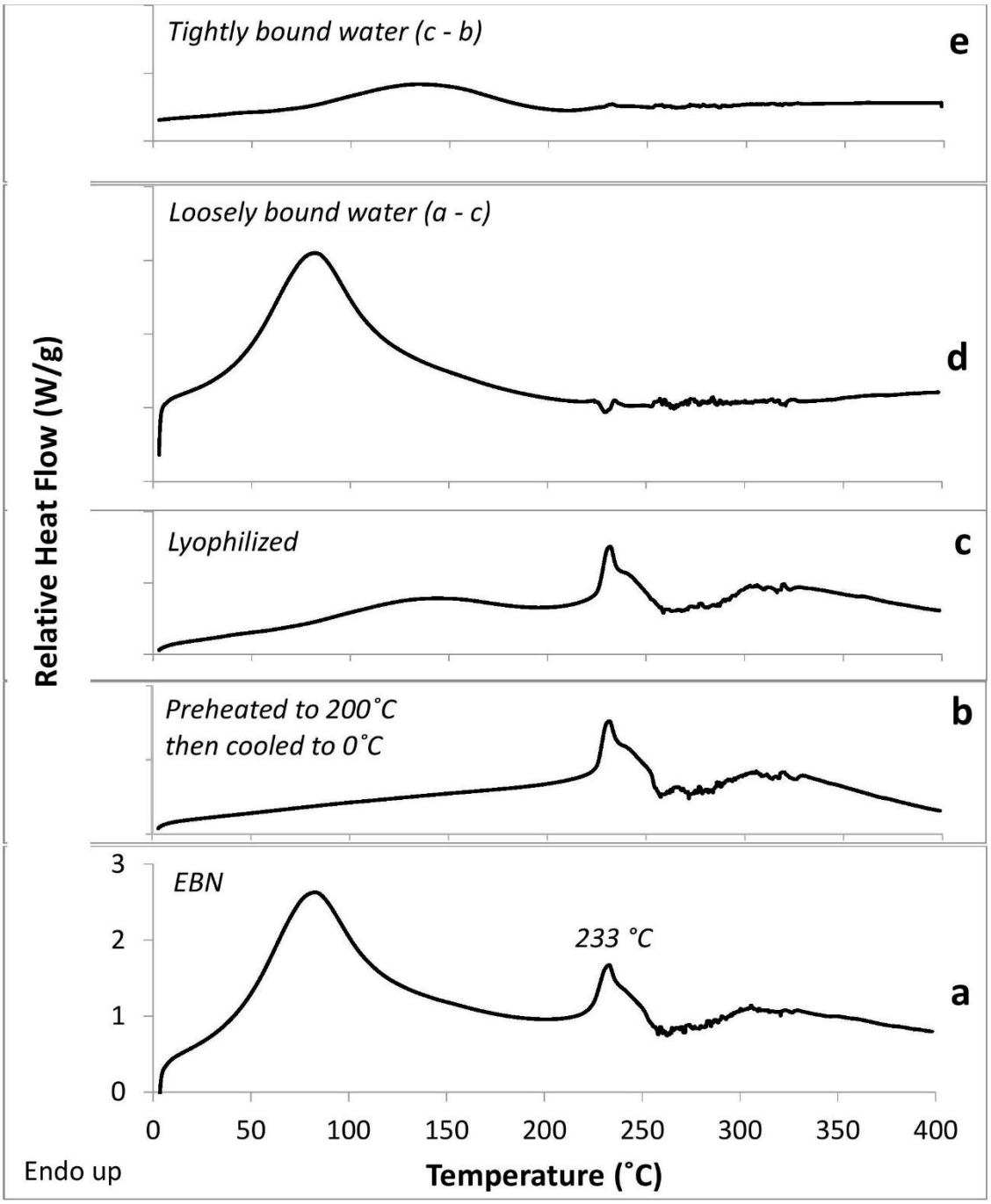

Figure 3.2 DSC curves of Port Dickson EBN samples: a. heating scan from 0°C to 400°C; b. sample was first heated to 200°C, then cooled to 0°C prior to heating scan from 0°C to 400°C; c. heating scan of a lyophilized sample from 0°C to 400°C; d. the difference curve (a – c), showing the loosely bound moisture of EBN; e. the difference curve (c – b), showing the tightly bound moisture of EBN.

Figures 3.2b-e uses DSC to shed more light on the bound water. For Figure 3.2b, the EBN was first heated to 200°C to remove the bound water, cooled to 0°C, and then DSC scanned from 0-400°C. Clearly, water has been removed as seen from the straight line in the DSC curve (0-200°C), and in the range of 200-400°C is identical to that of Figure 3.2a. For Figure 3.2c, the EBN was first lyophilized to remove the loosely bound water, before the DSC scan from 0-400°C. Here, we see that the lyophilization has removed the loosely bound water, leaving behind the more tightly bound water which appears in the range 83-200°C, whilst from 200-400°C it is identical to that of Figure 3.2a and 3.2b. The TG curve of lyophilized EBN sample showed that it has about 5% by weight of tightly bound water, which means that the raw EBN has roughly 1.5:1 ratio of loosely bound to tightly bound water molecules.

By subtracting the DSC curve in Figure 3.2c from Figure 3.2a, we obtain the bell-shaped DSC curve for the loosely bound water shown in Figure 3.2d, with an endothermic peak at 83°C. Similarly, by subtracting the DSC curve in Figure 3.2b from Figure 3.2c, we obtain the bell-shaped DSC curve for the tightly bound water, shown in Figure 3.2e, with a peak at 140°C. The loosely bound water would correspond to water molecules surrounding the glycoprotein polymer and in between polymer chains, while the tightly bound water would correspond to the water molecules strongly hydrogen bonded with the polysaccharides and polypeptides in the coils of the glycoprotein chain.

This phenomenon of loosely bound and tightly bound water should be quite prevalent in food materials. Here, it has implications for the wide use of hydrogen peroxide, as a bactericide and bleaching agent in the bird's nest cleaning industry. Some of the H_2O_2 may be tightly hydrogen bonded in the coils of the glycoprotein chains, just like the tightly bound water, and may remain trapped in the EBN on drying typically below 60°C, and this could present a food hazard. It may be necessary to heat dry the cleaned EBN at above 100°C to dislodge and

decompose the hydrogen peroxide, or to reduce it in the moist EBN with permitted reducing agents like ascorbic acid, or by enzymatic decomposition with catalase, before drying.

3.3.3 Edible Type I Adulterants in EBN

Edible Type I adulterants – coralline seaweed, tremella fungus, agar, fish bladder, pork rind - are solids which have some distinct differences in their surface structure that permit identification using a microscope. Coralline seaweed and fish bladder are naturally slightly pinkish red and yellow in color, respectively, but can be bleached with hydrogen peroxide (3% w/w) to obtain a translucent light-yellow color to blend in with the EBN strands when added as adulterants. The microscopic images of EBN and the Type I adulterants are shown in Figure 3.3.

EBN has translucent strands of 0.5-1 mm diameter and each strand is made up of a few layers. Coralline seaweed has jointed branches of thickness about 1 mm and is opaque. Tremella fungus is whitish yellow, frond-like, and opaque. Agar strands are made of transparent, crumpled, thin sheets. Fish bladder and pork rind have an uneven, bubbly surface. EBN and the Type I adulterants soften when moist and the adulterants can be adhered to the EBN as strips or pieces using gelatin or hydrolyzed collagen as glue.

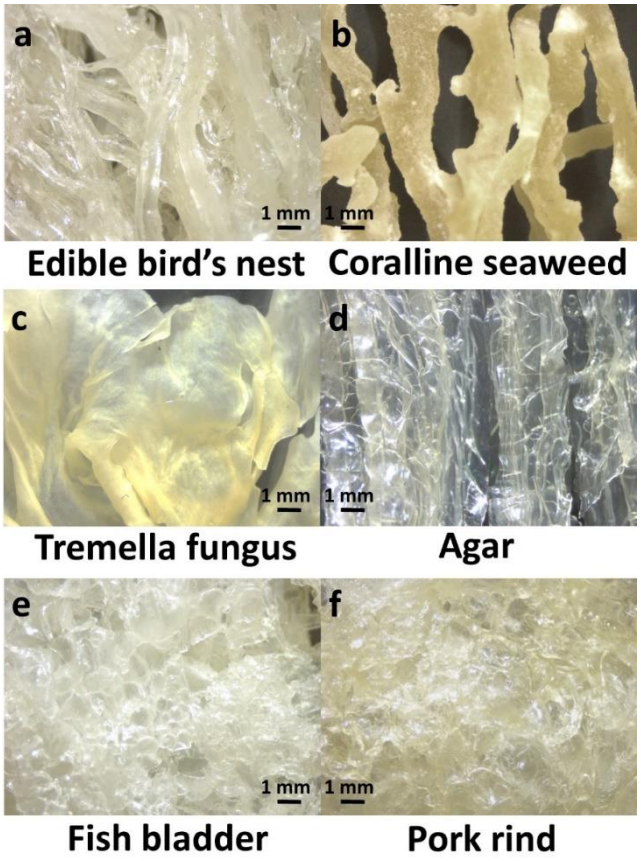

Figure 3.3 Microscopic images of EBN and Type I adulterants: a. EBN; b. Coralline seaweed; c. Tremella fungus; d. Agar; e. Fish bladder; f. Pork rind.

The TG and DTG curves of these commonly used Type I adulterants are shown in Figure 3.4. Clearly, the DTG band for each adulterant is unique and can be characterized by three parameters (temperature for the peak, peak height, and full width at half peak). Table 3.1 gives the unique set of parameters for the DTG bands of the adulterants in comparison with EBN. Coralline seaweed, tremella fungus, and agar are largely polysaccharides with the DTG maximum occurring at a lower temperature and overall a thinner band than that for fish bladder and pork rind which are largely polypeptides. It is also noted that agar shows two local maxima, with one of lower height than the other in the DTG curve. EBN being a glycoprotein has a temperature for the DTG maximum and a band width that falls between that of the polysaccharides and the polypeptides.

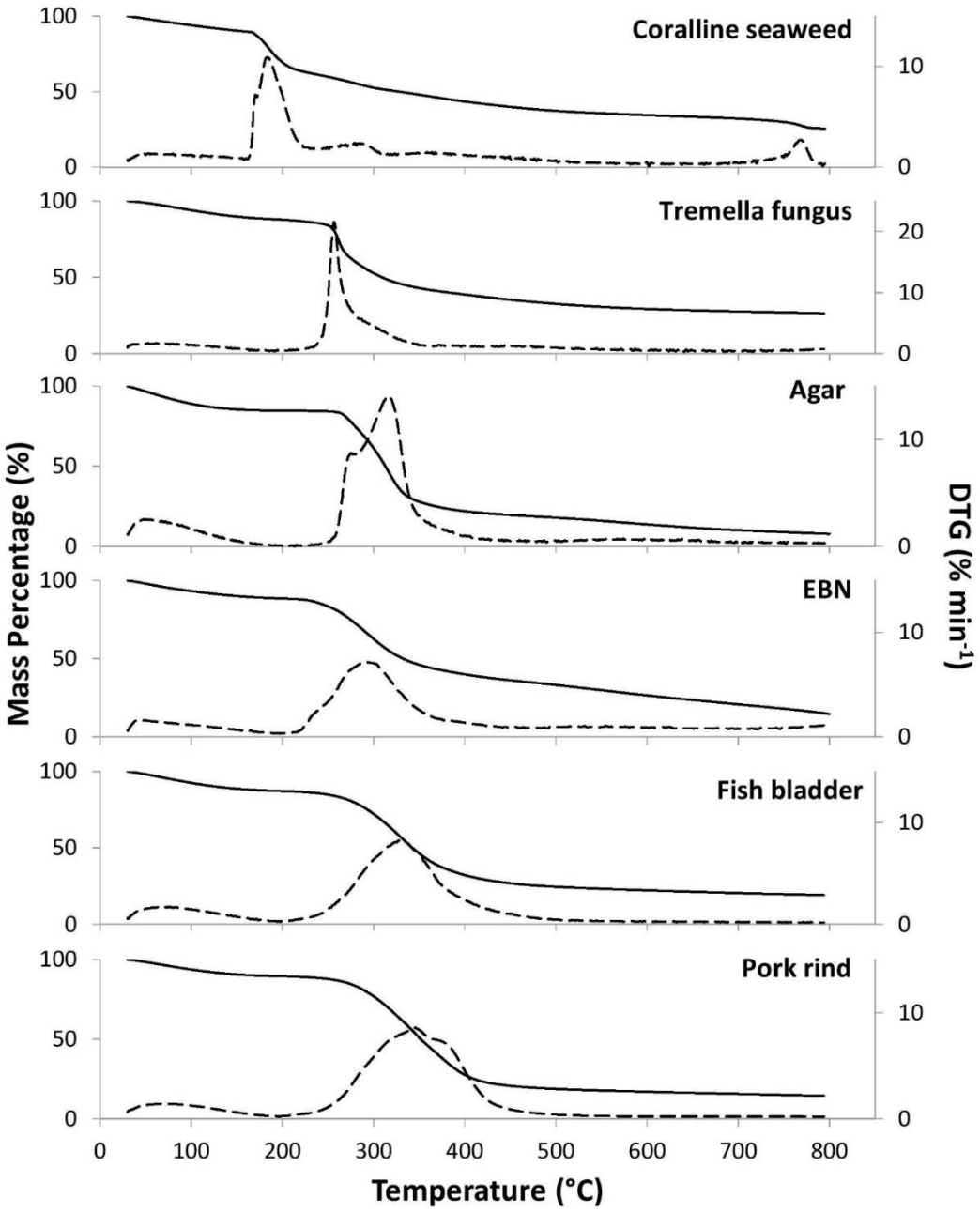

Figure 3.4 TG (solid line) and DTG (dashed line) curves of various Type I adulterants – Coralline seaweed, Tremella fungus, Agar, Fish bladder and Pork rind – versus unadulterated EBN. The DTG peaks for the polysaccharides – Coralline seaweed, Tremella fungus, and Agar – occur at a lower temperature than for EBN which is a glycoprotein, while those for the polypeptides – Fish bladder and Pork rind – occur at a higher temperature.

Table 3.1 Characterization parameters of DTG bands for Type I adulterants in comparison with unadulterated EBN.

Type I adulterant	Temperature of peak (°C)	Peak height (%/min)	Full-width at half peak (°C)
Coralline seaweed	182 ± 2	10.8 ± 0.1	33.7 ± 2.0
Tremella fungus	266 ± 1	22.4 ± 0.4	12.7 ± 0.9
Agar	275 ± 1, 316 ± 1	8.8 ± 0.2, 14.1 ± 0.1	64.0 ± 0.3
EBN	294 ± 3	7.2 ± 0.1	83.7 ± 1.6
Fish bladder	326 ± 3	8.5 ± 0.6	91.2 ± 4.0
Pork rind	344 ± 7	9.2 ± 0.2	105.5 ± 7.0

3.3.4 Composite of EBN with Edible Type II Adulterants

Type II adulterants are water soluble to give a transparent liquid which can be absorbed by the EBN, and on drying an amorphous composite material is obtained [4]. The common Type II adulterants are glucose, sucrose, hydrolyzed collagen and monosodium glutamate (MSG). Glucose and sucrose are also used as sweeteners in the cooking of EBN; hydrolyzed collagen is added as a health supplement; and MSG is a taste enhancer. The presence of type II adulterants cannot be detected with a microscope as they are embedded in the EBN matrix on drying without a change in physical appearance. However, TG and DTG in the temperature range of 25-500°C can be used to detect the presence of Type II adulterants.

For each sample of unadulterated EBN, we know the moisture content based on its TG/DTG curves and so we can calculate the amount of anhydrous EBN cement. After soaking in the adulterant solution and fan drying, the new weight will comprise moisture, adulterant,

and the same amount of anhydrous EBN cement. The amount of moisture is measured by TG/DTG, and we can thereby determine the amount of adulterant absorbed by the EBN cement. The average uptake of adulterants in the dried, composite EBN as a function of the concentration of adulterant solutions used are given in Table 3.2, and the results are plotted in Figure 3.5. The uptake of the saccharides – sugar and glucose – can be quite substantial, with as much as 41% and 32% w/w of sugar and glucose embedded in the dried composite EBN when soaked in 10% w/w of adulterant solutions. Similarly, for hydrolyzed collagen as much as 30% w/w of collagen is absorbed in the composite with EBN, and for MSG about 22% w/w of MSG is absorbed. There's a good linear correlation between the amount of adulterant absorbed, and the concentration of adulterant solution (up to 10% concentration) used to soak the EBN.

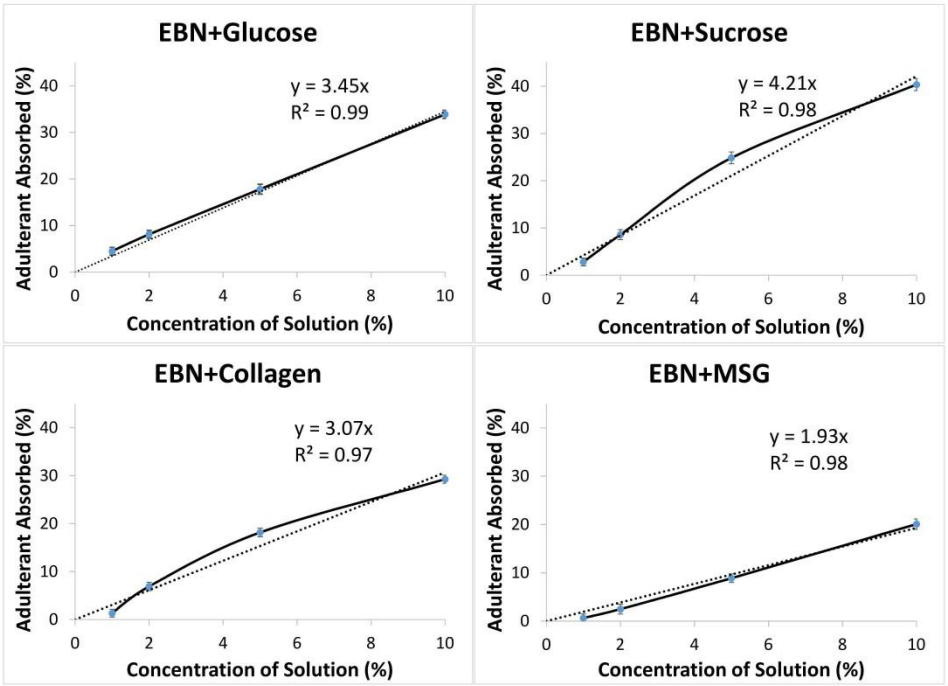

Figure 3.5 Graphs of the uptake of Type II adulterants by EBN versus concentration of adulterant solutions used in soaking. The plots are almost linear up to 10% concentration of soaking solutions.

Table 3.2 Mass percentage of moisture and Type II adulterants absorbed by EBN.

Type II adulterant	**Concentration (w/w) of Type II adulterant solution**	**Mass percentage of moisture in composite EBN by TG (%)**	**Mass percentage of adulterant absorbed by EBN (%)**
Glucose	1%	10.0 ± 0.2	4.5 ± 0.7
	2%	9.6 ± 0.2	8.1 ± 0.7
	5%	9.3 ± 0.7	17.8 ± 1.0
	10%	9.2 ± 0.3	33.9 ± 0.8
Sucrose	1%	9.9 ± 0.2	2.8 ± 0.7
	2%	9.0 ± 0.7	8.6 ± 1.0
	5%	7.8 ± 0.9	24.8 ± 1.2
	10%	6.1 ± 0.9	40.4 ± 1.2
Collagen	1%	10.1 ± 0.2	1.3 ± 0.7
	2%	10.3 ± 0.3	6.9 ± 0.8
	5%	10.7 ± 0.4	18.2 ± 0.8
	10%	11.1 ± 0.1	29.3 ± 0.7
Monosodium glutamate (MSG)	1%	10.2 ± 0.3	0.6 ± 0.7
	2%	10.0 ± 0.6	2.7 ± 0.9
	5%	10.6 ± 0.4	8.9 ± 0.8
	10%	10.0 ± 0.7	19.9 ± 1.0

The TG and DTG curves for the dried, composite EBN previously soaked in different concentrations of adulterant solutions - 1%, 2%, 5% and 10% w/w - in comparison with unadulterated EBN are shown in Figure 3.6. The DTG curves are presented as stack plots.

The trends in the TG and DTG curves for increasing concentration of adulterant solutions are quite similar in the case of EBN+Glucose and EBN+Sucrose. Both involve simple sugars absorbed in the EBN matrix. Each set of the TG curves shows a significant difference in mass loss in the temperature range of 170-330°C for increasing concentrations of adulterant solutions. The corresponding DTG curves show a peak around 190-220°C due to the melting and decomposition of the sugars and Maillard reactions with the protein (which occur at a fast pace at temperature above 180°C), and a corresponding decline in the band between 250-350°C due to a decrease in the weight percentage of proteins.[33-34]

Collagen is largely a protein, and since EBN has a high percentage of protein the TG curves for EBN+Collagen and EBN are rather similar up to about 320°C, but we note a general broadening of the DTG curves with increasing concentration of adulterant solutions. There is a slight increase in the new step at around 200-220°C due to melting and decomposition. For the salt MSG, the TG curves for EBN+MSG do not fan out as pronounced as those for EBN+Glucose and EBN+Sucrose in the temperature range of 200-300°C for the major decomposition step. The DTG curves show a new band at around 190-220°C due to melting and decomposition. There are ripples on the DTG curves in the temperature range 300-350°C, and the curves also broaden with increasing concentration of MSG solutions used. They can be attributed to the decomposition of dehydrated glutamate and pyroglutamate.[35]

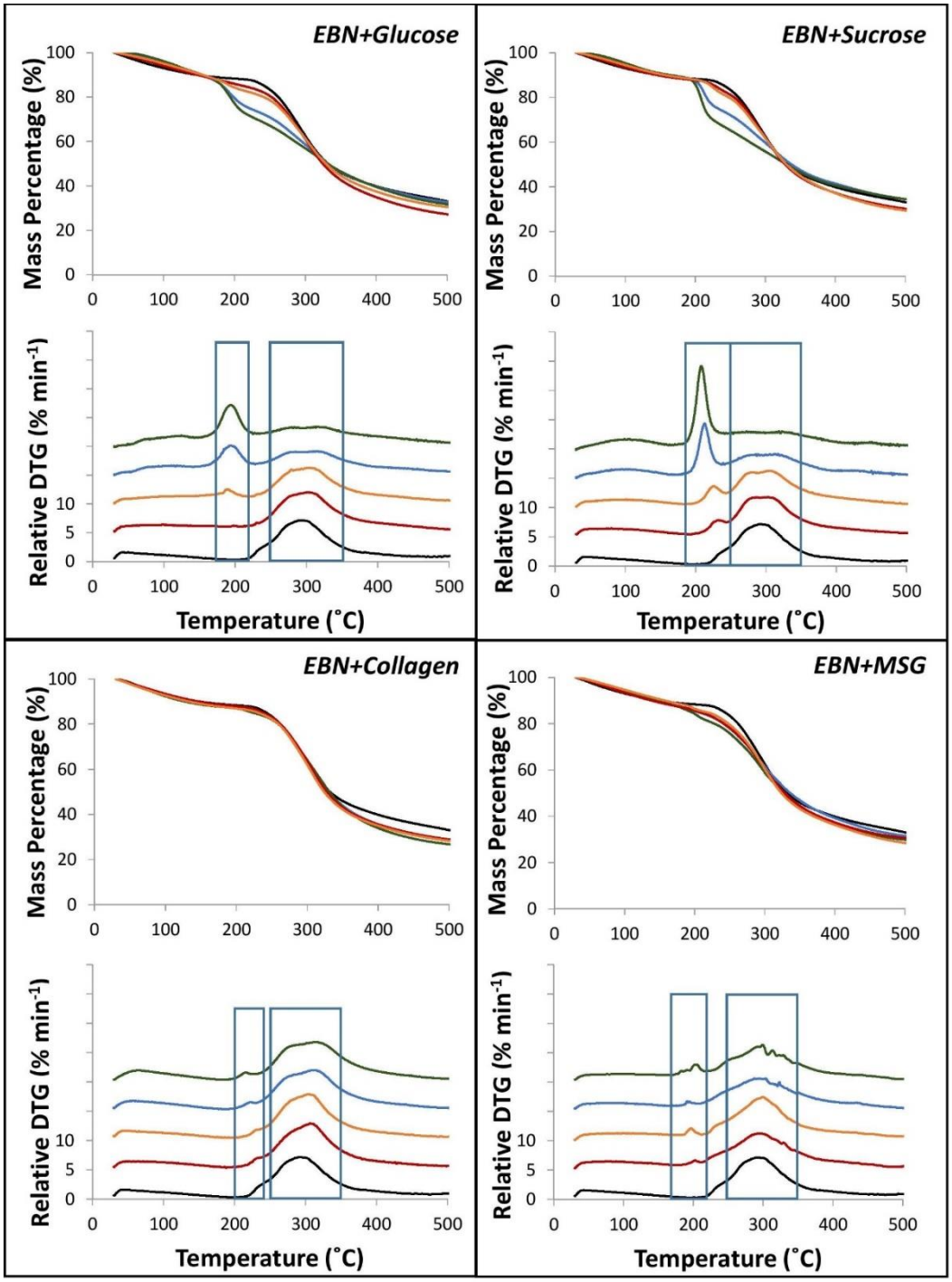

Figure 3.6 TG and DTG curves of EBN adulterated with Type II adulterants. Each subfigure corresponds to a Type II adulterant: adulterated EBN by soaking with 1% (red line), 2% (orange line); 5% (blue line) and 10% (green line) of Type II adulterant solutions. The comparison TG and DTG reference curves for unadulterated EBN are shown as black lines. The DTG curves are shown as stack plots, and the scale for the decomposition rate is for the unadulterated EBN.

The boxes in Figure 3.6 show the regions in the DTG curves where the decomposition pattern of the adulterated EBN differs from the raw EBN. Generally, they fall under two main temperature ranges: (a) 175-220°C, corresponding to melting and the onset of chemical decomposition, and (b) 250-350°C, corresponding to the decomposition step with higher mass loss. The differences in the DTG curves between Type II adulterated and unadulterated EBN are summarized in Table 3. Clearly, the TG and DTG curves of the unadulterated EBN can be used as a reference to check for adulteration in EBN. From the TG and DTG curves, one can infer that the detection limit of adulteration by thermal analysis is at the 1% w/w of soaking solution where the adulterant is present at the 2-4% w/w concentration in the dry EBN.

Table 3.3 Comparison of DTG thermograms between Type II adulterated and unadulterated EBN.

Type II adulterant	**Temperature range (°C) where the DTG curves are significantly different between adulterated and unadulterated EBN**
Glucose	175-220 (new band); 250-350 (decreased band height)
Sucrose	185-250 (new band); 250-350 (decreased band height)
Collagen	200-240 (new band); 250-350 (broadened band)
Monosodium glutamate (MSG)	175-220 (new band); 250-350 (broadened band with ripples)

Principal component analysis (PCA) is a statistical tool commonly used for data classification that is mathematically defined as an orthogonal linear transformation that transforms the data to a new coordinate system. As a result, the greatest variance lie on the horizontal coordinate (called the first principal component, PC1) and the second greatest variance is on the vertical coordinate (called the second principal component, PC2) in the score plot [36]. In our study, a PCA of all the DTG curves for EBN samples soaked in 2%, 5% and 10% w/w aqueous solutions of Type II adulterants, and that of the unadulterated EBN from three different geographical regions, using the DTG data from 150°C to 350°C, was carried out.

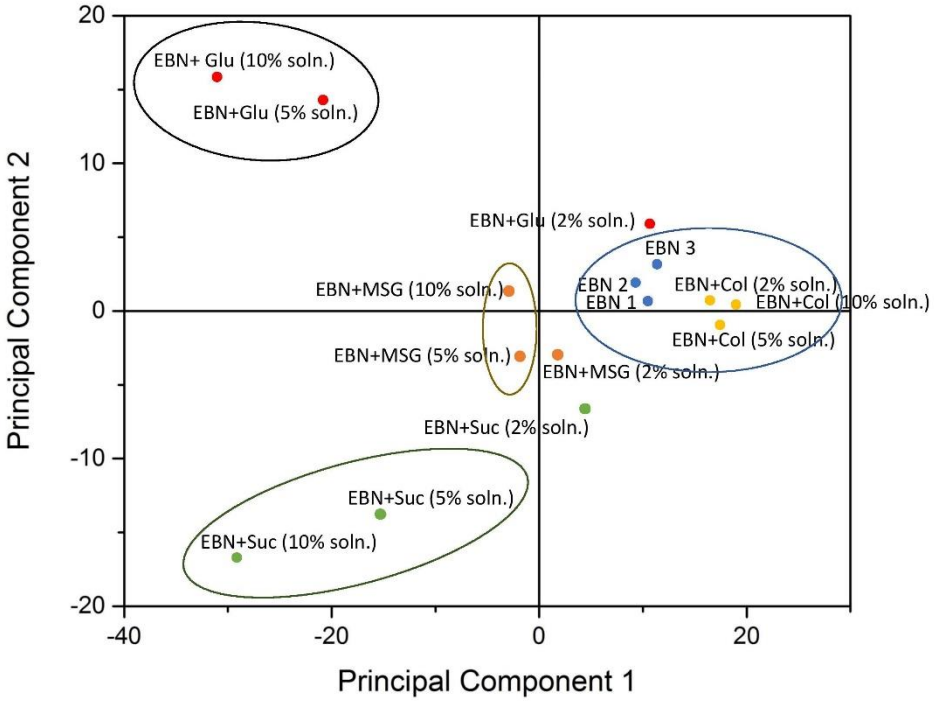

Figure 3.7 Principal component analysis (PCA) score plot of the DTG data in the temperature range 150°C to 350°C, comprising: (a) the DTG of unadulterated EBN from three different geographical regions, (b) DTG of adulterated EBN, for samples soaked in 2%, 5% and 10% w/w aqueous solutions of glucose, sucrose, MSG and collagen.

The first four principal components are responsible for the major variations (>94%). PC1 and PC2 which accounted for variance of 65% and 15% respectively, were used to plot

the 2-D PCA scatter score plot shown in Figure 3.7. By visual inspection, the separation among the data points can be observed along the PC1 horizontal axis and PC2 vertical axis. Samples with similarities are grouped together while dissimilar ones are spaced apart on the score plot. The formation of four clusters can be distinguished from Figure 3.7. The first one is for EBN adulterated with collagen samples and unadulterated EBN as there are high similarities between DTG curves for marine collagen and EBN. The remaining three clusters are for EBN adulterated with glucose, sucrose, and MSG respectively, due to the characteristic DTG peaks for glucose (175-220°C), sucrose (185-250°C) and MSG (175-220°C) arising from the decomposition of the adulterants. In agreement with the DTG curves in Figure 3.7, EBN adulterated with 2% w/w aqueous solutions are at the borderline of thermal analysis sensitivity, and the PCA points tend towards that of the first cluster for EBN and EBN adulterated with collagen.

3.4 Conclusion

We have shown that the EBNs of the swiftlet *Aerodramus fuciphagus*, from widely different geographic regions, have unique thermogravimetric (TG) and differential thermogravimetric (DTG) curves. From the TG and DTG curves, EBN is shown to have a total moisture content of 12.6%, which is about 5% higher than that reported in the literature by proximate analysis. Differential scanning calorimetry (DSC) showed that there are two kinds of bound water in EBN, and proximate analysis gives only the result for loosely bound water (7.5%). There is also about 5% of tightly bound water present in EBN. This finding should also apply to other food materials. The TG curve for EBN shows the main decomposition stage in the range of 200-735°C with a peak at about 294°C intermediate between that for polysaccharides and proteins which is consistent with EBN being a glycoprotein with both saccharides and proteins in the biopolymer.

Thermal analysis provides a fast, easy to use technique requiring small sample sizes to detect adulteration in EBN. The adulterated EBN will have a different set of TG and DTG curves from that of the reference unadulterated EBN. Both Type I, surface adhered adulterants, e.g. coralline seaweed, tremella fungus, agar, fish bladder and pork rind which can be picked out with a microscope, and Type II water-soluble adulterants, e.g. glucose, sucrose, hydrolyzed marine collagen, and MSG, which can be absorbed and bound inside the EBN matrix forming a uniform composite material, can be detected by thermal analysis. The detection limit of Type II absorbed adulterants by thermal analysis is at the 2-4% w/w concentration, depending on the adulterant, in the dry EBN.

3.5 References

1. Wang, C. C., The composition of Chinese edible bird's nest and the nature of their proteins. *Journal of Biological Chemistry* **1921,** *49* (2), 429-439.

2. Wieruszeski, J. M.; Michalski, J. C.; Montreuil, J.; Strecker, G.; Peter-Katalinic, J.; Egge, H.; van Halbeek, H.; Mutsaers, J. H.; Vliegenthart, J. F., Structure of the monosialyl oligosaccharides derived from salivary gland mucin glycoproteins of the Chinese swiftlet (genus Collocalia). Characterization of novel types of extended core structure, Gal beta(1----3)[GlcNAc beta(1----6)] GalNAc alpha(1----3)GalNAc(-ol), and of chain termination, [Gal alpha(1----4)]0-1[Gal beta(1----4)]2GlcNAc beta(1----.). *Journal of Biological Chemistry* **1987,** *262* (14), 6650-6657.

3. Marcone, M. F., Characterization of the edible bird's nest the "Caviar of the East". *Food Research International* **2005,** *38* (10), 1125-1134.

4. Shim, E. K. S.; Chandra, G. F.; Pedireddy, S.; Lee, S.-Y., Characterization of swiftlet edible bird nest, a mucin glycoprotein, and its adulterants by Raman microspectroscopy. *Journal of Food Science and Technology* **2016,** *53* (9), 3602-3608.

5. Yang, M.; Cheung, S.-H.; Li, S. C.; Cheung, H.-Y., Establishment of a holistic and scientific protocol for the authentication and quality assurance of edible bird's nest. *Food Chemistry* **2014,** *151*, 271-278.

6. Ding, Z.; Zhang, R.; Kan, Z., Quality and safety inspection of food and agricultural products by LabVIEW IMAQ vision. *Food Analytical Methods* **2015,** *8* (2), 290-301.

7. Chua, Y. G.; Chan, S. H.; Bloodworth, B. C.; Li, S. F. Y.; Leong, L. P., Identification of edible bird's nest with amino acid and monosaccharide analysis. *Journal of Agricultural and Food Chemistry* **2015,** *63* (1), 279-289.

8. Saengkrajang, W.; Matan, N.; Matan, N., Nutritional composition of the farmed edible bird's nest (Collocalia fuciphaga) in Thailand. *Journal of Food Composition and Analysis* **2013,** *31* (1), 41-45.

9. Lee, T. H.; Wani, W. A.; Poh, H. Y.; Baig, U.; Tan, T. T. E.; Nashiruddin, N. I.; Ling, Y. E.; Aziz, R. A., Gel electrophoretic and liquid chromatographic methods for the identification and authentication of cave and house edible bird's nests from common adulterants. *Analytical Methods* **2016,** *8* (3), 526-536.

10. Ma, F.; Liu, D., Sketch of the edible bird's nest and its important bioactivities. *Food Research International* **2012,** *48* (2), 559-567.

11. Zhang, S.; Lai, X.; Liu, X.; Li, Y.; Li, B.; Huang, X.; Zhang, Q.; Chen, W.; Lin, L.; Yang, G., Competitive enzyme-linked immunoassay for sialoglycoprotein of edible bird’s nest in food and cosmetics. *Journal of Agricultural and Food Chemistry* **2012,** *60* (14), 3580-3585.

12. Wu, Y.; Chen, Y.; Wang, B.; Bai, L.; Wu, R.; Ge, Y.; Yuan, F., Application of SYBRgreen PCR and 2DGE methods to authenticate edible bird's nest food. *Food Research International* **2010,** *43* (8), 2020-2026.

13. Lin, J.-R.; Zhou, H.; Lai, X.-P.; Hou, Y.; Xian, X.-M.; Chen, J.-N.; Wang, P.-X.; Zhou, L.; Dong, Y., Genetic identification of edible birds’ nest based on mitochondrial DNA sequences. *Food Research International* **2009,** *42* (8), 1053-1061.

14. Huang, L.; Chen, Y.; Liu, G.; Li, S.; Liu, Y.; Gao, X., Non-isothermal pyrolysis characteristics of giant reed (Arundo donax L.) using thermogravimetric analysis. *Energy* **2015,** *87*, 31-40.

15. Torrecilla, J. S.; García, J.; García, S.; Rodríguez, F., Application of lag-k autocorrelation coefficient and the TGA signals approach to detecting and quantifying

adulterations of extra virgin olive oil with inferior edible oils. *Analytica Chimica Acta* **2011,** *688* (2), 140-145.

16. Manara, P.; Vamvuka, D.; Sfakiotakis, S.; Vanderghem, C.; Richel, A.; Zabaniotou, A., Mediterranean agri-food processing wastes pyrolysis after pre-treatment and recovery of precursor materials: A TGA-based kinetic modeling study. *Food Research International* **2015,** *73*, 44-51.

17. Santos, O. V.; Corrêa, N. C. F.; Soares, F. A. S. M.; Gioielli, L. A.; Costa, C. E. F.; Lannes, S. C. S., Chemical evaluation and thermal behavior of Brazil nut oil obtained by different extraction processes. *Food Research International* **2012,** *47* (2), 253-258.

18. Siracusa, V.; Blanco, I.; Romani, S.; Tylewicz, U.; Dalla Rosa, M., Gas permeability and thermal behavior of polypropylene films used for packaging minimally processed fresh-cut potatoes: a case study. *Journal of Food Science* **2012,** *77* (10), E264-E272.

19. Ruttarattanamongkol, K.; Petrasch, A., Oxidative susceptibility and thermal properties of moringa oliefera seed oil obtained by pilot-scale subcritical and supercritical carbon dioxide extraction. *Journal of Food Process Engineering* **2016,** *39* (3), 226-236.

20. Vecchio, S.; Cerretani, L.; Bendini, A.; Chiavaro, E., Thermal decomposition study of monovarietal extra virgin olive oil by simultaneous thermogravimetry/differential scanning calorimetry: Relation with chemical composition. *Journal of Agricultural and Food Chemistry* **2009,** *57* (11), 4793-4800.

21. Colombo, A.; Ribotta, P. D.; León, A. E., Differential scanning calorimetry (dsc) studies on the thermal properties of peanut proteins. *Journal of Agricultural and Food Chemistry* **2010,** *58* (7), 4434-4439.

22. Tolstorebrov, I.; Eikevik, T. M.; Bantle, M., A DSC determination of phase transitions and liquid fraction in fish oils and mixtures of triacylglycerides. *Food Research International* **2014,** *58*, 132-140.

23. Blanco, I.; Siracusa, V., Kinetic study of the thermal and thermo-oxidative degradations of polylactide-modified films for food packaging. *Journal of Thermal Analysis and Calorimetry* **2013,** *112* (3), 1171-1177.

24. Tomaszewska-Gras, J., Rapid quantitative determination of butter adulteration with palm oil using the DSC technique. *Food Control* **2016,** *60*, 629-635.

25. Dahimi, O.; Rahim, A. A.; Abdulkarim, S. M.; Hassan, M. S.; Hashari, S. B. T. Z.; Siti Mashitoh, A.; Saadi, S., Multivariate statistical analysis treatment of DSC thermal properties for animal fat adulteration. *Food Chemistry* **2014,** *158*, 132-138.

26. Nur Azira, T.; Amin, I., 12 - Advances in differential scanning calorimetry for food authenticity testing a2 - Downey, Gerard. In *Advances in Food Authenticity Testing*, Woodhead Publishing: 2016; pp 311-335.

27. Bozec, L.; Odlyha, M., Thermal denaturation studies of collagen by microthermal analysis and atomic force microscopy. *Biophysical Journal* **2011,** *101* (1), 228-236.

28. Tegza, M.; Andreyeva, O.; Maistrenko, L., Thermal analysis of collagen preparations. *Cheminė technologija* **2012,** *1* (59), 40-45.

29. Stern, K. H., High temperature properties and decomposition of inorganic salts Part 3, nitrates and nitrites. *Journal of Physical and Chemical Reference Data* **1972,** *1* (3), 747-772.

30. Tromp, R.; Rubloff, G. W.; Balk, P.; LeGoues, F. K.; van Loenen, E. J., High-Temperature SiO_2 Decomposition at the SiO_2/Si Interface. *Physical Review Letters* **1985,** *55* (21), 2332-2335.

31. Sayi, Y. S.; Yadav, C. S.; Shankaran, P. S.; Chhapru, G. C.; Ramakumar, K. L.; Venugopal, V., Thermal decomposition of nitrogenous salts under vacuum. *International Journal of Mass Spectrometry* **2002,** *214* (3), 375-381.

32. Lehman, R. L.; Gentry, J. S.; Glumac, N. G., Thermal stability of potassium carbonate near its melting point. *Thermochimica Acta* **1998,** *316* (1), 1-9.

33. Chen, X.-M.; Liang, N.; Kitts, D. D., Chemical properties and reactive oxygen and nitrogen species quenching activities of dry sugar–amino acid maillard reaction mixtures exposed to baking temperatures. *Food Research International* **2015,** *76, Part 3*, 618-625.

34. Benzing-Purdie, L. M.; Ripmeester, J. A.; Ratcliffe, C. I., Effects of temperature on Maillard reaction products. *Journal of Agricultural and Food Chemistry* **1985,** *33* (1), 31-33.

35. Nunes, R. S.; Cavalheiro, É. T. G., Thermalbehavior of glutamic acid and its sodium, lithium and ammonium salts. *Journal of Thermal Analysis and Calorimetry* **2007,** *87* (3), 627-630.

36. Zhang, X.; Qi, X.; Zou, M.; Liu, F., Rapid authentication of olive oil by Raman spectroscopy using principal component analysis. *Analytical Letters* **2011,** *44* (12), 2209-2220.

Chapter 4 Nitration of Tyrosine in the Mucin Glycoprotein of Swiftlet Edible Bird's Nest Changes its Color from White to Red

Abstract

The edible bird's nest (EBN) of the swiftlet *Aerodramus fuciphagus* is largely a mucin glycoprotein. It is usually white in color, but there also exist the more sought after red or 'blood' EBN which is orange-red in color. The basis of the orange-red color has been a puzzle for a long time. Conjectures for the orange-red color have included hemoglobin in the EBN, oxidation of iron, an ovotransferrin-iron complex, feed taken by the swiftlets, structural coloration, and nitric oxide (NO) binding with the glycoprotein. Here, we show that it is the nitration of the tyrosyl residue, giving rise to the colored 3-nitrotyrosyl (3-NTyr) residue in the glycoprotein, as the real cause of the orange-red color. Evidence for the 3-NTyr residue comes from: (a) the detection and quantitative analysis of 3-NTyr in EBN by enzyme-linked immunosorbent assay, (b) the ultraviolet-visible absorption spectra of red EBN as a function of pH being similar to 3-nitrotyrosine (3-NT), (c) the change in the color of red EBN from yellow at low pH to orange-red at high pH just like 3-NT, and (d) the Raman spectrum of red EBN showing strong Raman nitro bands at 1330 cm^{-1} (symmetric $–NO_2$ stretch) and 825 cm^{-1} ($–NO_2$ scissoring bend). The high concentrations of nitrite and nitrate in red EBN are also explained.

4.1 Introduction

Swiftlets of genus *Aerodramus fuchiphagus*, native to the Indo-Pacific region, build edible bird's nest (EBN), also known as cubilose or nest cement, which is an unusual amorphous, composite material of strands of mucin glycoprotein (*ca*. 90% by weight) strengthened largely with their own bird feathers (*ca*. 10% by weight). The mucin glycoprotein is secreted like saliva in copious amounts from a pair of sublingual glands under the tongue of the swiftlet during breeding. In living systems, mucin glycoprotein is only present in tiny amounts; however EBN is a material with the highest known concentration of mucin glycoprotein, and more than a million kilograms of EBN are harvested annually. The raw EBN is moistened and cleaned of feathers, sand grains, etc., with tweezers, leaving behind strands of clean, white glycoprotein to be used as food or medicine. When cooked, EBN is believed to have exceptional nutritional and medicinal properties. It is one of the most expensive Asian food delicacies today and has been prescribed in traditional Chinese medicine for more than a thousand years. Recent studies have shown that EBN can inhibit influenza virus infection, stimulate the immune system, and promote epidermal growth.[1]

The EBN mucin glycoprotein is a polymer with a protein backbone and many dendritic carbohydrate chains attached to it. The proximate analysis of EBN revealed that it contains *ca.* 62% by weight of protein, made up of 17 types of amino acids, with the most abundant being serine, valine, tyrosine, isoleucine, aspartic acid and asparagine, glutamic acid and glutamine, and phenylalanine, and the distinct absence of tryptophan, cysteine, and proline.[2-5] The dendritic carbohydrates make up *ca.* 27% by weight and the major saccharides are sialic acid, galactose, N-acetylgalactosamine, N-acetylglucosamine, fucose, and mannose.[5-6] The rest are moisture (*ca.* 8%), ash/minerals (*ca.* 2%),[7] and fat (< 1%).[5]

There are several colors of EBN available in the market – white (Figure 4.1A shows a natural white EBN), various shades of light yellow or golden, and red EBN (Figure 4.1B shows

a natural red EBN from a bird house). The latter is often addressed as ‘blood’ nest due to its color. Commercially, the more common cleaned, white EBN costs about US$3,000/kg today, with the price fluctuating based on supply and demand, while the less common red EBN costs several times more, as the red EBN is perceived to have superior nutritional and medicinal properties over the white EBN. Today, the trade in EBN is a multibillion dollar industry annually. As a result of the lucrative return of red EBN, some EBN processors have used various methods, including dyeing and fumigation with swiftlet ‘bird soil’ (feces), to convert the white EBN into red ‘blood’ nest.[8]

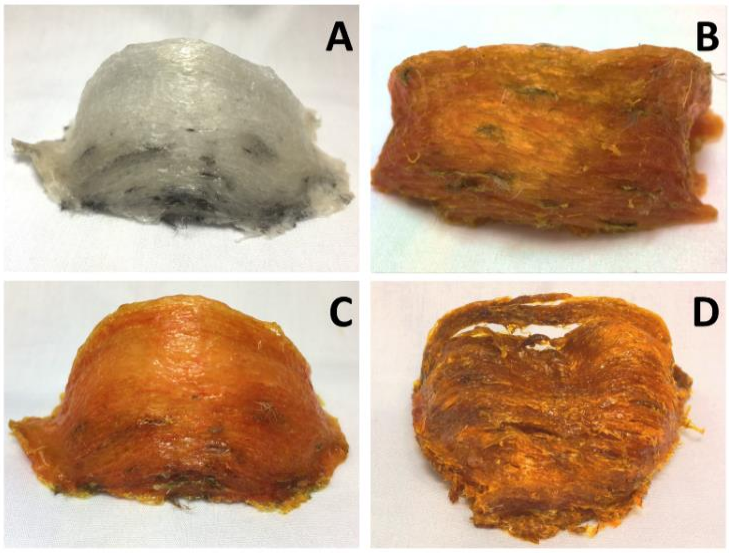

Figure 4.1 A. White EBN; B. Natural red EBN; C. HNO_2 fumigated EBN; and D. Xanthoproteic (HNO_3+H_2SO_4) reacted EBN.

Contrary to a long-held belief, red ‘blood’ EBN is a misnomer as it contains no hemoglobin.[9] In any case, we would not expect hemoglobin to be present in swiftlet saliva unless the bird was injured or sick to regurgitate blood. Marcone found that: (a) the substance giving the red color is neither water soluble nor lipid/solvent extractable, (b) white and red EBN both have ovotransferrin, and red EBN has a relatively higher amounts of iron compared to white EBN, and so it was suggested that an ovotransferrin-iron complex could be the cause

of the red color in red EBN.[5] The red color is also not a structural coloration (light interference effect) as both the white and red nests are made of similar amorphous cement-like material from the dried, clear liquid gel of mucin glycoprotein initially secreted through the beak of the same species of swiftlet. The coloration appears after the initial white EBN has been formed.

Recently, But *et al.*[8] showed that red EBN could be produced by fumigating white EBN either with vapor from unwashed swiftlet bird soil (feces), simulating the environment in some bird houses that accumulate the bird soil to produce colored nests, or with nitrous acid (HNO_2) vapor from a solution of sodium nitrite in 2% hydrochloric acid (Figure 4.1C shows a red EBN prepared by HNO_2 fumigation for 30 days). The similarity in the outcome is because the vapor from the bird soil also contains HNO_2 produced by bacterial decomposition of the protein/nitrogen-rich bird soil. Clearly, an ovotransferrin-iron complex cannot be the cause of the red color in these experiments. In analogy to sodium nitrite liberating nitric oxide (NO) and forming NO-myoglobin to give the deep red color of cured meat, it was conjectured that perhaps NO produced in the nitrous acid vapor equilibrium could similarly bind to the glycoprotein of EBN to give a red color. However, But *et al.*[8] noted that the chemistry of the color change from white to red EBN remains unknown.

The xanthoproteic reaction, using a mixture of concentrated nitric and sulfuric acids, is a standard biochemical test that gives a positive yellow to a deep red substance in proteins with aromatic amino acids, e.g. tyrosine, phenylalanine or tryptophan, due to nitration of the aromatic ring. Now, EBN is a glycoprotein containing substantial amounts of the aromatic amino acids tyrosine and phenylalanine, and it reacts positively at room temperature, giving a red color (Figure 4.1D shows a xanthoproteic reacted EBN). Clearly, the natural red EBN, the HNO_2 fumigated EBN, and the xanthoproteic reacted EBN in Figure 4.1B-D all have a similar red color. It is known that nitration of phenylalanine by the xanthoproteic reaction requires heat as the aromatic ring is not activated, but for tyrosine, it proceeds readily at room temperature

due to ring activation by the phenolic –OH group. So, the red color is most likely due to the nitration of the glycoprotein tyrosine residues to give 3-nitrotyrosyl (3-NTyr) residues. It remains for us to show that the 3-NTyr residue is practically absent in the white nest, but present significantly in the natural red EBN, the HNO_2 fumigated EBN, and the xanthoproteic reacted EBN, and 3-NTyr is the cause of the red color.

An anti-3-NTyr antibody enzyme-linked immunosorbent assay (ELISA) kit can be used to detect and quantitatively measure the 3-NTyr in EBN. Further evidence for 3-NTyr come from: (a) the UV-Vis absorption spectroscopy of solubilized red EBN showing pH-dependent absorption spectra similar to that of free 3-nitrotyrosine (3-NT), (b) the change in the color of red EBN strands from yellow at low pH to red at high pH, consistent with the UV-Vis absorption spectra of red EBN and 3-NT, and (c) Raman microspectroscopy showing the presence of the nitro group in red EBN.

4.2 Materials and methods

4.2.1 Edible bird's nest (EBN) and other materials

Raw white and natural red EBN samples produced by the species *Aerodramus fuciphagus* were obtained from bird houses from different geographical locations in Southeast Asia: Port Dickson (West Malaysia), Lahad Datu (East Malaysia), and Makassar (Indonesia). All standard chemicals used were analytical grade. Ultrapure water (18.2 MΩ cm) was prepared with Sartorius Arium Lab water purification system (Germany) and used for all experiments. Sodium nitrite, silver nitrate, and citric acid were purchased from Sigma-Aldrich Chemicals (St Louis, MO). Hydrochloric acid, sulfuric acid, and nitric acid were purchased from Fisher Scientific Chemicals (Hampton, NH). Urea, disodium hydrogen phosphate, sodium hydroxide, sodium carbonate, and sodium bicarbonate were purchased from VWR Chemicals (Radnor, PA). L-tyrosine and L-phenylalanine were purchased from NowFoods

(Bloomingdale, IL). 3-NT ELISA kit was purchased from Abcam (UK). Citric acid and disodium hydrogen phosphate were used to make buffers from pH 4 to 8, and sodium carbonate and sodium bicarbonate were used to make buffers from pH 9 to 10.

4.2.2 Fumigation of white EBN by nitrous acid to produce red EBN

EBN was fumigated with nitrous acid vapor to convert to red EBN.[8] A solution of sodium nitrite (200 mg) in 2% HCl (20 mL) was poured into a 250 mL glass beaker. A small empty glass bottle was placed at the bottom of the beaker as support for a glass petri dish containing the EBN so that it is above the fumigating solution. The glass beaker was then sealed with a paraffin film and kept in the dark at room temperature, and the color change in the EBN was monitored at regular intervals for up to 30 days, with a change of the $NaNO_2$-HCl solution every 7 days, during which time the EBN changed color from white to yellow to orange and finally to red.

4.2.3 Xanthoproteic reaction to produce red EBN

A whole piece of moistened raw white EBN (about 6 g) was dipped in a nitrating acid mixture (500 mL; 69% nitric acid: 98% sulfuric acid: water (5: 4: 95 v/v)) for *ca.* 5 seconds, removed and fan-dried for *ca.* 10 min at 25°C and *ca.* 50% relative humidity, and the dipping and drying was repeated for about 30 times, until the EBN turned yellow. The dipping and drying helped to retain the shape of the EBN and to better control the rate of nitration. Next, the dipping and drying were repeated for 30 times with water to rinse off residual acid to stop the reaction. Finally, 1 mM sodium hydroxide solution was sprayed on the surface of the nitrated EBN to neutralize any remaining acid, followed by fan-drying for *ca.* 10 min. The process was repeated several times, and the EBN turned red as shown in Figure 4.1D.

4.2.4 Synthesis of 3-nitrotyrosine (3-NT) and 4-nitrophenylalanine (4-NP)

3-NT was synthesized by reacting L-tyrosine with an acid mixture of nitric acid and sulfuric acid to generate the nitronium ion for electrophilic aromatic substitution.[10] The product was characterized by nuclear magnetic resonance (NMR) spectroscopy and liquid chromatography-mass spectroscopy (MS). ^{1}H NMR spectra were recorded on a JOEL 400 (Japan) at 400 MHz, and mass spectra were recorded on a Thermo Finnigan LCQ Fleet Mass Spectrometer (San Jose, CA) using water as a solvent. ^{1}H NMR (400 MHz, D_2O) δ/ppm: 8.03 (s, 1H, aromatic proton), 7.57 (dd, 1H, J_1 = 9 Hz, J_2 = 2 Hz, aromatic proton), 7.17 (dd, 1H, J_1 = 9 Hz, J_2 = 2 Hz, aromatic proton), 4.22 (t, J = 8 Hz, 1H, -CH), 3.26 (multiplet, 2H, -CH_2). LC-MS (ESI) m/z: $[M + H]^+$ Calcd for $C_9H_{10}N_2O_5 + H^+$, 227.19; found 226.88.

4-NP was synthesized from phenylalanine in the same way as 3-NT by electrophilic aromatic substitution of the nitronium ion,[11] and subjected to reverse-phase high-performance liquid chromatography (RP-HPLC) for further purification. The mixture was injected onto the Agilent ZORBAX SB-C18 column (9.4 x 250 mm, 5 µm) (Santa Clara, CA) and eluted with eluent A (water: acetonitrile: trifluoroacetic acid = 95: 5: 0.1) and a linear gradient of eluent B (water: acetonitrile: trifluoroacetic acid = 50: 50: 0.1) for 20 min, followed by a washing and re-equilibration step. The injection volume was 400 µL at a flow rate of 3 mL min^{-1}, and the UV absorbance of the eluents was monitored at 280 nm. The major product eluted at 11.5 min was characterized by NMR and LC-MS. ^{1}H NMR (D_2O) δ/ppm: 8.20 (d, 2H, J = 9 Hz, aromatic proton), 7.51 (d, 2H, J = 8 Hz, aromatic proton), 4.40 (t, 1H, J = 7 Hz, -CH), 3.39 (multiplet, 2H, -CH_2). LC-MS (ESI) m/z: $[M + H]^+$ Calcd for $C_9H_{10}N_2O_4 + H^+$, 211.19; found 210.99.

4.2.5 Microscopic images of red EBN strands with change in pH

Carl Zeiss Stemi 305 Trino Greenough system with Stand K EDU and spot illuminator K LED (Germany) was used to obtain the microscopic images of EBN strands. The images were captured and recorded with microscopy camera Axiocam 105 color and Carl Zeiss ZEN

Lite software. EBN strands were soaked in the respective buffer solutions for 10 min and fan dried for 15 min at 25°C and *ca.* 50% relative humidity, before the images were taken.

4.2.6 Solubilization and lyophilization of EBN

About 0.1 g of white or red EBN was frozen in liquid nitrogen, pulverized, and sieved through 0.5 mm mesh. The EBN was rinsed with water (4 L) to remove any nitrate/nitrite in the EBN. Subsequently, the residue was further soaked and rinsed with 0.05 M urea (200 mL) to remove any residual nitrite, and finally rinsed with water (4 L) again. We will call this cleaned EBN residue. It was then added to 1 M sodium hydroxide (5 mL) and stirred until the EBN dissolved (*ca*. 12 hours). The solubility of the EBN was about 20 g/L. The solution was centrifuged, and the supernatant was ultrafiltered with Sartorius Vivaspin 20 ultrafiltration tube (MWCO 3000 Da) using water as eluent to remove any excess sodium hydroxide and salt present. The neutral EBN solution was lyophilized and stored at 4°C. We will call the product lyophilized EBN.

4.2.7 Enzyme-linked immunosorbent assay (ELISA)

The ELISA was conducted using the commercially available 3-NTyr sandwich ELISA kit. A calibration curve utilizing 3-NTyr labeled bovine serum albumin (BSA) in the working range from 8 to 1000 ng mL^{-1} was fitted using a four-parameter logistic algorithm in Origin Pro 9.0 (Northampton, MA). Lyophilized white or red EBN samples, silver nitrate, and sodium nitrite were appropriately diluted for the analysis, and triplicate measurements were carried out for each sample. 3-NTyr labeled BSA and incubation buffer were used as the positive and negative control, respectively. The absorption at 600 nm was recorded at 15 min after the addition of the horseradish peroxidase (HRP) enzyme development solution with Tecan 96-well plate spectrophotometer (Switzerland). The concentrations of 3-NTyr in the lyophilized EBN samples were determined

4.2.8 UV-Visible spectroscopy

A series of solutions (~1 g L^{-1}) at different pH were made by adding the lyophilized EBN, 4-NP, or 3-NT into pH buffers with pH from 4 to 10. The pH of the solutions was monitored with a Mettler Toledo benchtop pH meter (Switzerland). The absorption spectra of the solutions, in Fisher-Scientific 1 cm path-length quartz cuvette cell, were then recorded from 250 to 600 nm with a Shimadzu UV-1800 UV-Vis spectrophotometer (Japan).

4.2.9 Raman microspectroscopy

Cleaned white or red EBN residues were pre-soaked in 0.01 M sodium hydroxide to deprotonate the 3-NTyr residue so as to intensify the Raman bands of the nitro group, and fan dried for *ca.* 12 hours at 25°C and *ca.* 50% relative humidity before measurement. Raman spectra of the EBN were collected with the Nanophoton Ramantouch microspectrometer (Japan) using the 532 nm laser excitation and instrument parameters (LU Plan Fluor 100 X, 600 gr mm^{-1}, 28 mW, 30 s, and 24°C).

Pure 3-NT (0.1 mg) was dissolved in 1 M sodium hydroxide (10 µL), deposited on a silicon substrate, and the solvent was allowed to evaporate slowly in a covered petri dish for *ca.*72 hours before the Raman measurement. The Raman spectrum of 3-NT was also collected using the 532 nm laser excitation, but with lower power (3 mW, 180 s, and 24°C) to minimize fluorescence.

Each sample was measured in triplicate over different spots, and the average Raman spectrum was baseline-corrected with the Origin Pro 8.0 software.

4.3 Results and Discussion

4.3.1 Fumigation of white EBN with nitrous acid vapor and by xanthoproteic reaction to produce red EBN

But *et al.*[8] showed that red EBN can be formed by fumigating the white EBN with HNO_2 vapor formed by the reaction between sodium nitrite and hydrochloric acid or the vapor from 'bird soil' collected from bird houses. Figure 4.1 shows the natural white nest (A), natural red nest (B), red nest produced by HNO_2 fumigation (C), and red nest produced by the xanthoproteic reaction (D).

Figure 4.2 shows the red color development of a piece of raw white EBN when fumigated with a mixture of sodium nitrite and hydrochloric acid over a period of 30 days (d). The white EBN had turned yellow/golden after 1 d, orange-red after 5 d and gradually a terracotta red after 30 d. This can be explained by the increasing concentration of 3-NTyr residue in the EBN as the fumigation time increases.

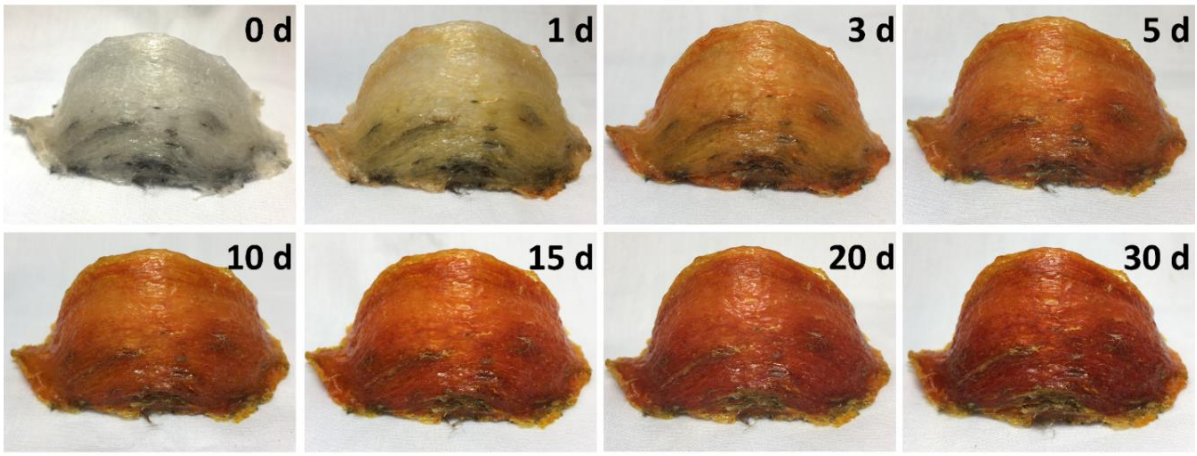

Figure 4.2 Development of the red color in EBN by HNO_2 fumigation from 0 – 30 days (d).

In fumigation, sodium nitrite and hydrochloric acid react steadily to yield nitrous acid vapor,

$$NaNO_2(aq) + HCl(aq) \rightarrow HNO_2(aq, g) + NaCl(aq) \quad . \qquad (1)$$

Nitrous acid undergoes disproportionation to yield reactive nitrogen species (RNS), e.g. NO_2 and •NO,[12-13]

$$2HNO_2 \rightleftharpoons \bullet NO_2 + \bullet NO + H_2O \quad . \qquad (2)$$

Besides reacting with glycoprotein tyrosine, the radicals can also undergo the following reactions,

$$2\bullet NO_2 \rightleftharpoons N_2O_4 \qquad (3)$$

$$N_2O_4 + 2H_2O \rightarrow NO_3^- + NO_2^- + 2H_3O^+ \quad . \qquad (4)$$

In the presence of atmospheric O_2, the oxidation of •NO can also occur,[14]

$$4\bullet NO + O_2 + 6H_2O \rightarrow 4NO_2^- + 4H_3O^+ \quad . \qquad (5)$$

The EBN in the bird house is thus exposed to an atmosphere containing $\bullet NO_2$, •NO, NO_2^-, and NO_3^-.

In analogy to protein tyrosine nitration in living systems, the reaction between the RNS and protein tyrosine can occur by a radical mechanism as shown in Scheme 4.1. The one electron oxidant $\bullet NO_2$ can undergo a slow reaction with the glycoprotein tyrosine to give the tyrosyl radical, and a further fast reaction with $\bullet NO_2$ gives 3-NTyr.[15-16] The tyrosyl radical can also react (slowly) with •NO to form the intermediate 3-nitrosotyrosyl residue which is rapidly oxidized to 3-NTyr, e.g. by HNO_3.[13, 15, 17] The intermediate 3-nitrosotyrosyl residue can be trapped by the addition of Hg(II) to give a red pigment as in Millon's test for tyrosine.[18]

The natural red EBN, Figure 4.1B, came from a bird house. In bird houses, there is swiftlet bird soil on the floor. The bird soil is rich in protein and nitrogenous compounds because the swiftlets feed on a high protein diet of aerial insects. Aerobic bacteria can feed on the bird soil, and its metabolism produces nitrous acid and nitric acid vapors. If the concentration of nitrous acid reaches a sufficient level in the largely enclosed bird house, it will

be absorbed by the white EBN initially built by the swiftlet on the walls and ceiling of the bird house, and reacts by Scheme 4.1 first to a yellow/golden color, then to red, and finally to a terracotta red as the concentration of 3-NTyr increases in the EBN, just as in Figure 4.2. Thus, even the white nest can have a small amount of 3-NTyr. Equations (4) and (5), and also nitric acid vapor from the bird soil, explains why red EBN would have a significant amount of nitrite and nitrate. This makes red EBN an unsafe food or health supplement, if not properly cleaned. The toxicity of high concentrations of nitrite and nitrate (found in thousands of parts per million (ppm) in red EBN) was what led China to put a ban on the sale of both white and red EBNs at one time.[19] The nitrate and nitrite in EBN, being water soluble, can be rinsed away, and this is carried out before analyzing for 3-NTyr to avoid interference.

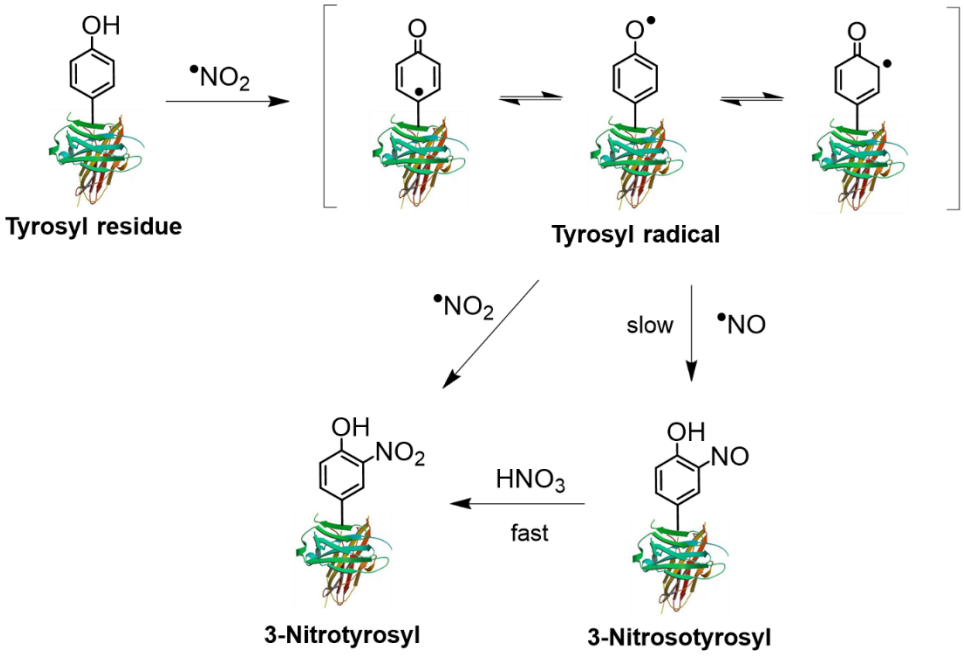

Scheme 4.1 The reactions between the protein tyrosine residues and reactive nitrogen species - •NO_2 and •NO – to produce 3-NTyr during HNO_2 fumigation. The illustration is not to scale as the mucin glycoprotein is a 3D giant macromolecule in comparison to the tyrosine residue. For the sake of clarity, only one tyrosine residue is shown.

In the xanthoproteic reaction of EBN with a mixture of nitric and sulfuric acids to give red EBN, significant amounts of 3-NTyr is formed by Scheme 4.2. By conjugation with sulfuric acid, nitric acid produces a nitronium ion (NO_2^+), which is the active species in electrophilic aromatic nitration,

$$HNO_3(aq) + 2H_2SO_4(aq) \rightleftharpoons NO_2^+(aq) + H_3O^+(aq) + 2HSO_4^-(aq) \quad . \qquad (6)$$

The nitronium ion reacts with the aromatic ring to form a nitrotyrosyl arenium ion, and subsequently the H^+ is eliminated by a nucleophile, H_2O, and a neutral 3-NTyr is formed. [10, 20]

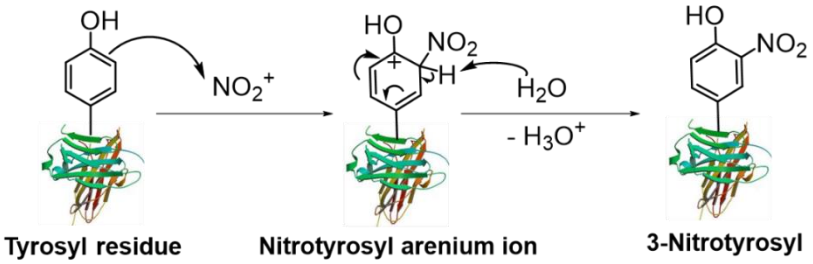

Scheme 4.2 Electrophilic aromatic substitution reaction by the nitronium ion, NO_2^+, on the protein tyrosine residues in the xanthoproteic reaction to produce 3-NTyr.

4.3.2 Determination of 3-NTyr in white and red EBN with ELISA

An anti-3-NTyr ELISA kit was used to detect and quantify 3-NTyr in natural white EBN, natural red EBN, HNO_2 fumigated EBN and xanthoproteic reacted EBN. The concentrations of 3-NTyr detected, and the degree of protein tyrosine nitration are shown in Table 4.1.

Table 4.1 Concentrations of 3-nitrotyrosine residue found in white and red EBNs by ELISA test.

Sample	[3-nitrotyrosine] (ppm)	EBN tyrosyl nitration degree (%)
Natural white EBN	2.5 ± 1.2	< 0.0034
Natural red EBN	$(9.84 \pm 1.24)x10^2$	0.90 ± 0.11
EBN fumigated with $NaNO_2$/HCl for 30 days	$(2.53 \pm 0.45)x10^3$	2.32 ± 0.41
Xanthoproteic reacted EBN	$(8.28 \pm 1.64)x10^3$	7.60 ± 1.50

The concentrations of 3-NTyr in red EBNs are hundreds to thousands of times higher than in white EBN. In the natural white EBN, the concentration of 3-NTyr is very low 2.5 ± 1.2 ppm, while natural red EBN and HNO_2 fumigated EBN contained $(9.84 \pm 1.24)x10^2$ ppm and $(2.53 \pm 0.45)x10^3$ ppm of 3-NTyr, respectively. It was observed that a higher degree of nitration could be achieved if the fumigation time was lengthened or the surface area of the EBN was increased, e.g. by pulverization. The xanthoproteic reaction gave a more effective nitration of the glycoprotein tyrosine, and the red EBN produced had an even higher concentration of 3-NTyr, $(8.28 \pm 1.64)x10^3$ ppm. The EBN tyrosyl nitration degree in Table 4.1, ranging from <0.0034% for natural white EBN to about 7.6% for the xanthoproteic reacted EBN, was calculated based on 87.2 mg tyrosine per g of EBN.[5]

4.3.3 Color change in the red EBN strands as a function of pH

A color change as a function of pH, like an indicator, was observed in strands of red EBNs when they were soaked in the respective buffers and air-dried. Figure 4.3 shows the microscopic images where a color change from light yellow/golden to a deep red can be

observed when the buffer changed from acidic to alkaline pH. The natural red EBN and HNO_2 fumigated EBN were pale yellow from pH 2 to 5, then an orange hue developed from pH 6 to 9, and finally a deep red was seen from pH 10 to 13. The color intensity of natural red EBN is lower than HNO_2 fumigated EBN due to the lower concentration of the 3-NTyr chromophore. A similar color change (not shown) occurred with strands of the xanthoproteic reacted red EBN.

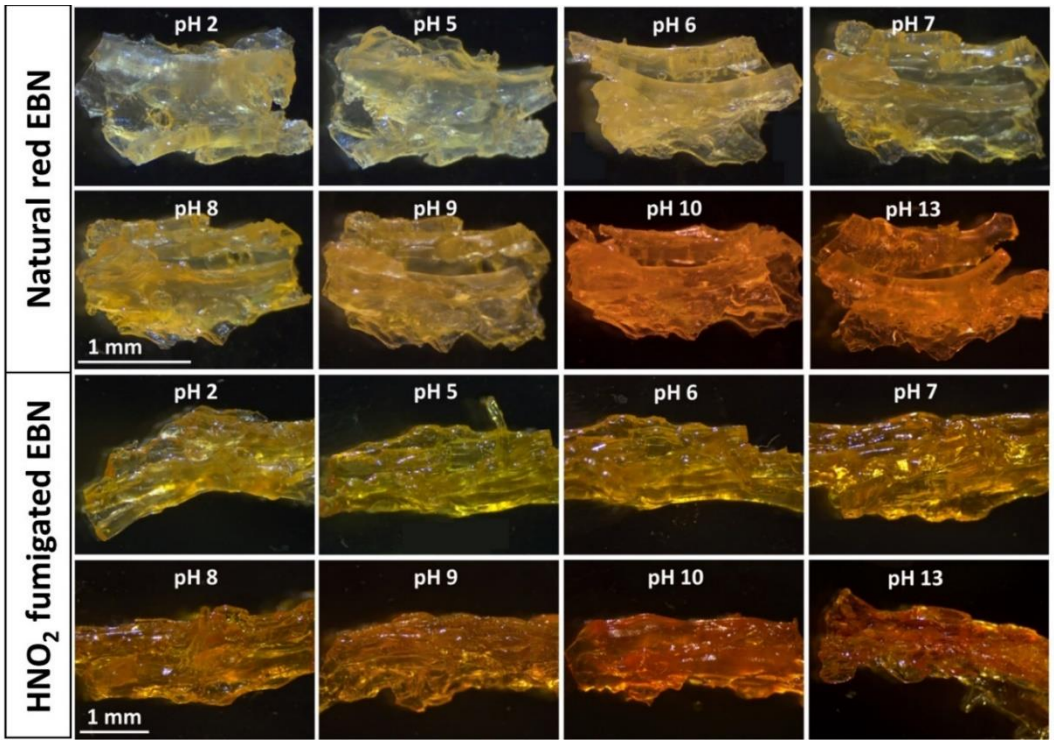

Figure 4.3 Color change in strands of natural red EBN (top panel) and HNO_2 fumigated EBN (bottom panel) as pH is varied from 2 to 13, observed under the microscope.

4.3.4 UV-Vis absorption spectra of 4-nitrophenylalanine and 3-nitrotyrosine as a function of pH

Figure 4.4A shows the absorption spectra of 4-nitrophenylalanine (4-NP) as a function of pH from 4 to 10. It absorbs in the UV region and would not show any visible color. The absorption bands are similar with a maximum at 280 nm for pH 4-8, and a maximum at 290 nm for pH 9-10. There would be a gradual change in the absorption band from one form to

another at around pH 9, due to the change from protonated to deprotonated amine on the amino acid as phenylalanine has $pK_{a2} \approx 9.1$.

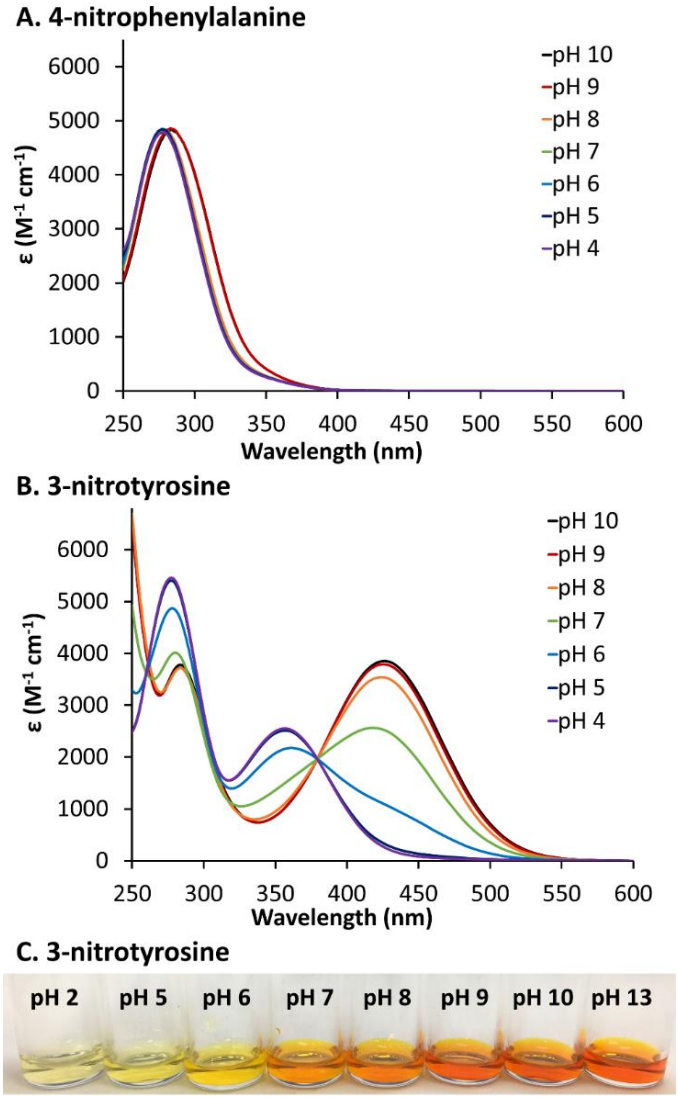

Figure 4.4 UV-Vis absorption spectra of A. 4-nitrophenylalanine, and B. 3-nitrotyrosine – pH 10 (black), pH 9 (red), pH 8 (orange), pH 7 (green), pH 6 (blue), pH 5 (indigo) and pH 4 (purple); and C. Color change of 3-nitrotyrosine solution (5 g L^{-1}) from yellow to red with pH from 2 to 13.

In the UV-Vis absorption spectra of 3-NT, the hydroxyl (-OH) auxochrome in 3-NT, conjugated with the nitro ($-NO_2$) group chromophore, when deprotonated (to $-O^-$) will give a bathochromic shift of the absorption. The absorption spectra of 3-NT (Figure 4.4B) in acidic

solutions, with –OH intact, show an absorption maximum at 358 nm. As the pH is increased, the absorption at 358 nm gradually decreases, and the absorption with a 427 nm maximum for the deprotonated phenolate -O^- form of 3-NT increases. The color change due to the phenol-phenolate reversible equilibrium and the presence of an isosbestic point at 380 nm makes 3-NT, with a pK_a of 7.1, an indicator.[21-22]

The color change of 3-NT solutions from light yellow to red as the pH is changed from 2 to 13, is shown in Figure 4.4C. Clearly, the color change with pH for red EBN strands in Figure 4.3 is similar. It suggests that the chromophore present in red EBN is likely to be 3-NT. The phenylalanine in EBN is much less readily nitrated compared to tyrosine, and even if it is nitrated, its absorption is in the UV region and will not show any visible color change with pH.

4.3.5 UV-Vis absorption spectra of white and red EBN as a function of pH

To ascertain that the absorbing chromophore in red EBN is 3-NTyr, the absorption spectra of solubilized white and red EBNs were investigated. Figure 4.5 shows the absorption spectra of white EBN as a function of pH. The absorption falls in the UV region and is nearly pH independent. The absorption band at 280 nm is due to the π-π^* transition of the aromatic amino acids – tyrosine and phenylalanine – in EBN.[23]

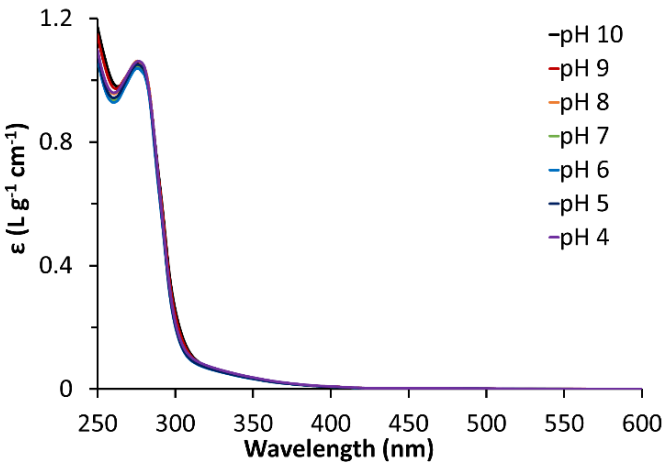

Figure 4.5 pH independent UV-Vis absorption spectra of solubilized white EBN – pH 10 (black), pH 9 (red), pH 8 (orange), pH 7 (green), pH 6 (blue), pH 5 (indigo) and pH 4 (purple).

Figures 4.6A-C show the absorption spectra as a function of pH for the three types of red EBNs – natural, HNO_2 fumigated, and xanthoproteic reacted. The corresponding difference spectra between the red and white EBNs, Figures 4.6D-F, would reveal the absorbing chromophore. They each show a bathochromic shift with a clear resemblance to the pH-dependent absorption spectra for 3-NT (Figure 4.4B), with absorption maxima at *ca.* 360 nm in acidic medium, shifting to *ca.* 430 nm in basic medium, and an isosbestic point at *ca.* 380 nm. The absorptivity ε in Figures 4.6A-C is given in terms of the concentration (g L^{-1}) of EBN, and then was scaled using the concentration of 3-NTyr determined by ELISA in Table 4.1 for the respective red EBNs to give the molar absorptivity of 3-NTyr in EBN in Figures 4.6D-F. It corresponds well to the molar absorptivity of pure 3-NT at the 427 nm absorption maximum, within the margin of error of the determination of 3-NTyr concentration by ELISA. The nitration could also produce a small amount of 4-NP residue on the glycoprotein, and this has not been subtracted out in Figures 4.6D-F; it would raise the difference absorption spectra only in the 290-350 nm region slightly, but would not affect the major band at around 427 nm.

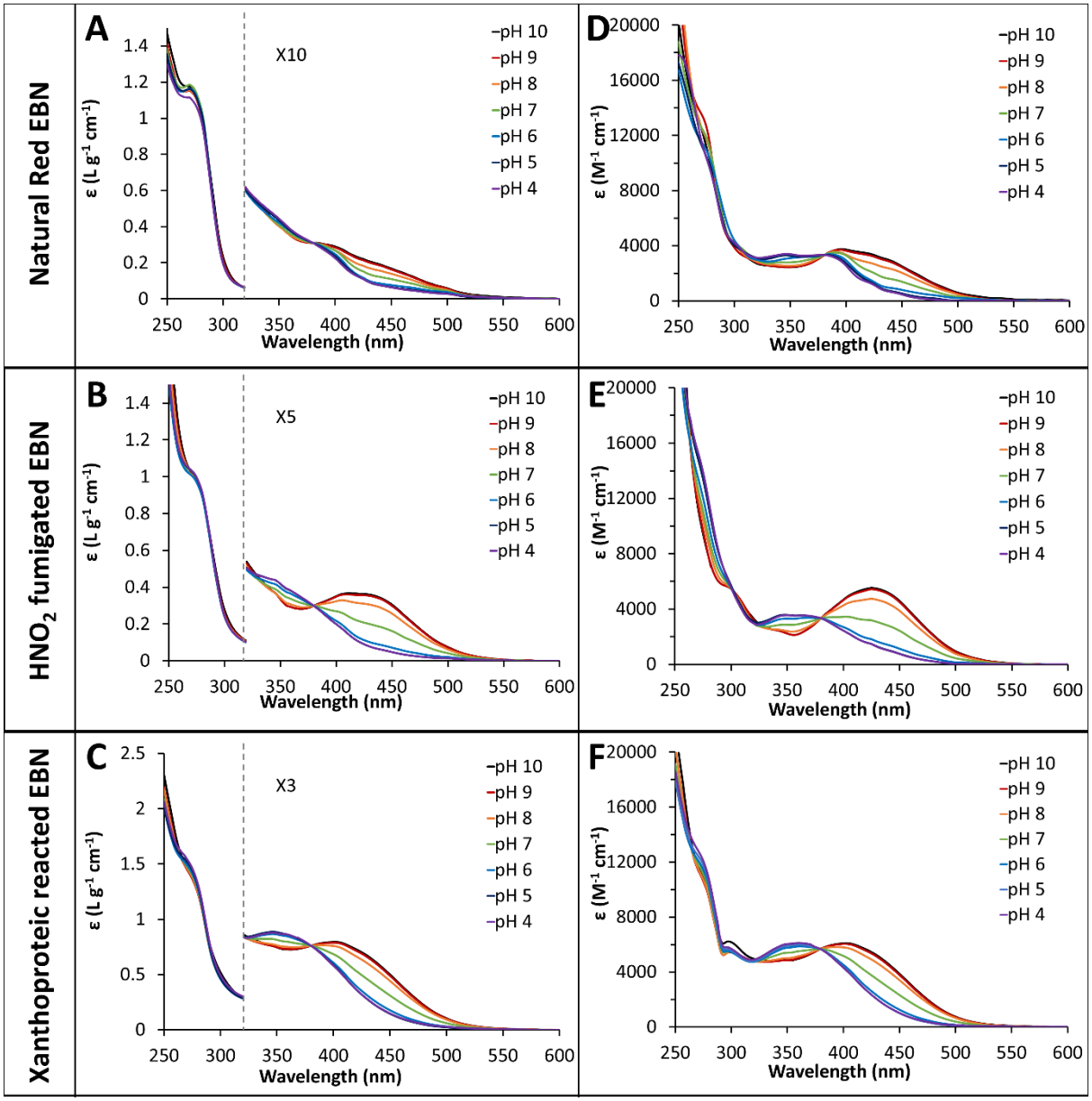

Figure 4.6 pH dependent UV-Vis absorption spectra (A - C) of A. natural red EBN (top panel), B. HNO_2 fumigated EBN (middle panel), and C. xanthoproteic reacted EBN (bottom panel) and the corresponding difference spectra (D - F) between red and white EBN – pH 10 (black), pH 9 (red), pH 8 (orange), pH 7 (green), pH 6 (blue), pH 5 (indigo) and pH 4 (purple). In (A-C), the absorption spectra in the region between 320-600 nm have been scaled up by an appropriate factor, as indicated, for visualization.

4.3.6 Raman spectra showing the nitro group in red EBN

Raman microspectroscopy with 532 nm laser excitation was used to confirm the presence of the nitro group in red EBN. The Raman spectra of white EBN, natural red EBN, HNO_2 fumigated EBN, xanthoproteic reacted EBN, and pure 3-NT are shown in Figures 4.7A-E, respectively. The two rectangular boxes in Figures 4.7B-D frame the spectral regions where the red EBNs differ significantly from the white EBN. The red EBNs show a strong Raman band at 1330 cm^{-1} which is due to the symmetric $–NO_2$ stretch, and a strong Raman band at 825 cm^{-1} which is due to the $–NO_2$ scissoring bend.[24-25] These two $–NO_2$ Raman bands are also present in the Raman spectrum of 3-NT, Figure 4.7E.

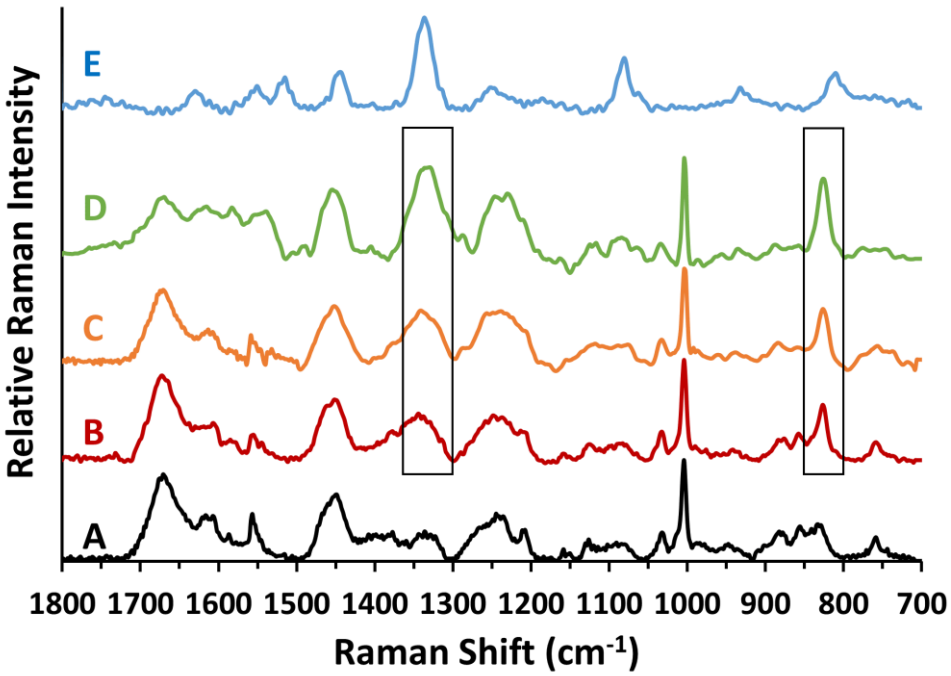

Figure 4.7 Comparison of Raman spectra of A. raw white EBN (black), B. natural red EBN (red), C. HNO_2 fumigated EBN (orange), D. xanthoproteic reacted EBN (green), and E. 3-nitrotyrosine (blue). The boxes over the red EBNs show: (a) the 1330 cm^{-1} Raman band which is due to the symmetric $–NO_2$ stretch, and (b) the 825 cm^{-1} Raman band which is due to the $–NO_2$ scissoring bend. These bands are also present in 3-nitrotyrosine.

4.3.7 EBN as a scavenger for reactive nitrogen species

The presence of 3-NTyr in red nest is a post-translational modification. The 3-NTyr pigment, with a $pK_a \approx 7.1$, behaves like an indicator and exhibits a color change from yellow in acid to red in alkali, with the color change occurring around pH 7.

Generally, protein nitration by RNS is a complex process. It has been suggested that protein nitration is dependent upon the proximity of protein tyrosine to the nitration source, but not all tyrosine residues in a protein are equally susceptible to nitration. There is no specific amino acid consensus sequence or specific protein primary structure that determines the site of tyrosine nitration.[26-27] From our results, it was found that EBN is quite readily nitrated. The high concentration of asparagine/aspartic acid (60.1 mg g^{-1}), glutamine/glutamic acid (48.9 mg g^{-1}), and glycine (21.1 mg g^{-1}) residues[5] in EBN might be responsible for this, as it has been noted that the acidic amino acids (glutamic acid or aspartic acid) or turn-inducing amino acids (proline and glycine) in the vicinity of the targeted tyrosine are the characteristic features observed for nitrated proteins.[28]

In vivo, a high concentration of RNS can induce pathological effects on our body, and the protein-bound tyrosine in our organs and tissues react with RNS to form 3-NTyr.[29-30] The level of protein nitration is clinically viewed as a marker of oxidative or nitrative stress.[31-32] For this reason, a food material like EBN that is able to mop up RNS may help to alleviate disease-related nitrative stress.[33-36] This could be one of the new benefits in the prescription of EBN in traditional Chinese medicine. White EBN, where >99% of the tyrosine residues are not nitrated would therefore be more beneficial than the colored yellow, golden, orange or red EBNs where a portion of the tyrosine residues would have already been spent, i.e. converted to 3-NTyr.

Preliminary results show that EBN is also a very strong antioxidant, with higher antioxidant capacity than black garlic, ginseng or goji berry, and white EBN is a stronger antioxidant compared to red EBN. Part of the antioxidant capacity of EBN arises from the protein bound tyrosine, so tyrosine plays multiple roles of mopping up RNS as well as free radicals and oxidants. This work is ongoing.

4.4 Conclusion

Our findings, based on color change with pH, UV-Vis spectra as a function of pH, and Raman microspectroscopy on red EBN, provide conclusive evidence for the nitration of tyrosine residues in the mucin glycoprotein of EBN to yield 3-NTyr which gives rise to the red color. The 3-NTyr is found to be practically absent in the white nest, but present significantly in the natural red EBN, the HNO_2 fumigated EBN, and the xanthoproteic reacted EBN. As the tyrosyl residues in EBN mucin glycoprotein is highly susceptible to nitration, it suggests that mucin glycoproteins (present widely in our bodies) can act as scavengers for reactive nitrogen species in disease conditions and could be one of the benefits for the use of white EBN in traditional Chinese medicine and as a health supplement. We believe that our work can stimulate more research, at a molecular level, on the use of this abundant (white EBN) mucin glycoprotein to create new and safe drugs related to the long-held benefits attributed to the consumption of EBN.

4.5 References

1. Chua, L. S.; Zukefli, S. N., A comprehensive review of edible bird nests and swiftlet farming. *Journal of Integrative Medicine* **2016,** *14* (6), 415-428.

2. Chua, Y. G.; Chan, S. H.; Bloodworth, B. C.; Li, S. F. Y.; Leong, L. P., Identification of edible bird's nest with amino acid and monosaccharide analysis. *Journal of Agricultural and Food Chemistry* **2015,** *63* (1), 279-289.

3. Shim, E. K. S.; Chandra, G. F.; Pedireddy, S.; Lee, S.-Y., Characterization of swiftlet edible bird nest, a mucin glycoprotein, and its adulterants by Raman microspectroscopy. *Journal of Food Science and Technology* **2016,** *53* (9), 3602-3608.

4. Oda, M.; Ohta, S.; Suga, T.; Aoki, T., Study on food components: the structure of N-linked asialo carbohydrate from the edible bird's nest built by Collocalia fuciphaga. *Journal of Agricultural and Food Chemistry* **1998,** *46* (8), 3047-3053.

5. Marcone, M. F., Characterization of the edible bird's nest the "Caviar of the East". *Food Research International* **2005,** *38* (10), 1125-1134.

6. Ma, F.; Liu, D., Sketch of the edible bird's nest and its important bioactivities. *Food Research International* **2012,** *48* (2), 559-567.

7. Shim, E. K. S.; Chandra, G. F.; Lee, S.-Y., Thermal analysis methods for the rapid identification and authentication of swiftlet (Aerodramus fuciphagus) edible bird's nest – a mucin glycoprotein. *Food Research International* **2017,** *95*, 9-18.

8. But, P. P.-H.; Jiang, R.-W.; Shaw, P.-C., Edible bird's nests—How do the red ones get red? *Journal of Ethnopharmacology* **2013,** *145* (1), 378-380.

9. Paydar, M.; Wong, Y. L.; Wong, W. F.; Hamdi, O. A. A.; Kadir, N. A.; Looi, C. Y., Prevalence of nitrite and nitrate contents and its effect on edible bird nest's color. *Journal of Food Science* **2013,** *78* (12), T1940-T1947.

10. Burtch, E. A.; Jones-Wilson, T. M., A green starting material for electrophilic aromatic substitution for the undergraduate organic laboratory. *Journal of Chemical Education* **2005,** *82* (4), 616.

11. Qiu, J.; Xu, B.; Huang, Z.; Pan, W.; Cao, P.; Liu, C.; Hao, X.; Song, B.; Liang, G., Synthesis and biological evaluation of Matijing-Su derivatives as potent anti-HBV agents. *Bioorganic & Medicinal Chemistry* **2011,** *19* (18), 5352-5360.

12. Vione, D.; Belmondo, S.; Carnino, L., A kinetic study of phenol nitration and nitrosation with nitrous acid in the dark. *Environmental Chemistry Letters* **2004,** *2* (3), 135-139.

13. Goldstein, S.; Czapski, G.; Lind, J.; Merényi, G., Tyrosine nitration by simultaneous generation of ·NO and $\cdot O_2^-$ under physiological conditions: How the radicals do the job. *Journal of Biological Chemistry* **2000,** *275* (5), 3031-3036.

14. Ignarro, L. J.; Fukuto, J. M.; Griscavage, J. M.; Rogers, N. E.; Byrns, R. E., Oxidation of nitric oxide in aqueous solution to nitrite but not nitrate: comparison with enzymatically formed nitric oxide from L-arginine. *Proceedings of the National Academy of Sciences of the United States of America* **1993,** *90* (17), 8103-8107.

15. Radi, R., Nitric oxide, oxidants, and protein tyrosine nitration. *Proceedings of the National Academy of Sciences* **2004,** *101* (12), 4003-4008.

16. Cudic, M.; Dendane, M.; Houé-Levin, C.; Ducrocq, C., Nitration of angiotensin II by ·NO2 radicals and peroxynitrite. *European Journal of Biochemistry* **1999,** *265* (3), 967-971.

17. Sturgeon, B. E.; Glover, R. E.; Chen, Y.-R.; Burka, L. T.; Mason, R. P., Tyrosine iminoxyl radical formation from tyrosyl radical/nitric oxide and nitrosotyrosine. *Journal of Biological Chemistry* **2001,** *276* (49), 45516-45521.

18. Philpot, J. S. L.; Small, P. A., The action of nitrous acid on p-cresol and tyrosine. *Biochemical Journal* **1938,** *32* (3), 534-541.

19. Thorburn, C. C., The edible nest swiftlet industry in Southeast Asia: Capitalism meets commensalism. *Human Ecology* **2015,** *43* (1), 179-184.

20. de Queiroz, J. F.; de M. Carneiro, J. W.; Sabino, A. A.; Sparrapan, R.; Eberlin, M. N.; Esteves, P. M., Electrophilic aromatic nitration: Understanding its mechanism and substituent effects. *The Journal of Organic Chemistry* **2006,** *71* (16), 6192-6203.

21. Crow, J. P.; Beckman, J. S., Quantitation of protein tyrosine, 3-nitrotyrosine, and 3-aminotyrosine utilizing HPLC and intrinsic ultraviolet absorbance. *Methods* **1995,** *7* (1), 116-120.

22. Muta, Y.; Oneda, H.; Inouye, K., Anomalous pH-dependence of the activity of human matrilysin (matrix metalloproteinase-7) as revealed by nitration and amination of its tyrosine residues. *Biochemical Journal* **2005,** *386* (2), 263-270.

23. Metzler, D., Determining structures and analyzing cells. In *Biochemistry 2nd Edition: The Chemical Reactions of Living Cells*, Metzler, D., Ed. Academic Press: 2003; pp 95-160.

24. Quaroni, L.; Smith, W. E., Nitration of internal tyrosine of cytochrome c probed by resonance Raman scattering. *Biospectroscopy* **1999,** *5* (S5), S71-S76.

25. Passingham, C.; Hendra, P. J.; Hodges, C.; Willis, H. A., The Raman spectra of some aromatic nitro compounds. *Spectrochimica Acta Part A: Molecular Spectroscopy* **1991,** *47* (9), 1235-1245.

26. Souza, J. M.; Peluffo, G.; Radi, R., Protein tyrosine nitration—Functional alteration or just a biomarker? *Free Radical Biology and Medicine* **2008,** *45* (4), 357-366.

27. Gunaydin, H.; Houk, K. N., Mechanisms of peroxynitrite-mediated nitration of tyrosine. *Chemical Research in Toxicology* **2009,** *22* (5), 894-898.

28. Souza, J. M.; Daikhin, E.; Yudkoff, M.; Raman, C. S.; Ischiropoulos, H., Factors determining the selectivity of protein tyrosine nitration. *Archives of Biochemistry and Biophysics* **1999,** *371* (2), 169-178.

29. Kato, Y.; Ogino, Y.; Aoki, T.; Uchida, K.; Kawakishi, S.; Osawa, T., Phenolic antioxidants prevent peroxynitrite-derived collagen modification in vitro. *Journal of Agricultural and Food Chemistry* **1997,** *45* (8), 3004-3009.

30. Teixeira, D.; Fernandes, R.; Prudêncio, C.; Vieira, M., 3-nitrotyrosine quantification methods: Current concepts and future challenges. *Biochimie* **2016,** *125* (Supplement C), 1-11.

31. Misko, T. P.; Radabaugh, M. R.; Highkin, M.; Abrams, M.; Friese, O.; Gallavan, R.; Bramson, C.; Hellio Le Graverand, M. P.; Lohmander, L. S.; Roman, D., Characterization of nitrotyrosine as a biomarker for arthritis and joint injury. *Osteoarthritis and Cartilage* **2013,** *21* (1), 151-156.

32. Ahsan, H., 3-nitrotyrosine: a biomarker of nitrogen free radical species modified proteins in systemic autoimmunogenic conditions. *Human Immunology* **2013,** *74* (10), 1392-1399.

33. Huang, G.-J.; Sheu, M.-J.; Chen, H.-J.; Chang, Y.-S.; Lin, Y.-H., Inhibition of reactive nitrogen species in vitro and ex vivo by trypsin inhibitor from sweet potato 'Tainong 57' storage roots. *Journal of Agricultural and Food Chemistry* **2007,** *55* (15), 6000-6006.

34. Rodrigues, E.; Mariutti, L. R. B.; Mercadante, A. Z., Carotenoids and phenolic compounds from Solanum sessiliflorum, an unexploited amazonian fruit, and their scavenging capacities against reactive oxygen and nitrogen species. *Journal of Agricultural and Food Chemistry* **2013,** *61* (12), 3022-3029.

35. Sousa, C.; Valentão, P.; Ferreres, F.; Seabra, R. M.; Andrade, P. B., Tronchuda cabbage (Brassica oleracea l. Var. Costata dc): Scavenger of reactive nitrogen species. *Journal of Agricultural and Food Chemistry* **2008,** *56* (11), 4205-4211.

36. Yen, G.-C.; Lai, H.-H., Inhibition of reactive nitrogen species effects in vitro and in vivo by isoflavones and soy-based food extracts. *Journal of Agricultural and Food Chemistry* **2003,** *51* (27), 7892-7900.

Chapter 5 Conclusion and Future Work

As a health supplement and medicine, edible bird's nest (EBN) is reputed to have many benefits ranging from stimulating the immune system to ameliorating the effects of aging on the skin, and hence it has been consumed in large quantities. It is the most abundant source of mucin glycoprotein known, and more than one million kilograms of EBN are harvested annually. Due to these reasons, understanding of the properties of EBN mucin glycoprotein at the molecular level has gained increasing interest in recent years.

In this thesis, the chemistry of the mucin glycoprotein of EBN produced by the species *Aerodramus fuciphagus* was explored. The four main research objectives that were set for this thesis were achieved through different experimental studies conducted and discussed in the respective chapter.

Firstly, the aim to characterize the properties of mucin glycoprotein in EBN was achieved with Raman microspectroscopy and thermal analysis instruments. While the demand for EBN remains a pressing problem till date, greater awareness of the properties of EBN is of paramount importance when it comes to achieving a holistic evaluation of the benefits and values of EBN. Our findings showed that both analytical tools provided useful information of EBN that has never been reported before. The unique Raman spectrum of EBN showed vibrational lines that are attributed to protein and saccharides, while the unique thermogravimetry (TG), differential thermogravimetry (DTG) and differential scanning calorimetry (DSC) curves showed the thermal decomposition characteristics of the glycoprotein, tightly and loosely bound moisture content, and ashes content of EBN. The unique fingerprinting of EBN samples from different geographical places suggested that they are generally made of the same material by the species *Aerodramus fuciphagus*. In addition,

the unique fingerprinting served as the analytical standards to authenticate and check for adulterants that may be introduced into EBN with a profit motive.

Secondly, we classified the edible adulterants into two types. Type I adulterants which are adhered on the surface have some distinct differences in their morphological structure that permit identification using a microscope, while advanced analytical tools are required to detect the Type II adulterants that are absorbed and embedded in the EBN cement. The ability of EBN to absorb a significant amount of Type II adulterants was also shown, which means that it could be used as a matrix for drug delivery.

We found that both analytical tools have their own exceptional advantages of checking for the authenticity of EBN. Raman microspectroscopy is a non-invasive and label-free technique that can rapidly provide comprehensive information on food analysis. The band frequencies and the relative intensities of the bands in the Raman spectra, as complemented by the high spatial resolution of Raman microspectroscopy is useful in identifying Type I or Type II adulterants that might either be lumpy or uniformly distributed across the EBN cement. On the other hand, thermal analysis tools offer a straightforward and fast technique that only requires a small sample size to check for adulterants in EBN. Moreover, the principal component analysis was applied to convert the correlated variables in the spectra or curves into linearly uncorrelated variables which helped draw a distinction between adulterated and unadulterated EBN samples. Therefore, these two proposed techniques could be put into service for establishing a quality assurance platform for EBN and could be featured in the official regulatory protocol for the import and export of EBN, so that more predictable and reproducible results could be achieved in the future.

Thirdly, a series of comprehensive studies were planned and conducted to reveal the underlying mechanism of the reddening process of EBN. The myth of the red color in the red

EBNs that has perpetuated among Chinese communities for over centuries has finally been uncovered. We have been able to identify the molecular basis for the red color by biochemical (ELISA test) and spectroscopic (UV-Vis and Raman) methods which have never been done before. Contrary to the earlier conjectures, the nitration of the mucin glycoprotein, particularly on the tyrosyl residues to produce 3-nitrotyrosyl (3-NTyr) is the real cause of the red color. The nitrous acid generated from bacterial decomposed bird's dropping or the reaction between sodium nitrite and hydrochloric acid reacts with the tyrosyl residues on EBN mucin glycoprotein, thereby leading to the formation of the colored 3-NTyr residue.

As discussed in the forth chapter, evidences for the 3-NTyr residue came from the anti-3-nitrotyrosine ELISA which showed significantly higher 3-NTyr content in red EBN, UV-Vis absorption spectra of red EBN as a function of pH which was akin to that of pure 3-nitrotyrosine (3-NT), color change of red EBN at different pH just like 3-NT, and Raman microspectroscopy which identified the presence of nitro bands of 3-NTyr in red EBN. The research has also shown that EBN is able to scavenge reactive nitrogen species (RNS) through the nitration of the tyrosyl residue on mucin glycoprotein. The red EBN could in fact be unsafe for human consumption due to the high amounts of nitrite and nitrate present, and some of the glycoprotein tyrosine would have been spent in being nitrated, and so the belief that red EBN is superior to white EBN is wrong. Besides solving the puzzle of the basis of red color, the findings of the chemical nature and mechanisms of the color modification in glycoprotein might have some deeper implications in the food industry.

Overall, the work that has been done throughout the entire duration of this Ph.D. project has broadened and deepened our understanding towards the properties and the chemistry of the mucin glycoprotein in EBN. In summary, two new techniques that offer remarkable stability in checking the authenticity of EBN has been proposed to tackle the challenges of adulteration.

On a separate note, the molecular basis and chemistry of the striking red color in red EBN that has remained the realm of hypothesis and legend for hundreds of years has been explained.

Last but not least, there are still many unknowns about EBN, including the molecular structure of the EBN mucin glycoprotein and the *in vivo* mechanism of the putative health effects. Therefore, more efforts are required to shed more light on it. Hopefully, we are able to comprehensively understand the EBN and feasibly synthesize the mucin glycoprotein in the near future, so that more people can receive the benefits from this fascinating nutraceutical.